Investigating novel roles for exogenous and endogenous Galectin-3 in leukocyte recruitment to the inflamed microcirculation

Miss Beatrice Rose Gittens

A thesis submitted to Queen Mary University of London (Barts and the London School of Medicine and Dentistry) in partial fulfilment of the requirements for the degree of Doctor of Philosophy

Centre for Biochemical Pharmacology,

William Harvey Research Institute,

Barts and the London School of Medicine and Dentistry.

Charterhouse Square, London, EC1M 6BQ.

I, Beatrice Rose Gittens, confirm that the research included within this thesis is my own work or that where it has been carried out in collaboration with, or supported by others, that this is duly acknowledged below and my contribution indicated. Previously published material is also acknowledged below.

I attest that I have exercised reasonable care to ensure that the work is original, and does not to the best of my knowledge break any UK law, infringe any third party's copyright or other Intellectual Property Right, or contain any confidential material.

I accept that the College has the right to use plagiarism detection software to check the electronic version of the thesis.

I confirm that this thesis has not been previously submitted for the award of a degree by this or any other university.

26th November 2013

Details of collaboration and publications:

Collaboration with Prof. S. Nourshargh from the Centre for Microvascular Research, WHRI who provided $CX_3CR1^{gfp/+}$ mice. I carried out intravital microscopy using these mice, collected and stained the cremasters *ex vivo* as detailed in Methods; Dr J. Bodkin of the Centre for Microvascular Research, WHRI then took confocal images (Shown in Figure 4.7C) of vessel segments, as detailed in Methods.

Publications listed in Section 1.10.

ABSTRACT

This study uses *in vivo* and *ex vivo* imaging to explore the hypothesis that galectin-3 (Gal-3) acts as a positive regulator of leukocyte recruitment to the inflamed microcirculation. In addition to this, due to its localisation both within and outside the cell, the effect of exogenous as well as the role of endogenous Gal-3 was investigated. Leukocyte recruitment in the cremasteric microcirculation of wild-type (C57BL/6), Gal-$3^{-/-}$ and $CX_3CR1^{gfp/+}$ mice was assessed by intravital microscopy following intra-scrotal injection of PBS, IL-1β, TNF-α or Gal-3 and intravenous administration of anti-Ly6G to label neutrophils. Concurrently, these responses were investigated further with the use of the parallel plate flow chamber assay, confocal microscopy, flow cytometry, PCR analysis and proteome profile array.

Treatment with IL-1β and TNF-α significantly reduced leukocyte rolling velocities in WT mice, an effect that was absent in Gal-$3^{-/-}$ mice. These observations were repeated in the flow chamber where Gal-$3^{-/-}$ leukocytes did not capture to E-selectin and initiate downstream changes in their activation state and cell morphology. Flow cytometric analysis showed that Gal-$3^{-/-}$ neutrophils express reduced PSGL-1 in response to TNFα and that basally both neutrophils and monocytes display reduced HPA and PNA lectin binding – suggesting that the Gal-$3^{-/-}$ leukocytes have an altered glycophenotype. Furthermore, Gal-$3^{-/-}$ neutrophils express reduced CD11b basally and after TNFα treatment, though both Gal-$3^{-/-}$ neutrophils and monocytes express comparable levels of L-selectin.

Finally, Gal-3$^{-/-}$ endothelial cells express reduced ICAM-1 basally and after TNFα or IL-1β treatment, in addition to expressing reduced E-selectin after IL-1β treatment only. Since these cell adhesion molecules are involved in slow rolling, their reduced expression in Gal-3$^{-/-}$ animals may provide the answer behind reduced slow rolling. In addition, a significant reduction in cell emigration was observed in the Gal-3$^{-/-}$ mice treated with IL-1β when compared to their wild type counterparts, which could be due to impaired expression of cell adhesion molecules and an altered cell surface glycoproteome in these animals.

Administration of recombinant Gal-3 to WT mice resulted in a dose-dependent reduction in rolling velocity associated with increased numbers of adherent and emigrated leukocytes, approximately 50% of which were Ly6G-positive neutrophils. Administration of Gal-3 to $CX_3CR1^{gfp/+}$ mice confirmed that approximately equal numbers of monocytes are also recruited in response to this lectin. After 4 h treatment with the lectin the cremaster contained increased mRNA for IL-1β, TNFα, KC, MCP-1 and IL-6; increased protein expression of these mediators with the exception of IL-1β, was confirmed by proteome profile array alongside IFNγ, MIP-2 and MIP-1α. The recombinant lectin was not acting directly on the leukocytes, which was confirmed in the flow chamber by treating Gal-3$^{-/-}$ leukocytes with recombinant Gal-3 and wild type plasma, by flow cytometric analysis of CD11a/b/c, CD44, PSGL-1 and L-selectin expression after treatment, and by intravenous administration of the lectin during intravital microscopy. Finally, endothelial cells treated *in vitro* with

Gal-3 did not increase ICAM-1 or E-selectin expression however, treatment *in vivo* followed by confocal analysis indicated possible increases in PECAM-1, VCAM-1 and E-selectin expression.

These data suggest the mechanisms mediating leukocyte rolling are impaired in Gal-3 null$^{-/-}$ mice and support a role for Gal-3 as a positive regulator of neutrophil and monocyte trafficking. In conclusion, this study unveils novel biology for exogenous and endogenous Gal-3 in controlling vascular inflammation.

ACKNOWLEDGEMENTS

First and foremost, I would like to thank my supervisor Dr Dianne Cooper. Thank you for giving me the opportunity to work with you on Galectins! Your enthusiasm, capacity for both understanding and teaching and last but not least, patience has helped keep me motivated throughout the three years. Finally, thank you for reading through my thesis (and Experimental Biology conference presentations), even when on maternity leave.

Thank you also to my second supervisor Professor Mauro Perretti for his guidance throughout my studentship. It has been an absolute privilege to work in your laboratory; your insight and passion in Galectin taskforces, conference presentation dry-runs, lab meetings and journal clubs has been invaluable.

Along the way I have worked with many members of the Centre for Biochemical Pharmacology and the William Harvey Research Institute, past and present – from learning new techniques in the lab to troubleshooting in the tearoom – thank you! I would also like to acknowledge the British Heart Foundation, who have funded this research (Grant number FS/10/009/28166).

On a personal note, I am grateful to my family and friends for their support, which has never gone unnoticed over the years - for their words of encouragement and reassurance when it was needed and for generally looking after me; thank you. Lots of love to my parents, especially - I would not have got to this stage without you.

LIST OF FIGURES

ABBREVIATIONS

Ab	Antibody
ANOVA	Analysis of variance
APC	Allophycocyanin
APS	Ammonium persulphate
BBS	Bicarbonate buffered solution
BCA	Bicinchoninic acid
BMDM	Bone marrow-derived macrophages
BSA	Bovine Serum albumin
$CaCl_2$	Calcium chloride
CAM	Cell adhesion molecule
CFSE	Carboxyfluorescein succinimidyl ester
CRD	Carbohydrate recognition domain
CRP	C-reactive protein
Ct	Cycle threshold value
DAPI	4',6-diamidino-2-phenylindole
DMEM	Dulbecco's modified Eagle's medium
DMSO	Dimethylsulfoxide
DNA	Deoxyribonucleic acid
DTT	Dithioreitol
EAE	Experimental autoimmune encephalomyelitis
ECL	Enhanced chemiluminescence
ELISA	Enzyme-linked immunosorbent assay
ERK	Extracellular signal-regulated kinase
ESAM	Endothelial cell-selective molecule
ESL-1	E-selectin ligand-1
EtOH	Ethanol
FAK	Focal adhesion kinase
FCS	Foetal calf serum
FITC	Fluorescein isothiocyanate
fMLF	N-formyl-Met-Leu-Phe
FSC	Forward-scattered light
Gal-3	Galectin-3
Gal-$3^{-/-}$	Galectin-3 knockout
GFP	Green fluorescent protein
Glycam-1	Glycosylation-dependent cell adhesion molecule-1
GPCR	G-protein coupled receptor
Gr-1	Granulocyte differentiation antigen-1
HBSS	Hank's Buffered saline solution
HEPES	4-(2-hydroxyethyl)-1-piperazineethanesulfonic acid
HEVs	High endothelial venules
HPA	*Helix pomatia* agglutinin
HRP	Horseradish peroxidase
HUVEC	Human umbilical vein endothelial cells
ICAM	Intercellular cell adhesion molecule
IgG	Immunoglobulin
IL	Interleukin
ILK	Integrin-linked kinase
IVM	Intravital microscopy
i.a.	Intraarticular

i.n.	Intranasal
i.p.	Intraperitoneal
i.s.	Intrascrotal
i.t.	Intratracheal
i.v.	Intravenous
JAM	Junctional adhesion molecule
JNK	c-Jun N-terminal kinase
KC	Keratinocyte-derived chemokine
kDa	Kilo Dalton
LacNAc	N-acetylactosamine
LAD-I	Leukocyte adhesion deficiency type-I
LBRC	Lateral border recycling compartment
LEL	*Lycopersicon esculentum* lectin
LFA-1	Lymphocyte function associated antigen-1
LN_2	Nitrogen (liquid phase)
LPS	Lipopolysaccharide
LT	Leukotriene
mAb	Monoclonal antibody
Mac-1	Macrophage antigen-1
MAdCAM-1	Mucosal addressin cell adhesion molecule-1
MAL-II	*Maackia amurensis* lectin II
MAPK	Mitogen activated protein kinase
MCP-1	Monocyte chemoattractant protein-1
MEK	MAPK/ERK kinase
MerTK	Mer receptor tyrosine kinase
MFI	Median fluorescence intensity
Mgat5	β1,6-N-acetylglucosaminyl transferase 5
MLCK	Myosin light chain kinase
MLEC	Murine lung endothelial cell
mRNA	Messenger RNA
L-NAME	N^G-Nitro-L-arginine methyl ester
L-PHA	*Phaseolus vulgaris* leucoagglutinin
NF-κB	Nuclear factor kappa B
OA	Osteoarthritis
PAF	Platelet-activating factor
PAGE	Polyacrylamide gel electrophoresis
PBMC	Peripheral blood mononuclear cells
PBS	Phosphate buffered saline
PE	Phycoerythrin
PECAM-1	Platelet-endothelial cell adhesion molecule-1
PI3K	Phoshoinositide-3 kinase
PMN	Polymorphonuclear cell
PNA	Peanut agglutinin
ppGalNAcTs	N-acetylgalactosaminyltransferase
PPP	Platelet-poor plasma
PS	Phosphatidylserine
PSGL-1	P-selectin glycoprotein ligand-1
PTX	Pertussis toxin
PVDF	Polyvinylidene difluoride
RA	Rheumatoid arthritis

rGal-3	Recombinant galectin-3
RNA	Ribonucleic acid
ROS	Reactive oxygen species
RT-PCR	Real-time polymerase chain reaction
s.c.	Sub-cutaneous
SDF-1α	Stromal cell-derived factor-1α
SDS	Sodium dodecylsulphate
SEM	Standard error of the mean
siRNA	Small interfering ribonucleic acid
sLe^X	Sialyl $Lewis^X$
SNA	*Sambucus nigra* lectin
SSC	Side-scattered light
TAE	Tris-acetate-EDTA
TBS	Tris buffered saline
TEMED	Tetramethylethlenediamine
TNF-α	Tumour necrosis factor-α
VAP-1	Vascular adhesion protein-1
VCAM	Vascular cell adhesion molecule
VE-Cadherin	Vascular endothelial cadherin
VEGF-R2	Vascular endothelial growth factor receptor-2
VLA	Very late antigen
WT	Wild type
β3GalT5	β3-galactotransferase 5

TABLE OF CONTENTS

Chapter 1: Introduction

1.1 Galectin-3 is a unique member of the galectin superfamily

Galectin-3 (Gal-3) is a member of the highly conserved β-galactoside-binding family of animal lectins, which are differentially expressed in a wide range of cells including many immune cells (Cooper *et al*., 2012). The group comprises 15 lectins characterized by large carbohydrate-recognition domains (CRD) in their C-terminals which may be folded into five or six β-pleated sheets and bind their ligands in the absence of divalent cations (Dhirapong *et al*., 2009). The family can be further subdivided according to the tertiary structure of their CRD (Figure 1.1).

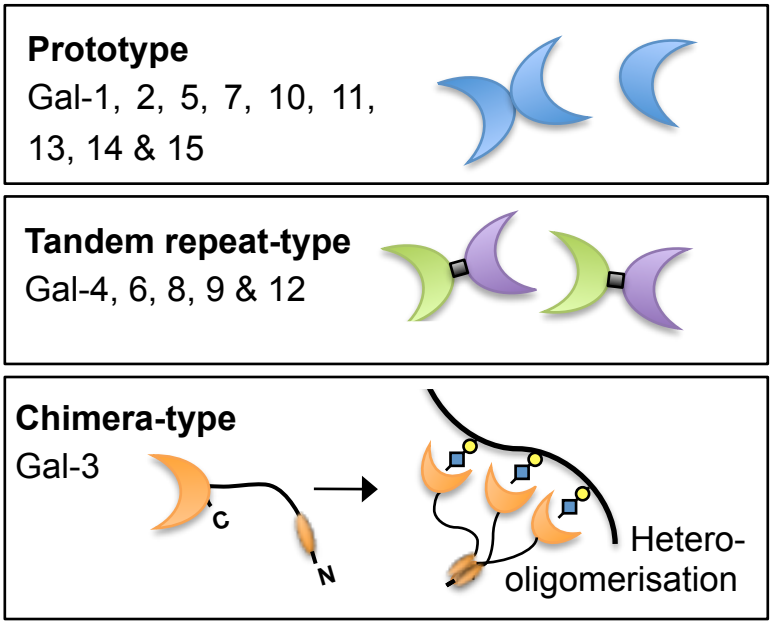

Figure 1.1 The Galectin family.
The galectin family of β-galactoside-binding proteins display distinct tertiary and quaternary structures by which they can be divided into three sub-groups, as shown. The unique structure of Gal-3 enables its self-oligomerisation upon ligand binding.

The prototype galectins Galectin-1, -2, -5, -7, -10, -11, -13, -14 and -15 all have one CRD that can exist as a single lectin or as a dimer. The tandem repeat-type galectins Galectin-4, -6, -8, -9 and -12 all display two CRDs in a single polypeptide chain. Gal-3 is the first lectin to be labelled as a chimeric molecule as it is known to contain one CRD of two anti-parallel β-sheets, one 5-stranded and the other 6-stranded – this one containing the amino acid side chains which form the sugar binding site. Crucially, this is joined to a relatively flexible non-lectin extended N-terminal made up of proline-, tyrosine- and glycine-rich motifs (de Boer *et al*., 2010). The Lgals3 gene is located on chromosome 14 and is formed by 6 exons and 5 introns totalling 17 kilobases; exons IV-VI code for the 135 amino acid C-terminus while exon III and part of exon II code for the 100-150 amino acid N-terminus (Argüeso and Panjwani, 2011). This structure, unique among the galectins, is thought to contribute to many of the singular properties of Gal-3.

Each galectin is able to bind the N-acetylactosamine (LacNAc) disaccharide units found both terminally and internally in N- and O-glycans on glycoreceptors for the lectins, these are most commonly glycoproteins but also include glycolipids (Di Lella *et al*., 2011). Specifically, Gal-3 binds glycoproteins that have been post-translationally modified by the glycosyltransferase Mgat5 (β1,6-N-acetylglucosaminyl transferase 5) which is responsible for the addition of β1,6 branched N-acetlyglucosamine to the α-linked mannose of biantennary N-linked oligosaccharides (Figure 1.2). Gal-3 has also been identified as a

receptor for advanced glycation end products (AGE), which are produced when reducing sugars react with proteins to form highly reactive glycoproteins that have been implicated in diabetes and cardiovascular diseases as well as normal process such as chemotaxis and cytokine release from activated cells (Vlassara *et al*., 1995).

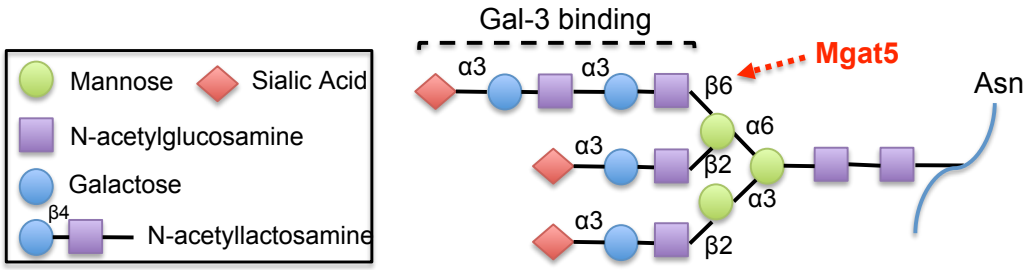

Figure 1.2 Gal-3 binding preference.
Gal-3 binds terminal or internal N-glycans produced by post-translational modification with β1,6 N-acetylglucosaminyltransferase V (Mgat5).

The prototype, tandem repeat-type and chimera-type galectins are, respectively, able to homodimerise, heterodimerise or hetero-oligomerise in the presence of multivalent ligands. When acting extracellularly, galectin-glycan interactions result in large cell surface lattices distinct for each member, thus initiating divergent functions. Specifically, Gal-3 CRD binding to glycan ligands results in conformational changes in the backbone protein loops of the N-terminal that enables the molecule to oligomerize and form heterogeneous and disorganised lattices, displaying positive cooperativity of this binding. In this way, Gal-3 is able to bind glycans at the plasma membrane and through self-assembly results in the cross-linking of these oligosaccharides on the cell surface, initiating intracellular effector signalling pathways (Henderson and Sethi, 2009).

The approximately 30kDa Gal-3 can also exert its effects intracellularly where it oligomerizes; the resulting large aggregates being able to exert many different effects on cellular pathways. Indeed, it is known to bind a number of proteins involved in intracellular signalling including Bcl-2, a protein important for programmed cell death with which Gal-3 shares an NWGR amino acid sequence (Haudek *et al*., 2010). Early studies found that the lectin is itself phosphorylated at Ser^{6} and Ser^{12} on the N-terminus by kinases including casein kinase I and that this resulted in reduced ligand binding, suggesting that the ratio between the two forms would regulate its function, a similar mechanism to that proposed for the selectins (Mazurek *et al*., 2000). More recently, it has been found that though both forms can be found in the nucleus, only the phosphorylated lectin is detected in the cytosol. Indeed, Gal-3 can carry out nuclear splicing of pre-mRNA along with Galectin-1, a process which evidently would have far-reaching effects inside the cell (Liu *et al*., 2002).

Gal-3 is expressed in the majority of human and murine immune cells, in both species it is predominantly produced by macrophages (Forsman *et al*., 2008). Gal-3 belongs to a small group of proteins that can be secreted in the absence of a classical signal sequence, possibly via interaction with extracellular matrix proteins; thus, it is localised primarily in the cytoplasm but also the nucleus and, significantly for this thesis, in the extracellular compartment (de Boer *et al*., 2010). Since it was first investigated in the 1980s Gal-3 can influence many cellular processes

that have direct effects on the continuation and resolution of the inflammatory response.

Since its characterization, Gal-3 has been implicated in a diverse group of human pathologies, many of which have been replicated in murine models of disease (Cooper *et al*., 2012). In healthy adults, levels of circulating Gal-3 average at ~7ng/mL and this is increased by 2-3 fold in infectious disease such as bacterial sepsis, viral lower respiratory tract infections and candidaemia (Ten Oever *et al*., 2013). Its expression was previously found to be upregulated in certain types of lymphomas while downregulated in breast, colon and ovarian carcinomas; furthermore, levels of circulating Gal-3 are again increased in metastatic disease (Sano *et al*., 2000, Iurisci *et al*., 2000). In addition to this, it is up-regulated in the foam cells of atherosclerotic lesions (Nachtigal *et al*., 1998). In a murine model of pneumonia, Gal-3 accumulated in the alveolar space of *S. pneumoniae*-infected lungs, this was closely correlated with the onset of neutrophils to the area (Sato *et al*., 2002). Additionally, Gal-3 has been localized to sites of joint destruction in the synovial tissue of rheumatoid arthritis (RA) patients and furthermore, was found to be increased in these tissues when compared to those from healthy controls or osteoarthritis (OA) patients (Ohshima *et al*., 2003). Gal-3 has also been shown to act similarly in the CNS, where it was upregulated following experimental stroke and this correlated closely with ischaemia (Yan *et al*., 2009). These disease states, particularly RA, stroke and *S. pneumoniae* infection, all involve large inflammatory

responses characterised by leukocyte infiltration to the inflamed area. Thus, it is possible that Gal-3 is exerting its effects by mediating this leukocyte recruitment, a process imperative to the onset and ultimately, conclusion, of acute and chronic inflammatory disorders.

1.2 The leukocyte recruitment cascade

Leukocytes are fundamental to both the acute and chronic phases of the immune response. The large group of haematopoietic stem cell-derived immune cells can be divided into two groups based on their morphology – granulocytes such as neutrophils, basophils, eosinophils and mast cells as well as agranulocytes such as lymphocytes, monocytes and macrophages. Regardless of their specific function, an important hallmark of all leukocytes is their ability to migrate quickly to the area of inflammation. The basic mechanisms underlying leukocyte recruitment have been extensively studied both *in vivo* and *in vitro*; from this a model of cell movement across the endothelial cell wall has been formed (Figure 1.3). Briefly, recruitment in post capillary venules involves five stages – initial capture and rolling, activation, firm adhesion, crawling and finally transmigration (Petri *et al*., 2008, Ley *et al*., 2007).

1.2.1 Capture and rolling

The initial tethering, rolling and subsequent slow rolling of leukocytes is mediated primarily by selectins, which are Ca^{2+}-dependent type-I transmembrane glycoproteins. E- and P- selectin are found on the vascular endothelium and L-selectin is found on the surface of many leukocytes; all bind P-selectin Glycoprotein-1 (PSGL1) and other glycosylated cell surface ligands, many of which carry the tetrasaccharide sialyl Lewis X (sLe^x) (Sperandio *et al*., 2009). It was originally shown by immunogold electron microscopy that PSGL-1 is localised to the tips of microvilli on quiescent neutrophils, monocytes, eosinophils, basophils and

lymphocytes and is not stored intracellularly, allowing for instantaneous association between the leukocytes and vascular endothelium (Bruehl *et al*., 1997). Additional E-selectin ligands include E-selectin ligand-1 (ESL1) and the hyaluronan receptor, CD44. It is possible that E-selectin is more important in humans whereas P-selectin is more predominant in murine tissues (Pan *et al*., 1998).

L-selectin is constitutively expressed on neutrophils, monocytes and lymphocytes; following cell activation it is rapidly shed from the cell surface to concentrated clusters on the microvilli. It is a comparatively short molecule enabling optimal cell interactions with the endothelia at the initial tethering and rolling stages (rolling velocity >100μm/s) (Stein *et al*., 1999). L-selectin also enables secondary leukocyte capture, whereby leukocytes can capture other leukocytes before further strengthening of interactions with the endothelia on E- and P-selectin (Ley *et al*., 2007).

P-selectin is constitutively expressed in Weibel-Palade bodies of the endothelia, which, when stimulated by many inflammatory mediators fuse with the plasma membrane within minutes; thus P-selectin is also important for initial tethering and rolling. P-selectin clustering on the endothelia via clathrin-coated pits increases the strength of selectin binding to neutrophils *in vitro* (Setiadi and McEver, 2003). Studies in P-selectin$^{-/-}$ mice have shown that P-selectin mediates rolling at velocities of approximately 40μm/s in response to cytokine-induced inflammation as well as surgery-induced trauma (Sundd *et al*., 2011).

E-selectin is not stored intracellularly, rather it is newly synthesised upon activation of the endothelial cells and has been shown to be upregulated in as little as 2h following cytokine treatment (Jung and Ley, 1997). E-selectin is predominantly responsible for slow rolling on the endothelia; in E-selectin$^{-/-}$ mice neutrophil slow rolling (<5μm/s) in response to TNFα was absent (Sundd *et al*., 2011). The dramatic decrease in rolling velocity on E-selectin has been partly attributed to an association with the β_2-integrins (Kunkel *et al*., 2000). It is thought that upon binding of E-selectin to its ligand PSGL-1, the integrin LFA-1 becomes partially activated in a Syk-dependent manner allowing slow rolling, but not arrest on ICAM-1 (Zarbock *et al*., 2007). This is reviewed in more detail in section 1.2.2.

The selectins are clearly an important group of molecules for leukocyte recruitment, however studies have shown that there may be distinct routes of recruitment which exclude these molecules, such as α4–integrin-induced rolling and molecules which may be able to replace selectins such as α4–integrin-like CD44 and vascular adhesion protein-1 (VAP-1) (Petri *et al*., 2008).

1.2.2 Activation and firm adhesion

Leukocyte activation and firm adhesion involves the integrin family of transmembrane heterodimers formed from one of 18 α subunits and one of 8 β subunits so far identified and which may exist in one of three conformational states classified according to the affinity with which they bind their ligands. These are the low-affinity bent state, the intermediate-affinity state where the integrin is extended however the headpiece and thus binding site is closed and finally the high-affinity open headpiece extended formation (Hogg *et al*., 2011). Once in close contact with the endothelium the leukocytes become activated and this initiates integrin-dependent pathways through inside-out signalling, which mediate firm adhesion via a conformational change of the integrin that allows firm binding with their leukocyte ligands. It is thought that the α_4–integrins such as very late antigen-4 (VLA-4) and the more prominent β_2-integrins such as lymphocyte function associated antigen-1 (LFA-1) and macrophage-1 antigen (Mac-1) can be fully activated by shear flow in the vessel after E-selectin inside-out signalling, facilitating cell arrest on the vessel wall (Green *et al*., 2004).

Initial integrin activation commonly occurs through the action of chemokines presented by endothelial cells binding GPCRs on the leukocyte cell surface. In neutrophils, these $G\alpha_{i2}$-coupled receptors most probably result in PLC-β activation, intracellular Ca^{2+} fluctuations and subsequent activation of the guanine nucleotide exchange factor (GEF) CalDAG-GEFI and its target Rap1. In comparison, further investigation

since the Zarbock *et al.* (2007) findings have reported that neutrophil rolling on both E-and P-selectin can initiate the inside-out integrin pathways that cause LFA-1 to enter the extended but not high-affinity conformation, in the absence of chemokine signalling. This was dependent on PSGL-1 binding and syk activation via the src family tyrosine kinase FGR, which in turn phosphorylated the immunoreceptor tyrosine-based activation motif (ITAM)-containing molecules DAP-12 and FcRγ before recruiting syk itself (Kuwano *et al*., 2010). This complements work carried out using co-coated chamber slides in the *in vitro* flow assay showing that neutrophil engagement with E-selectin activates β_2-integrin binding to ICAM-1, which was blocked by neutralising antibodies against E- and L-selectin, PSGL-1 or inhibitors of p38 mitogen-activated protein kinase (MAPK) (Simon *et al*., 2000). Further, cross-linking of E-selectin on human umbilical vein endothelial cells (HUVEC) resulted in MAPK/ERK kinase (MEK)-dependent MAPK activation, which was brought about by interaction with Ras and Raf-1 to upregulate the pro-inflammatory early response gene *c-fos* (Hu *et al*., 2000).

There are differences in the two activation routes described; selectin-dependent neutrophil activation is much slower than activation induced by chemokine signalling, which is almost instantaneous. Furthermore, it is thought the added force of the shear flow in vessels enables chemokine-mediated activation to cause the high affinity, open headpiece

conformation of the integrin, suggesting that further layers of regulation occur *in vivo* (Kuwano *et al*., 2010).

Once firm adhesion is fully effected, ICAM-1 dimers preferentially bind these LFA-1 and MAC-1 integrin ligands and through Src-dependent phosphorylation of the actin cytoskeleton the dimers form a concentrated cluster on the endothelial cell under the leukocyte which continues to surround the cell as it transmigrates through the vessel wall (Yang *et al*., 2006). VCAM-1 preferentially binds VLA-4 on monocytes and lymphocytes; clustering of this adhesion molecule in the later stages of the recruitment cascade has also been described. This clustering of ICAM-1 and VCAM-1 is thought to aid the later stage of transmigration by leading to increases in cytosolic free Ca^{2+} and the subsequent loosening of the endothelial tight junctions via VE-cadherin phosphorylation. ICAM-2 is constitutively expressed on endothelial cells and preferentially binds β_2-integrins, some studies report a functional role for ICAM-2 in neutrophil adhesion though its real relevance is still unclear and overall modest (Muller, 2011). Finally, activation also induces neutrophil surface relocation of the selectin ligand PSGL-1 from the microvilli to the newly-formed uropod, perhaps allowing for smoother transendothelial migration by disengaging bonds to the surface of the endothelial cell (Bruehl *et al*., 1997).

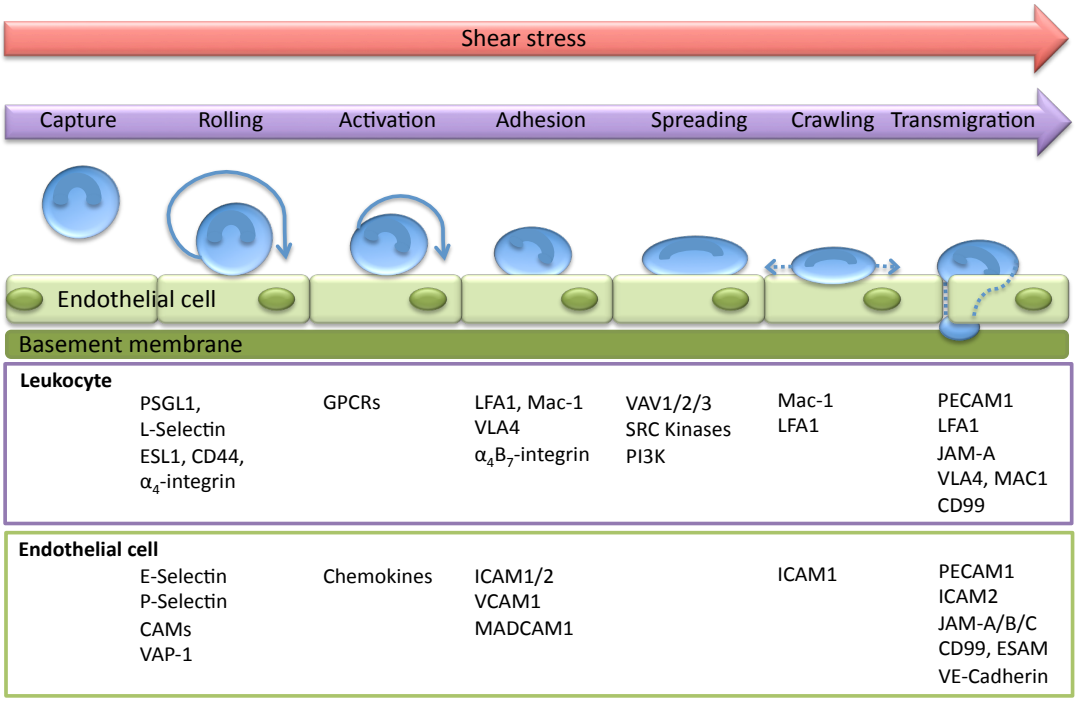

Figure 1.3 The leukocyte recruitment cascade.
Many leukocyte and endothelial cell molecules work in concert to coordinate the leukocyte recruitment cascade in a sequential manner. The distinct stages include initial tethering, rolling, activation, slow rolling, adhesion, crawling and finally para- or transcellular transmigration. PSGL-1, P-selectin glycoprotein ligand-1; ESL1, E-selectin ligand 1; CAM, cell adhesion molecule; VAP-1, vascular adhesion protein-1; LFA1, lymphocyte function-associated antigen-1; Mac-1, macrophage-1 antigen; VLA4, very late antigen-4; ICAM, intracellular CAM; VCAM, vascular CAM; MADCAM1; mucosal vascular addressin CAM-1, PI3K, phosphoinositide 3-kinase; Jam, junctional adhesion molecule; ESAM, endothelial cell-selective adhesion molecule.

1.2.3 Crawling and Transmigration

The process of crawling is thought to aid leukocyte emigration as the cells search out endothelial cell junctions and appropriate places to transmigrate (Wojciechowski and Sarelius, 2005). It was first identified as a critical step in the cascade by visualising monocyte transmigration through endothelial cells *in vitro* (Schenkel *et al*., 2004). Leukocyte crawling is also integrin-dependent, with Mac-1 having a dominant role. *In vivo* wild type neutrophils migrated to PECAM-1-stained junctions but neutrophils lacking Mac-1 failed to do so. In addition, inhibition of neutrophil crawling via Mac-1 antibody caused leukocytes to migrate at the point of their adherence resulting in a higher proportion of transcellular as opposed to paracellular migration of these cells (Phillipson *et al*., 2006).

Though it has been shown that leukocyte subtypes behave differently under different conditions, all subtypes can migrate across the endothelia both transcellularly and paracellularly. For example, neutrophils often emigrate at tricellular points of the endothelial barrier whereas monocytes often migrate at endothelial cell tight junctions and there is mounting evidence that lymphocytes prefer the transcellular route (Burns *et al*., 2000, Carman and Springer, 2004). Several endothelial cell junctional molecules are involved primarily in this stage of recruitment, these include platelet endothelial cell adhesion molecule -1 (PECAM-1), ICAM-2, junctional cell adhesion molecules A-C (JAM-A/B/C), CD99 (also known as MIC2), endothelial cell-selective molecule (ESAM) and

vascular-endothelial-cadherin (VE-cadherin). PECAM-1, CD99 and JAM-A on the endothelia bind in a homophilic manner to their counterparts on transmigrating leukocytes and neighbouring endothelial cells; JAM-B and JAM-C bind VLA-4 and Mac-1, respectively; ICAM-2 binds LFA-1 and Mac-1 and ESAM binds unidentified ligands on leukocytes (Ley *et al*., 2007).

As described above, firm adhesion of the leukocyte involves the clustering of ICAM-1 and VCAM-1 at the endothelial cell membrane and this step initiates further stages, which aid paracellular transmigration by weakening the endothelial cell tight junctions. VCAM-1 multimerisation leads to increases in cytosolic free Ca^{2+}, activation of Rac-1, production of reactive oxygen species and consequent protein kinase Cα activation, which in turn leads to the phosphorylation of VE-cadherin and its subsequent dissociation from the actin cytoskeleton (Muller, 2011). ICAM-1 clustering also increases intracellular Ca^{2+} ion concentration as well as initiating p38 MAPK pathways, which result in activation of RhoA. The increase in cytosolic Ca^{2+} brought about by ICAM-1 and VCAM-1 clustering as well as the activation of RhoA signalling collectively activates myosin light chain kinase (MLCK) and consequently leads to endothelial cell contraction. The leukocyte is then guided through the weakened tight junction between endothelial cells by the junctional molecules present on the leukocyte and at the endothelial border. It is thought that the endothelial cell is able to direct a pool of molecules to aid this process; for example, VE-cadherin is directed away from the junction

whereas PECAM-1 and JAM-A migrate towards it (Ley *et al*., 2007). Specifically, Mamdouh *et al.* showed that intracellular PECAM-1 is targeted and recycled to a pool of molecules connected to the endothelial cell surface during transmigration and later termed the lateral border recycling compartment (LRBC) (Mamdouh *et al*., 2003, Mamdouh *et al*., 2008).

The molecules involved in this stage vary according to the type of stimulus that is applied to the inflamed zone, and whether it predominantly activates the endothelia or the leukocytes themselves. Stimuli known to activate the endothelial cells include ischaemia/reperfusion injury as well as the cytokine IL-1β; neutrophil transmigration elicited by the latter stimuli was shown to require ICAM-2, JAM-A then PECAM-1 in distinct but sequential steps (Woodfin *et al*., 2009). These junctional molecules were found not to be necessary for transmigration elicited by TNFα, LTB4 or N-formyl-Met-Leu-Phe (fMLF) – three stimuli known to activate leukocytes directly. The same study reported that following TNFα stimulation, antibody blockade of Mac-1 and JAM-C reduced leukocyte transmigration; this was in accordance with earlier studies describing a role for JAM-C in monocyte and neutrophil transmigration (Bradfield *et al*., 2007, Chavakis *et al*., 2004).

Transcellular migration is known to occur in the CNS and more commonly in *in vitro* models, it was first described convincingly *in vivo* using a guinea pig model of skin inflammation (Feng *et al*., 1998). Clustering of

ICAM-1 is thought to play a role in initiating transcellular migration and overexpression of this molecule was shown to increase migration via this pathway (Yang *et al*., 2005). In order for a pathway to form in the endothelial cells, it is reported that ICAM-1 ligation leads via F-actin interactions to the transport of caveolin-1 to the cell membrane and further stabilisation of channels by vimentin (Ley *et al*., 2007). In addition to this, Muller suggested that ICAM-1 clustering may lead to recruitment of the LBRC, which is essential for transcellular migration (Muller, 2011). By this mechanism, the junctional molecules present throughout paracellular migration also play a part in transcellular migration, as they are contained within the LBRC. The junctional molecules CD99, PECAM-1 and JAM-A surround neutrophils and monocytes transmigrating transcellularly, though studies using blocking antibodies against CD99 and PECAM-1 confirmed that only these two molecules were essential for leukocyte transcellular transmigration (Mamdouh *et al*., 2009).

Many factors can alter the mode of leukocyte recruitment; for example, the tissue localisation, the type of stimulus or how long the endothelium has been activated for, as well as what leukocyte subtype is predominantly being recruited. Furthermore, these factors may alter the catalogue of molecules that the cells are using to migrate to the site of injury and much work has shown that these may differ from the classical selectin and integrin ligands that have been so well characterised (Kubes and Kerfoot, 2001, Sato *et al*., 2002, Li *et al*., 2006, Hogg and Doerschuk, 1995, Mizgerd *et al*., 1997). Investigating the roles of these factors in

leukocyte recruitment may have many implications for inflammatory diseases such as RA and stroke where this process plays a large part. In order to establish whether Gal-3 may be an alternative molecule involved in leukocyte recruitment, taking into account its relevance in a wide variety of pathologies in addition to its intra- and extracellular localisation, it is important to examine both exogenous effects and endogenous roles on leukocyte subsets individually.

1.3 Galectin-3 roles and effects on Neutrophils

Neutrophils are integral cells of the innate immune system and constitute the first line of defence against invading pathogens. Gal-3 is expressed in human neutrophils and at much lower levels in murine neutrophils though both species express Gal-3 surface ligands such as CD66 (Sato *et al*., 2002, Farnworth *et al*., 2008). Many *in vivo* and *in vitro* studies carried out in human as well as in murine systems indicate a role for Gal-3 in the recruitment of neutrophils to the inflamed zone. Sano *et al.* reported that Gal-3 acts as a chemoattractant for human neutrophils *in vitro* and that Gal-3 induced their recruitment to a mouse air-pouch model (Sano *et al*., 2000). Studies have also examined the role of Gal-3 in murine models of *Streptococcal pneumoniae* lung infection, where neutrophil extravasation in response to the pathogen is predominantly β_2-integrin-independent (Mizgerd *et al*., 1999). This is in contrast to *Escherichia coli*-induced alveolar inflammation, where tight adhesion and subsequent emigration of the neutrophils through the vascular endothelium is reduced by β_2-integrin antibody blockade (Hogg and Doerschuk, 1995). Accumulation of Gal-3 in the lungs correlated with neutrophil emigration to the alveoli during infection and low levels of Gal-3 were bound to the neutrophil cell surface (Sato *et al*., 2002). Farnworth *et al.* demonstrated that Gal-3$^{-/-}$ mice developed more severe lung injury and reduced neutrophil recruitment, which was restored by administration of exogenous Gal-3 (Farnworth *et al*., 2008). Nieminen *et al.* found that there was a reduction in the number of neutrophils recruited to the alveolar space of Gal-3$^{-/-}$ mice at 24h after infection; they reported no

effect on mice infected with *E.Coli*, suggesting that Gal-3 facilitates β_2-integrin-independent migration of neutrophils to the infected alveoli during lung inflammation (Nieminen *et al*., 2008).

Another study indicating a stimulus-specific role for Gal-3 found that endogenous Gal-3 was required for acute neutrophil recruitment to *Leishmania major*-infected murine air pouches in those mice infected with the LV39 strain but not the Friedlin strain. This was without any defects in macrophage, monocyte, lymphocyte or eosinophil recruitment and not due to any differences in cytokine production or neutrophil mobility and capacity to phagocytose. Furthermore, Gal-3 binds the *L.major* glycan epitope ($Gal\beta_{1\text{-}3})_n$ and is then cleaved; interestingly Friedlin strain does not contain high levels of this epitope, suggesting complex regulation via different routes for Gal-3 roles (Bhaumik *et al*., 2013). Indeed, the study drew two conclusions; firstly that Gal-3 was released and accumulated in exudates in response to *L.major* bacterial challenge. Secondly, since it could also initiate neutrophil recruitment when injected alone to murine air pouches, the authors suggested that Gal-3 was acting as a damage-associated molecular pattern (DAMP) molecule, which interacts directly with the neutrophils. This is in addition to recent research suggesting that along with other galectins, Gal-3 is starting to be classified as a pattern recognition receptor itself (Cerliani *et al*., 2011).

Murine models of sterile peritonitis have also been employed to investigate exogenous and endogenous Gal-3 effects on leukocyte,

specifically neutrophil, trafficking. Thioglycollate broth elicits peak leukocyte recruitment at 6h, this was unchanged in Gal-3$^{-/-}$ mice; however, these animals displayed reduced neutrophil recruitment at 3, 6 and 9 h post-treatment when compared to wild type counterparts (Alves *et al*., 2013). Another study which did not look at these early time-points found Gal-3$^{-/-}$ mice had reduced peritoneal granulocytes after 4 days and furthered this by confirming that in this setting, the mutant cells had a normal rate of apoptosis and macrophage phagocytosis suggesting that defects in recruitment are singularly down to an inability to traffic properly (Colnot *et al*., 1998). In contrast, peritoneal treatment with exogenous recombinant Gal-3 (rGal-3) did not alter neutrophil influx in a carrageenan model of rat peritonitis despite levels of Gal-3 being increased in peritoneal lavage fluid and extravasated neutrophils at 4 h post-treatment in wild type animals (Gil *et al*., 2006). In accordance with this, Mgat5$^{-/-}$ mice, which display reduced Gal-3 ligands on the cell surface, had reduced leukocyte extravasation to the peritoneal cavity after treatment with thioglycollate broth, suggesting that it is extracellular Gal-3 that affects trafficking directly. The authors suggested that Gal-3 cross-linked Mgat5-modified N-glycans on cytokine receptors at the cell surface, and obstructed their depletion by constitutive endocytosis, for example the TGFβ receptor (Partridge *et al*., 2004). Hsu *et al.* (2000) have investigated this further and observed that thioglycollate broth-elicited peritoneal inflammatory cells from Gal-3$^{-/-}$ mice had much reduced NFκB activation. In contrast to earlier studies however, these authors also saw increased levels of apoptosis and altered cell morphology in macrophage

cultures of Gal-3$^{-/-}$ cells compared to wild type counterparts (Hsu *et al*., 2000).

Human neutrophils have been investigated under static conditions *in vitro*; adhesion to an endothelial monolayer was increased 5-fold in the presence of exogenous Gal-3 (Sato *et al*., 2002). Furthermore, Gal-3 promotes human neutrophil adherence to the extracellular matrix proteins laminin and at higher concentrations, fibronectin. This effect is dependent on the carbohydrate recognition domain and amino terminal of Gal-3 as well as being temperature and Ca^{2+}/Mg^{2+}-dependent, suggesting that Gal-3 oligomerizes at the cell surface (Kuwabara and Liu, 1996). Taken together, these data indicate that Gal-3 may act as a soluble adhesion molecule for neutrophils.

Gal-3 has additional effects on neutrophils that may be central to its inflammatory role. There has been some debate over direct Gal-3 effects on neutrophils. Initial studies reported that it was able to induce an oxidative burst in exudated hence primed neutrophils but not in peripheral blood neutrophils. Neutrophil priming occurs *in vivo* during migration and *in vitro* can be induced by pre-incubation with, amongst others, LPS, IL-8 (low concentration) or cytochalasin B. It occurs in degrees and via granule mobilisation, intracellular Ca^{2+} fluctuations and increased phosphorylation activity, to enable neutrophils to rapidly respond once they have reached their target site (Almkvist *et al*., 2001). Cytochalasin B was used to show an increase in Gal-3-mediated oxidative burst and

reactive oxygen species (ROS) production when compared to unprimed cells (Yamaoka *et al*., 1995). Karlsson *et al.* furthered these studies by examining differences in NADPH-oxidase activity in peripheral or human skin blister neutrophils, which responded much more to Gal-3. They also distinguished two signals in the cell response to Gal-3 – extracellular release of ROS attributed to plasma membrane NADPH-oxidase activated by Gal-3 receptors in the gelatinase and secretory granules, as well as intracellular ROS production attributed to Gal-3 receptors activating NADPH-oxidase in the specific granule membrane (Karlsson *et al*., 1998). In contrast to this, more recent studies looking at different markers of activation have shown Gal-3 can indeed activate naïve as well as primed neutrophils, causing L-selectin shedding within 5 min and IL-8 release after 30 min in these cells; in both cases CRD binding and N-terminal oligomerization was required. Furthermore, the study showed that Gal-3 was cleaved by the serine protease neutrophil elastase in primed cells upon its CRD binding and suggested that this regulation of Gal-3 activity was coupled to its internalisation (Nieminen *et al*., 2005). Particularly relevant to neutrophil recruitment, Farnworth *et al*. demonstrated that 30 min treatment with recombinant Gal-3 also caused L-selectin shedding on human neutrophils as well as CD11b upregulation on both human and mouse neutrophils (Farnworth *et al*., 2008).

Human recombinant Gal-3 increased the phagocytic capacity of isolated human neutrophils; this response was dependent on p38 MAPK phosphorylation and disruption of this pathway abrogated these effects

(Fernández *et al*., 2005). Finally, there is work indicating a role in neutrophil apoptosis – some studies show that Gal-3 is protective, most likely due to intracellular mechanisms of action whereas when acting extracellularly it may induce apoptosis (Farnworth *et al*., 2008, Fernández *et al*., 2005). In the case of human neutrophils, Gal-3 is able to induce phosphatidylserine (PS) exposure in the absence of cell death and it was suggested that Gal-3 would act as an immunomodulatory molecule via this function (Stowell *et al*., 2008).

1.4 Gal-3 roles and effects on Monocytes and Macrophages

Monocytes and macrophages are vital members of the innate immune system, monocytes arrive at the site of injury quickly before differentiating into macrophages, which can engulf invading pathogens and cell debris. Despite this, much less is known about Gal-3 roles and effects in these cells. Gal-3 is expressed in both cell types and monocyte differentiation into macrophages as well as stimulation with IL-4 results in increased expression of the lectin (van Stijn *et al*., 2009). It has also been found in both peritoneal and alveolar murine macrophages and can be released from the latter without compromising plasma membrane integrity. The same study found that *S. pneumoniae* infection increased the expression of Gal-3 in alveolar macrophages as well as stimulating its release from these cells (Sato *et al*., 2002).

There is also evidence that supports the view that Gal-3 may affect recruitment of monocytes and macrophages. The lectin can act as a chemoattractant for human monocytes where it is chemokinetic at low concentrations (10-100nM) and chemotactic at higher concentrations (~1μM). This biological property did not occur *via* any known chemoattractant receptors; it was coupled to an increase in intracellular Ca^{2+} in addition to being Pertussis toxin-sensitive, suggesting a role for G-inhibitory protein coupled receptors in some Gal-3 actions. Similarly, Gal-3 induces macrophage chemoattraction and is one of few chemokines that have been shown to do so. Its chemoattractant properties have been confirmed *in vivo* with increased numbers of monocytes recruited to mouse air-pouches in response to Gal-3 (Sano *et al*., 2000).

In actions separate to those affecting chemoattraction, exogenous application of Gal-3 triggered human macrophages and peripheral blood monocytes to produce superoxide (Liu *et al*., 1995). It also affected macrophage phagocytosis, possibly due to its localisation in the phagosome, where it could interact with binding partners including Alix (Chen *et al*., 2005). In human cells exogenous Gal-3 increased the proportion of macrophages that engulfed apoptotic neutrophils, as well as the number engulfed by each cell; the authors proposed that Gal-3 acted as an opsonin between the macrophage and the apoptotic cell (Karlsson *et al*., 2009). These observations are repeated in murine models where Gal-$3^{-/-}$ macrophages displayed impaired phagocytic capacity of apoptotic

neutrophils (Farnworth *et al*., 2008). Recent work established that Gal-3 acts as an 'eat-me' ligand for macrophages by binding to the phagocytosis receptor mer receptor tyrosine kinase (MerTK) and leading to its autophosphorylation (Caberoy *et al*., 2012).

Gal-3 can also regulate the differentiation of macrophages into alternative lineages, which have been associated with various pathologies including fibrotic diseases, asthma, and atherosclerosis (MacKinnon *et al*., 2013). Classical M1 macrophages are produced by IFNγ/LPS stimulation and release higher levels of IL-12 than IL-10, whereas alternatively activated M2 macrophages are typically brought about by IL-4/IL-13 stimulation and release low levels of both cytokines. Cytotoxic and pro-inflammatory M1 macrophages effect the initial inflammatory response to injury whereas the M2 cells drive the resolution of inflammation by promoting tissue repair. Gal-3$^{-/-}$ bone marrow-derived macrophages (BMDM) displayed no defect in IFNγ/LPS –induced TNFα and IL-6 production. However, Gal-3$^{-/-}$ BMDMs treated with IL-4/IL-13 showed much reduced arginase-1 activity when compared to their wild type counterparts, suggesting the cells were not able to enter the M2 state; these results were replicated in *in vivo*-derived peritoneal macrophages. Furthermore, IL-10-induced deactivation of BMDMs was measured in inhibition of LPS-induced TNFα release and was unchanged between the two genotypes. Additionally, M2 BMDMs were found to release Gal-3; co-incubation with a Gal-3 CRD inhibitor or an inhibitor of the macrophage-binding partner for Gal-3, CD98, blocked this IL-4-mediated arginase-1 activation. CD98 is known

to constitutively associate with the β_1 integrins and through this association results in focal adhesion kinase (FAK) and phoshoinositide-3 kinase (PI3K) activation. Upon further investigation, alternative activation of THP-1 differentiated macrophages was driven by Gal-3 binding to CD98 resulting in subsequent PI3K activation and a Gal-3 feedback loop (MacKinnon *et al*., 2008). Research from the same group found that Gal-3 has significant roles in the pathogenesis of atherosclerosis and that deletion of this lectin is associated with reduced M2 macrophages in the plaque, which had previously been linked to increased atherosclerosis susceptibility (Waldo *et al*., 2008, MacKinnon *et al*., 2013).

1.5 Gal-3 roles and effects on secretory leukocytes

Gal-3 is expressed and secreted in both human and murine mast cells, where it was specifically localised to the secretory vesicles by electron microscopy (Craig *et al*., 1995, Frigeri and Liu, 1992). Murine mast cells null for Gal-3 exhibited lower levels of degranulation and decreased production of cytokines in response to IgE cross-linking on the cell surface, which are both vital processes of these cells (Chen *et al*., 2006). In addition, exogenous Gal-3 induces mediator release from these cells, which is thought to occur by the cross-linking of IgE and its receptor FcεRI on the cell surface (Frigeri *et al*., 1993).

Gal-3 has been localized to the secretory vesicles of human basophils though its effects on these important secretory cells are less well characterised (Craig *et al*., 1995). In contrast, Gal-3 roles in eosinophils

where it is expressed both intra- and extracellularly have been investigated, especially in models of allergic airway inflammation and the murine air pouch model where Gal-3 increased the number of eosinophils that migrated to the site of inflammation (Truong *et al*., 1993, Sano *et al*., 2000). Gal-3 expression is increased in murine lungs with allergic asthma and Gal-$3^{-/-}$ mice display reduced lung and airway eosinophilia in response to acute and chronic allergen (Ovalbumin) challenge, respectively (Ge *et al*., 2010). Further investigation showed endogenous Gal-3 is required for rolling of bone marrow-derived eosinophils on VCAM-1 and showed a trend to be required for stable adhesion on ICAM-1 under conditions of flow. This was in addition to its requirement for subsequent activation-induced morphological changes such as cell spreading and protrusion formation as well as intracellular Gal-3 being vital for eosinophil migration to eotaxin-1 in transwells (Ge *et al*., 2013). These findings could be split into extracellular versus intracellular roles for the lectin. Extracellular Gal-3 enables clustering of the eosinophil stable adhesion receptor αM in lipid rafts by cross-linking CD66b, with which it is constitutively associated on the cell surface (Yoon *et al*., 2007). Additionally, Rao *et al.* (2007) found extracellular Gal-3 could bind glycoprotein receptors including integrin $\alpha 4\beta 1$ and support eosinophil rolling and adhesion under flow by interacting with VCAM-1 (Rao *et al*., 2007b). Not much is known in terms of Gal-3 binding to extracellular glycans and initiating signalling pathways inside the cell; however, a study in mammary epithelial tumour cells showed exogenous Gal-3

increased PI3K and FAK activation as well as F-actin turnover, which are all required for eosinophil trafficking (Lagana *et al*., 2006).

Conversely, intracellular Gal-3 could regulate eosinophil adhesion molecule expression. This has been shown for the intracellular trafficking of epidermal growth factor receptor; in association with Alix, endogenous Gal-3 enables correct trafficking of the protein to the cell surface thus promoting keratinocyte migration (Liu *et al*., 2012). Indeed, eosinophil migration to eotaxin-1 was dependent on intracellular Gal-3 and this may be due to direct regulation of kinases, though this has so far only been investigated in pancreatic tumour cells where Gal-3 activated Ras with downstream extracellular signal-related kinase (ERK) resulting in increased cell invasion (Song *et al*., 2012). These data highlight the pleiotropic cell and injury type-specific roles of Gal-3 and suggest that Gal-3 may mediate recruitment of some of the less prominent leukocytes thus impacting much more on the inflammatory response by changing numbers of lowly expressed cells.

1.6 Gal-3 roles and effects on the adaptive immune response

Gal-3 is expressed in both human and murine dendritic cells, which act as the antigen-presenting cells of the innate immune system, by transferring information to the adaptive immune system. In a role which would have great effects on immune responses, Gal-3 is thought to suppress Th1 responses by reducing the levels of IL-12 released from Dendritic cells in

response to microbial challenge by *Toxoplasma gondii* (Bernardes *et al*., 2006). In terms of leukocyte recruitment, intracellular Gal-3 can increase the migratory profile of dendritic cells while accumulating in lipid rafts (Hsu *et al*., 2009b). Additionally, extracellular Gal-3 increased their adhesion to the endothelia, a property that correlated with the higher number of glycans on the surface of mature dendritic cells (Vray *et al*., 2004).

Gal-3 is lowly expressed in resting CD4 and CD8 positive T-cells, though is constitutively present in regulatory and memory T-cells and can be induced, for example, by T-cell receptor (TCR) ligation (Hsu *et al*., 2009a). The lectin is able to regulate T-cell activation and functions to maintain homeostasis, specifically by binding and self-oligomerising on N-glycans of the TCR thus restricting its lateral mobility and subsequent signal transduction (Demetriou *et al*., 2001). In terms of lymphocyte migration, Gal-3 did not increase their trafficking to murine air pouches and did not behave as a chemoattractant for these cells *in vitro* (Sano *et al*., 2000). However, it has been documented that Gal-3 promotes Th17 cell responses, especially in experimental autoimmune encephalomyelitis (EAE) models; Gal-$3^{-/-}$ mice displayed reduced demyelination and macrophage infiltration compared to wild type animals and *in vitro* Gal-3 was associated with increased IL-17 and IFNγ synthesis and reduced IL-10 production (Jiang *et al*., 2009). In a separate model investigating BSA antigen–induced arthritis, Gal-$3^{-/-}$ mice had significantly less joint erosion and cartilage damage; this was coupled to decreased IL-17-producing T-

cells in the spleen and reduced levels of sera TNFα and IL-6 in these animals compared to wild type controls (Forsman *et al*., 2011). The study also observed a partial phenotype recovery after administration of exogenous Gal-3, since this would predominantly affect the extracellular compartment it is likely that Gal-3 roles in arthritis involve the extracellular volume of this lectin.

Much research has been directed towards examining the effects of Gal-3 on lymphocyte proliferation and apoptosis as it is expressed in both T- and B-cells. Human leukaemia T-cells overexpressing Gal-3 display higher growth rates and resistance to apoptosis (Yang *et al*., 1996). In contrast, secreted extracellular Gal-3 signals T-cell apoptosis in murine and human cell lines; this was dependent on pre-existing cytoplasmic concentration of the lectin and the study proposed that CD7 and CD29 mediated this effect via cytochrome c and caspase-3 but not caspase-8 (Fukumori *et al*., 2003). Upon further investigation in T cells it has been found that intracellular Gal-3 is protective whereas actions of extracellular Gal-3 promote apoptosis in these cells (Nakahara *et al*., 2005). In B-cells, expression was increased in human B-cell lymphomas and in Gal-3$^{-/-}$ mice B-cells exhibited enhanced apoptosis (Acosta-Rodríguez *et al*., 2004, Hoyer *et al*., 2004). These data support the view that intracellular Gal-3 is protective and it is now thought that this is due to engaging intracellular apoptosis regulation pathways or by affecting mitochondrial homeostasis (Liu *et al*., 2002, Matarrese *et al*., 2000). In contrast,

extracellular Gal-3 induces apoptosis though the specific receptors and pathways involved have not been fully characterised.

1.7 Gal-3 roles and effects on endothelial cells

Gal-3 is expressed in endothelial cells and is localized predominantly at the cell membrane, along with surface ligands for the lectin (Sato *et al*., 2002). In HUVEC cells mRNA content confirmed Gal-3 expression, which was found to be almost exclusively present at the plasma membrane by flow cytometry. Immunohistochemical studies showed absence of Gal-3 expression in human liver endothelial cells whereas vessels of the kidney and placenta indicated low expression of the lectin. Gal-3 expression was unaltered after culture with 20% human serum though it has been reported that endothelial cells increase their expression on contact with tumour cells expressing specific carbohydrates on their surface (Thijssen *et al*., 2008). Gal-3 is proteolytically cleaved by matrix metalloproteinase-2 and this 27kDa fragment binds HUVEC with 20-fold higher affinity than the full-length 30kDa protein (Shekhar *et al*., 2004). In an *in vivo* model, upon *S. pneumoniae* infection murine alveolar vascular endothelial cells were thought to be among those increasing their Gal-3 expression (Sato *et al*., 2002) suggesting a role in leukocyte recruitment via the endothelia itself, which complements those which occur on the circulating leukocytes.

A recent paper examined whether Gal-3 could internalise to HUVEC and if so by which pathway; indeed, it was found that the lectin was endocytosed and then trafficked through one of two pathways. Gal-3 enters the cell upon ligand binding and reaches the early/recycling endosomes from where it is either recycled for exocytosis or targeted into

late endosomes or lysosomes (Gao *et al*., 2012). The authors suggest that these two pathways may be mediated by different receptors on the endothelial cell surface, which is in line with previous studies showing that HUVEC display high and low-affinity Gal-3 ligands (Nangia-Makker *et al*., 2000). These ligands were not identified and so far only a few others have been described, these include the main candidate integrin $\alpha v\beta 3$, integrin $\alpha 3\beta 1$, CD13 and VEGF-R2 (Markowska *et al*., 2010, Fukushi *et al*., 2004, Yang *et al*., 2007, Markowska *et al*., 2011).

Studies investigating the role of Gal-3 in angiogenesis have reported that soluble recombinant Gal-3 stimulates this process *in vitro* and *in vivo*, and that this may be due to its ability to induce locomotion of endothelial cells thus aiding the initial tube forming phase. This effect required the CRD of Gal-3, which bound at least two cell surface receptors on the endothelial cells before they significantly upregulated expression of integrin $\alpha v\beta 3$. Gal-3 can also modulate VEGF-mediated signalling through these integrins (Nangia-Makker *et al*., 2000, Markowska *et al*., 2010). Further investigation into vascular endothelial growth factor receptor-2 (VEGF-R2) induced angiogenesis showed that Gal-3 bound Mgat5-modified N-glycans on endothelial cell surface VEGF-R2, initiating its phosphorylation and retention at the membrane and promoting its pro-angiogenic function (Markowska *et al*., 2011).

Gal-3 has also been implicated in ischaemic injury repair. In the rat brain administration of Gal-3 neutralising antibodies diminished ischaemia-

induced angiogenesis and *in vitro* exogenous Gal-3 was shown to dose-dependently stimulate the proliferation of endothelial cells (Yan *et al*., 2009). Exogenous Gal-3 increased the number of angiogenic structures formed in a microglia-HUVEC co-culture model and this was associated with increased VEGF expression by BV2 microglial cells. The same study found extracellular Gal-3 increased the migratory profile of BV2 cells in scratch assays and Boyden-matrigel chambers. These effects were dependent on the serine/threonine kinase integrin-linked kinase (ILK), which acts via MAPK/ERK1/2 and PI3K/Akt pathways resulting in increased VEGF expression and subsequently, increased endothelial proliferation and migration (Wesley *et al*., 2013).

1.8 Possible mechanisms of Gal-3 action on leukocyte recruitment

There are many possible mechanisms of action of Gal-3 on inflammatory processes, especially leukocyte recruitment and it is probable that these operate in concert to exert its effects. One area of speculation is that of identifying Gal-3 ligands; studies using isolated human neutrophils and the HL-60 promyelocyte cell line have identified the CD66 proteins CD66a and CD66b as the major receptor candidates (Feuk-Lagerstedt *et al*., 1999). It was previously shown in neutrophils that receptors for Gal-3 must be mobilized to the cell surface from specific and gelatinase intracellular granules (Karlsson *et al*., 1998). Neutrophil granules were subsequently analysed by affinity chromatography and from this the CD66 proteins were identified as able to bind Gal-3. In addition to this, the subcellular localization of CD66 proteins are consistent with the proposed Gal-3 receptor distribution, as they are found in specific and gelatinase granules and are less well concentrated in the secretory vesicles or at the plasma membrane of unprimed cells (Feuk-Lagerstedt *et al*., 1999). It has since been reported that Gal-3 responsiveness is markedly increased upon gelatinase granule mobilisation; for example after LPS priming, which does not mobilise the specific granules, suggesting that it is these granules that store most Gal-3 binding partners (Almkvist *et al*., 2001).

The effects of binding to CD66 proteins have recently been under investigation. It was found that cross-linking of CD66b on peripheral

blood neutrophils mediates the release of IL-8 from intracellular stores (Schröder *et al*., 2006). IL-8 is known to be the major chemotactic factor for neutrophils, which suggests a mechanism for Gal-3 effects on neutrophil migration. Furthermore, the binding of both CD66a and CD66b can result in intracellular oxidative burst upon their cross-linking on the cell surface, a property that is often associated with Gal-3 binding (Jantscheff *et al*., 1996, Lund-Johansen *et al*., 1993). Finally, the cross-linking of antibodies binding to CD66b on neutrophils resulted in their increased adhesion to endothelial cells, a finding which may underlie the effects of Gal-3 on leukocyte recruitment (Skubitz *et al*., 1996). Further information on these molecules would provide interesting data for possible intracellular pathways of Gal-3, especially as signalling through CD66a and CD66b is known to differ.

Though Gal-3 may utilize many different pathways within leukocytes, it has been shown that in granulocytes, Gal-3-induced degranulation, phagocytosis and apoptotic rate is dependent on the p38 MAPK pathway (Fernández *et al*., 2005). This was demonstrated by p38 MAPK inhibition, which abrogated the effects of human recombinant Gal-3 as well as by analysis of p38 phosphorylation after incubation with human recombinant Gal-3. Interestingly, the major intracellular pathways of the MAPK family, ERK1/2, were unaffected by Gal-3. Additionally, it is possible that Gal-3 regulates levels of c-jun N-terminal kinase (JNK), another member of the MAPK family, which is an important regulator of apoptosis. However, JNK levels were found to differ only in mast cells of

Gal-3$^{-/-}$ mice, signalling that this is not a universal mechanism of action of the molecule (Liu *et al*., 2002). These data signal that Gal-3 may initiate some members of the MAPK family, which are known to respond to pro-inflammatory cytokines and alter gene expression, proliferation and apoptosis; though more information is needed to confirm specifically the pathways involved.

Gal-3 is one of a small number of molecules that have been proposed to act as soluble cell-cell and cell-cell matrix adhesion proteins and thus may have direct effects on leukocyte recruitment through this process. Sato *et al.* noted that the lectin mediates neutrophil adhesion to endothelia and that this is dependent on its self-oligomerization via its N-terminal domain; in addition, they noted that this effect was not due to the activation of any other adhesion molecule (Sato *et al*., 2002). Gal-3 oligomerization on the cell surface and the resultant receptor clustering has previously been linked to cell activation; it is now thought that this process can also lead to adhesion. Imaging studies have shown that Gal-3 clusters are concentrated at tricellular corners of the endothelium and adherent neutrophils, points of the vascular cell wall at which neutrophils are known to preferentially transmigrate (Nieminen *et al*., 2007), as discussed above. Similar observations have been found between eosinophils and breast carcinoma cells (Rao *et al*., 2007b). This mechanism of cross-linking has also been suggested for Gal-3 interactions with neutrophils and the extracellular cell matrix protein, laminin, where FITC-labelled Gal-3 was shown to aggregate on the

neutrophil cell surface (Kuwabara and Liu, 1996). Furthermore, binding studies suggest that Gal-3 mediates tight cell adhesion similar to that caused by the binding of β_2-integrins to their ligand ICAM-1 (Barboni *et al*., 1999). This is interesting as Gal-3 has been reported to have no effect on leukocyte recruitment in models where β_2-integrin-dependent migration is initiated, such as in *E. Coli* infection in the lungs and suggests that Gal-3 may be as important as the β_2-integrins in an equivalent role in another pathway. Thus, Gal-3 is involved in β_2-integrin-independent leukocyte migration by directly cross-linking leukocytes, endothelia and the extracellular matrix at specific points on the plasma membrane.

Previous work has also started to characterise the way in which Gal-3 may act as a chemoattractant for neutrophils, eosinophils, monocytes and macrophages. Work by Sano *et al.* established that Gal-3 most likely activates PTX-sensitive G-protein coupled receptors (GPCRs), suggesting that there is more than one type of receptor for Gal-3 and that they may be role- and cell type-specific. It is known that many chemoattractants and chemokines exert their effects via GPCRs and result in Ca^{2+} influx. However, there was no cross-reactivity between Gal-3 and other previously characterised chemokine receptors, suggesting that Gal-3 utilises an entirely new pathway. In addition to this, it was suggested that Gal-3 might activate different sets of receptors depending on its cell concentration as PTX inhibition varied in a Gal-3 concentration-dependent manner (Sano *et al*., 2000). Though this area

has been less well characterised, it will be important to establish the receptors involved in the lectin's role as a novel chemokine, as utilising this effect pharmacologically could prove to be very useful in modulating the inflammatory response.

These studies provide many answers to the question of Gal-3 mechanisms of action inside the cell; however, they undoubtedly raise many more questions that must be addressed. The prospect that Gal-3 receptors and the corresponding intracellular pathways may differ as a result of cell type, Gal-3 concentration and the effect exerted on the cell is an exciting one, as it suggests Gal-3 is a multi-faceted molecule which may be involved in many aspects of the immune response.

Gal-3 roles in leukocyte recruitment have been studied in *in vivo* models of inflammation, albeit using different tissues and inflammatory stimuli; the findings presented here are in keeping with published results, which are summarised in Table 1.1. Many investigations report reduced leukocyte infiltration of the affected tissue in Gal-$3^{-/-}$ mice; lower numbers of lymphocytes and eosinophils were recruited to OVA-challenged airways (Ge *et al*., 2010), there was reduced monocyte, macrophage and neutrophil recruitment to the CNS in a model of EAE (Jiang *et al*., 2009) and despite slightly conflicting reports using a thioglycollate broth model of peritonitis, two studies found reduced infiltration of neutrophils at either day 1 or 4 after insult (Hsu *et al*., 2000, Colnot *et al*., 1998). Farnworth *et*

al. found that Gal-3$^{-/-}$ mice exhibited more severe lung injury associated with reduced neutrophil recruitment at 15 h after *S. pneumoniae* infection, which is β_2-integrin-independent (Farnworth *et al*., 2008). This reduction in extravasated neutrophils at 12-24 h was also reported by Nieminen *et al.,* who found that recruitment was unaffected in β_2-integrin-dependent *E. Coli*-driven lung infection in Gal-3$^{-/-}$ animals (Nieminen *et al*., 2008). This is in slight contrast to the reduction in rolling velocity in Gal-3$^{-/-}$ mice presented here as slow rolling in TNFα-treated cremaster venules is dependent on β_2-integrins; since leukocyte velocities in CD18$^{-/-}$ mice treated with TNFα were approximately 3-fold higher than those in wild type mice (Jung *et al*., 1998). However, as these findings have been reported when investigating different vascular beds and responses to varied stimuli, they would involve different phenotypes such as adhesion molecule profiles and ultimately, distinct outcomes (Rao *et al*., 2007a). Indeed, taken together these investigations further suggest that Gal-3 is a multi-faceted molecule capable of interacting with and acting *via* different receptors in different cells and tissues.

1.9 Hypothesis and aims of this PhD studentship

As previously described with respect to different cell types, the involvement of Gal-3 in leukocyte trafficking during inflammation has been investigated using diverse *in vivo* models, which are summarised in Table 1.1. Reduced leukocyte infiltration to the area of insult was noted in models of *S. pneumoniae* infection (Farnworth et al., 2008), allergic airway inflammation (Ge et al., 2010), EAE (Jiang et al., 2009) and sterile peritonitis (Hsu et al., 2000, Colnot et al., 1998). This is in addition to work showing that treatment with the recombinant lectin increased neutrophil, monocyte and eosinophil but not lymphocyte recruitment to the murine air pouch, a useful *in vivo* model for looking at end-point cell numbers (Sano et al., 2000). In spite of what is already known, so far Gal-3 roles and effects on specific aspects of the leukocyte recruitment cascade *in vivo* and *in real time* have not been reported.

Thus the overarching hypothesis for this thesis is that *Gal-3 is a positive regulator of leukocyte, in particular neutrophil and monocyte recruitment in vivo*. In addition to investigating this and due to its localisation both within and outside the cell, both endogenous Gal-3 roles in leukocyte recruitment as well as exogenous Gal-3 effects on this inflammatory process were examined.

1.9.1 Aims

There are three separate aims of this studentship, these are:

1. Study the leukocyte and endothelium interactive events in post-capillary venules of Gal-3$^{-/-}$ mice.

The use of intravital microscopy to visualize in real time the vascular system and in particular, leukocyte recruitment will provide detailed information on this process. It will be important to first characterise responses of the leukocyte subsets to various inflammatory stimuli in wild type mice, before examining the same response in those that are null for Gal-3. This will be carried out using a fixed-time protocol where sham, IL-1β or TNF-α intrascrotal injections will be given 2 or 4h before IVM. Parameters such as leukocyte rolling velocity, rolling flux as well as the number of adherent and emigrated cells will be measured.

Concurrently, it will be important to confirm the genotype of the mice from the Gal-3$^{-/-}$ colony on a regular basis. Samples will undergo DNA extraction, PCR and subsequent gel analysis to confirm that they are null for Gal-3.

2. To determine the pharmacological effects of Gal-3.

The effect of exogenous Gal-3 can then be investigated by examining the pharmacological effects of Gal-3 itself; in the first case recombinant Gal-3 will be administered intrascrotally to examine its possible positive effects on recruitment. Any responses to the lectin can then be further

characterised *in vitro* with the use of flow cytometry, real-time PCR and the parallel plate flow chamber assay.

3. To pinpoint any effects of exogenous Gal-3 or defects caused by the lack of endogenous Gal-3 in relation to leukocyte sub-type.

Traditional bright-field microscopy methods cannot provide accurate information on the specific leukocyte subsets that may migrate in different environments; depending on previous results, the use of fluorescent dyes with intravital or static microscopy will enable Gal-3 roles and effects to be investigated further.

Table 1.1 Gal-3 in experimental models of inflammation

Model/Species	Inflammogen & Treatment	Result	Reference
Streptococcal pneumonia	Innoculum of *S. pneumoniae* or *E. coli* i.n.. rGal-3 i.n. immediate pre-treatment.	Reduced neutrophils but not macrophages in the alveoli of Gal-3$^{-/-}$ mice 24h but not 6h or 48h after infection. Levels of neutrophil extravasation were restored in Gal-3$^{-/-}$ mice treated with Gal-3 alongside *S. pneumoniae*. Responses absent in mice infected with *E. coli*.	Nieminen *et al.,* 2008
Streptococcal pneumonia	Innoculum of *S. pneumoniae* in PBS i.t., mice sacrificed at 15h. Recombinant Gal-3 (5μg) i.t. at time of inoculation.	Gal-3$^{-/-}$ mice exhibited more severe lung injury, septicaemia and a higher bacterial load alongside reduced neutrophil recruitment. Exogenous Gal-3 administration to Gal-3$^{-/-}$ animals reduced lung injury.	Farnworth *et al.,* 2008
Streptococcal pneumonia	Innoculum of *S. pneumoniae* or *E. coli* i.n., mice sacrificed up to 3 days after infection.	Accumulation of soluble Gal-3 in BALF correlated with neutrophil onset to the alveoli; emigrated neutrophils exhibited surface-bound Gal-3. Correlation absent in mice infected with *E. coli*.	Sato *et al.,* 2002
Peritonitis	Thioglycollate broth (1mL) i.p., mice sacrificed at 18h, day 2, day 3 or day 4.	Gal-3$^{-/-}$ mice displayed reduced granulocytes but not macrophages or lymphocytes in the peritoneal cavity 4 days after injection but not at earlier time-points.	Colnot *et al.,* 1998

(Continued)

Peritonitis	Thioglycollate broth (1mL) i.p., mice sacrificed at days 1-6.	Gal-3$^{-/-}$ mice displayed reduced total infiltrating leukocytes at days 1, 3 and 6 (not at days 2 and 4). Infiltrating neutrophils and macrophages were reduced in Gal-3$^{-/-}$ mice at day 1 (not at later time-points). Infiltrating lymphocytes were reduced in Gal-3$^{-/-}$ mice at days 2 and 4. Gal-3$^{-/-}$ leukocytes exhibited weaker NF-κB responses.	Hsu *et al.,* 2000
Chronic allergic airway inflammation	Mice sensitised with 50μg OVA/Al(OH)$_3$ s.c. on days 0, 7, 14, 21. Challenged with OVA (20μg) i.n. on days 23, 25, 28 then biweekly for 8 weeks. Mice sacrificed 24hr after final challenge.	Increased levels of Gal-3 found in OVA-challenged WT mice. Gal-3$^{-/-}$ mice exhibit reduced leukocyte airway infiltration and airway remodelling. Specifically reduced eosinophils and lymphocytes but not monocytes, macrophages and neutrophils.	Ge *et al.,* 2010
Experimental autoimmune encephalomyelitis (EAE)	Mice immunised s.c. with MOG$_{35-55}$/CFA. Pertussis toxin i.p. on days 0 and 2 after immunisation.	Gal-3$^{-/-}$ mice displayed attenuated EAE and reduced leukocyte infiltration of the CNS at day 18. Specifically, Gal-3$^{-/-}$ mice displayed reduced monocyte, macrophage and neutrophil but not T-cell recruitment.	Jiang *et al.,* 2009
Allergen-induced arthritis (AIA)	mBSA/CFA s.c. on day 0 and 7, mBSA i.a. in knee on day 21; mice sacrificed on day 28. Gal-3 (1.3μg/g body weight) i.p. on days 0, 3, 21 and 24.	Decreased AIA severity in Gal-3$^{-/-}$ mice, restored by the addition of exogenous Gal-3. At early stages of AIA (day 10) Gal-3$^{-/-}$ mice exhibited reduced levels of circulating TNFα and IL-6.	Forsman *et al.,* 2011

1.10 Publications

1.10.1 Related to this thesis

Investigating novel roles for exogenous galectin-3 in controlling vascular inflammation. [Manuscript in preparation]

1.10.2 Contribution to other publications during this PhD

Fu H., Kishore M., Gittens BR., Wang G., Komarowska I., Infante E., Ridley AJ, Cooper D., Perretti M. & Marelli-Berg FM. Self-recognition of the endothelium enables regulatory T-cell trafficking and defines the kinetics of immune regulation. Nat Commun (2014) [Corrections].

Gittens, BR., Wright, RD. & Cooper, D. Methods for assessing the effect of galectins on leukocyte trafficking. Methods Mol Biol (2013) [Ahead of print].

Iqbal AJ, Cooper D, Vugler A, Gittens BR, Moore A, Perretti M. Endogenous Galectin-1 Exerts Tonic Inhibition on Experimental Arthritis. J Immunol 191:171-7 (2013).

Rodriguez-Grande B, Blackabey V, Gittens B, Pinteaux E, Denes A. Loss of substance P and inflammation precede delayed neurodegeneration in the substantia nigra after cerebral ischaemia. Brain Behav Immun, 29: 51-61 (2013).

Cooper, D., Iqbal, A.J., Gittens, B.R., Cervone, C. & Perretti, M. The effect of galectins on leukocyte trafficking in inflammation: sweet or sour? Ann N Y Acad Sci 1253, 181-192 (2012).

Chapter 2: Materials and Methods

2.1 Animals

Breeding founders for the Gal-3$^{-/-}$ mouse colony were obtained from the Consortium for Functional Glycomics on a C57BL/6 background and a colony was established at Charles River UK. Male mice bearing green fluorescent protein (GFP) under their CX_3CR1 promoter were kindly donated by Prof. S. Nourshargh (QMUL, London). In all experiments age and sex-matched controls [wild type (WT) C57BL/6] were also purchased from Charles River UK. All animals were fed standard laboratory chow and water *ad libitim* and were housed in a 12h light-dark cycle under specific pathogen-free conditions. All experiments were performed with mice (20-28g), strictly following UK Home Office regulations (Guidance on the Operation of Animals, Scientific Procedures Act, 1986).

2.2 Intravital microscopy of the murine cremaster muscle

2.2.1 Exteriorisation of the murine cremaster muscle

Intravital microscopy (IVM) of the cremaster muscle was used to visualise leukocyte recruitment in real time. Male mice from wild type C57BL/6, monocyte GFP or Gal-3$^{-/-}$ strains were anaesthetised using a mixture of xylazine (7.5 mg/kg; Rompun) and ketamine (150 mg/kg; Narketan) made up in sterile dH_2O and mixed before intraperitoneal (i.p.) injection. Once anaesthetised, the mice were placed onto the viewing stage, which comprised a raised Perspex cylinder covered with a permanently attached glass coverslip. The raised cylinder also served as a small reservoir for warm bicarbonate buffered solution (BBS: 132nM sodium chloride (Sigma), 5mM Potassium Chloride (Sigma), 2mM Calcium

Chloride (AnalaR), 1mM Magnesium Sulphate (Sigma) and 20mM Sodium Hydrogen Carbonate (AnalaR), pH 7.4) to prevent the tissue from drying out, excess buffer was then drained away by attachment of the stage to vacuum suction. The BBS was used to wet the tissue throughout surgery and consequently was held at 37°C. Throughout the surgery, extreme care was taken to avoid agitating the cremaster muscle by touching the underlying tissue with any of the instruments used.

The skin and fascia covering the ventral aspect of the right scrotum was removed, exposing an area extending from the inguinal fold and to the distal end of the scrotum. Any remaining fascia was separated from the cremaster muscle using forceps and vannas scissors. Once the cremaster was cleared of fatty deposits the mouse was moved into position on a heat pack with the cremaster resting on the glass coverslip of the viewing stage (Figure 2.1A). A suture (BV1; Ethicon) was threaded through the distal point of the cremaster sack to secure and slightly extend the tissue. A cauteriser was used to score a line down the centre of the cremaster and also two lengths at the top edge of the muscle, forming a T-section (Figure 2.1B). Vannas scissors were then used to cut over the T-section and the cremaster was spread flat over the glass coverslip, four hooks were used to secure the cremaster in place (Figure 2.1C). The cauteriser was used to separate the vessel connecting the cremaster and the testicle, which was then separated from the cremaster using vannas scissors and secured out of the way of the viewing area (Figure 2.1D). The viewing stage was then moved to one of two

microscope set-ups with water immersion lenses to allow for continuous superfusion with BBS. Immediately before recording, the mice underwent a 30min stabilisation period which is critical for reducing the impact of the surgery itself on the leukocyte recruitment seen; for example, surgery quickly increases P-selectin expression thus affecting initial fast rolling of the leukocytes (Ley *et al*., 1995).

Brightfield recordings were carried out using a Zeiss Axioskop FS microscope with *a x*40 objective (Carl Zeiss Ltd) which was illuminated with a 12V, 100W halogen light source. An Optical Doppler Velocimeter (Microvascular Research Institute, Teas A&M University) was used to measure centerline red blood cell velocity and a video time-date generator (FOR-A company Ltd) sealed the date and stopwatch function onto the recordings. Fluorescence microscopy was carried out using an Olympus BX61W1 microscope with a x40 water immersion objective (Carl Zeiss Ltd.) connected to an Olympus BXUCB lamp, Uniblitz VCMD1 shutter driver and DG4-700 shutter instrument. The setup also used an Optical Doppler Velocimeter and a Hamamatsu C9300 digital camera with a Videoscope VS4-1845 image intensifier attached. All videos were captured using Slidebook 5.0 software from Intelligent Imaging TTL.

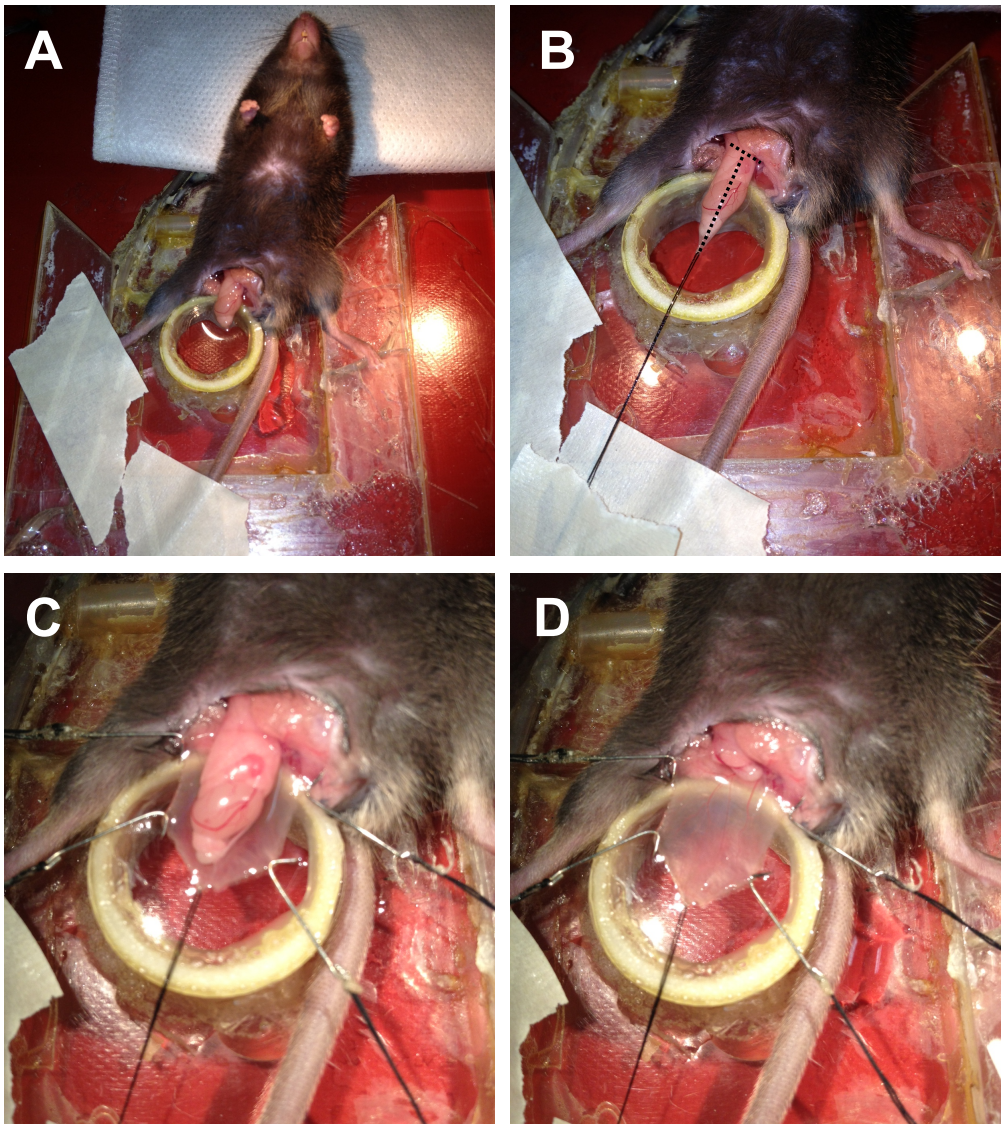

Figure 2.1 Preparation of the murine cremaster muscle for intravital microscopy
A) The skin and fascia covering the ventral aspect of the right scrotum is removed and the cremaster cleared of fatty deposits before the mouse is moved into position with the cremaster resting on the glass coverslip of the viewing stage and supported by a heat pack. **B**) A suture is threaded through the distal point of the cremaster sack and secured to slightly extend the tissue. The cauteriser is used to score a T-section down the centre of the cremaster (dotted line). **C**) The T-section is cut and the cremaster spread flat over the glass coverslip, four hooks are used to secure the cremaster in place. **D**) The testicle is then separated from the cremaster and secured out of the way of the viewing area.

Post-capillary venules with a diameter of 20-40μm, an adequate centerline velocity (≥500S^{-1}) and no branches within 100μm either side of the segment to be analysed were chosen. Vessel segments of 100μm in 3-5 vessels per mouse and of 3-5 mice per group were recorded for offline analysis. The analysis parameters are shown in Figure 2.2. Rolling flux was recorded as the number of leukocytes rolling past a specific point, averaged over 5 min. Rolling velocity was determined from the time taken for the leukocytes to travel 100μm. Adherent cells were those that were stationary on the vessel wall for more than 30 sec. Transmigrated cells were those found in the tissue 50μm by 100μm on either side of the vessel.

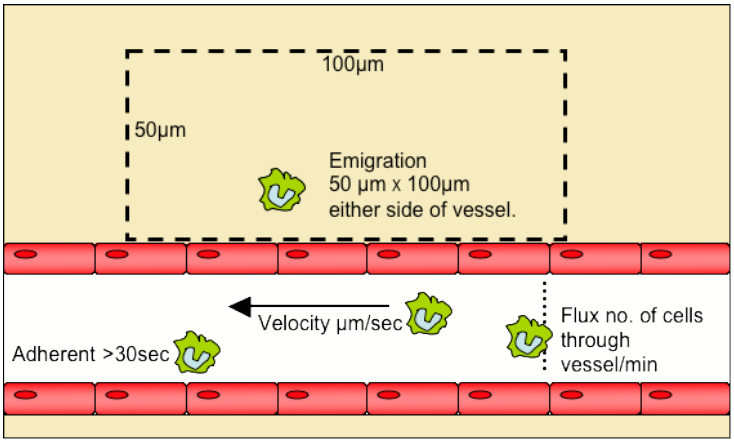

Figure 2.2 Analysis parameters of intravital microscopy

2.2.2 Cytokine-induced inflammation

To assess inflammation in the cremaster muscle, mice were-treated with an intrascrotal (i.s.) injection of PBS (sham), IL-1β (30ng), murine TNF-α (300ng; Gibco) and/or Gal-3 (200-1000ng) in a final volume of 400μl.

The injection was carried out 2 or 4h before the vessel was recorded, allowing time for the 30min stabilization period after the surgery had been completed, as shown in Figure 2.3. In order to perform the i.s. injection, mice were briefly anaesthetised with inhaled Isofluorane gas (approximately 5%: Baxter) and the scrotum gently extended to allow for a large injection site.

In addition to the i.s. injection, some animals also underwent a tail-vein intravenous (i.v.) injection of fluorescent antibody, rat anti-mouse Ly-6G (clone 1A8, 2μg; BD Pharmingen) in 200μL saline. This was administered approximately 15 min before the i.s. injection so that all circulating neutrophils were labelled before possible emigration into the cremaster muscle. The mice were heated in an incubated chamber set to 32°C until the tail vein was visible through the skin, typically for 10min, they were then transferred to a restrainer; the tail was exposed and pinched near the body to allow the tail vein to become prominent. The needle was inserted with the bevel facing upwards and the antibody solution administered carefully before the animal was replaced to its cage. Once recording, it was important to be careful not to expose the cremaster to excessive fluorescent excitation as the fluorophore faded quickly.

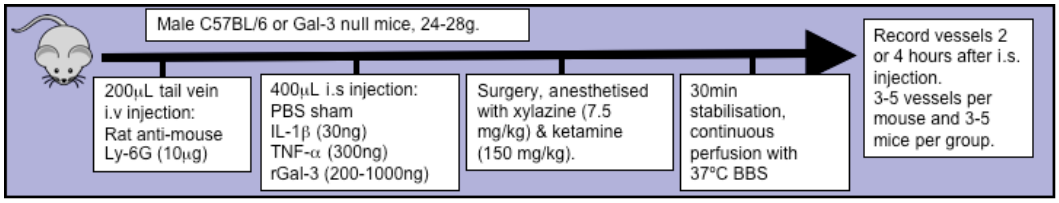

Figure 2.3 Protocol for analysis of inflammation in the cremaster muscle

2.2.3 Intravenous administration of recombinant Gal-3

To assess rGal-3 effects on circulating leukocytes prior to cremaster exteriorisation, the external jugular vein was exteriorised and cannulated with microtubing (Size 8.0) connected to a saline-filled syringe. Briefly, the skin covering the left submaxillary gland was removed and the salivary gland dissected away to allow access to the vein. The surrounding fascia was cleared and two sutures put in place, the upper suture was tied and an incision made before guiding the cannula into the vein and tying off the lower suture to hold it in place. Once the mouse was on the stage and a baseline recording had been made, 150ng rGal-3 or vehicle in 200μL saline was injected intravenously and subsequent recordings of cremaster post-capillary venules made at 10 min intervals for up to one hour.

2.3 *Ex vivo* confocal imaging of the murine cremaster muscle

Cremasters from $CX_3CR1^{gfp/+}$ mice treated intrascrotally for 4h with sham PBS or rGal-3 (1000ng, section 2.2.2) were exteriorised (section 2.5.1), spread flat onto wax sheets and then pinned in place using hooks made

from shortened 19.5G needles. The cremasters were then dissected away from the mouse and placed into a 5mL bijou container of 4% PFA in PBS for 10 min on ice before being washed twice in the same volume of PBS. Permeabilisation and blocking buffer was prepared as PBS containing 12.5% each of fetal bovine serum (FBS; Sigma) and normal goat serum (NGS; Sigma) and 0.5% Triton-X-100 (Sigma). The cremasters were removed from the wax, gently blotted on tissue then transferred to a 1.5mL microcentrifuge tube containing 500μL permeabilisation and blocking buffer and were incubated on a rotating wheel for 2h at room temperature. Primary antibodies against VE-Cadherin (Alexa Fluor® 555 conjugated, 1μL; donated by Prof. Nourshargh, QMUL) and MRP14 (Alexa Fluor® 647 conjugated, 0.5μL; donated by Prof. Nourshargh, QMUL) were diluted into PBS containing 5% each NGS and FBS; the cremasters were incubated in 200μL overnight at 4°C. The cremasters were then washed three times in 1mL PBS for 30 min each time on a rotating wheel before longer storage in PBS at 4°C. A coverslip was used to flatten the cremasters onto a microscopy slide and the vessels viewed using a Leica SP5 confocal microscope.

In addition to the above protocol, cremasters from wild type C57BL/6 mice treated intrascrotally for 4h with sham PBS, rGal-3 (1μg), rGal-3 plus lactose (1μg plus 30mM) or rTNFα (300ng) were collected and blocked/permeabilsed as above. The cremasters were then stained in TBS containing 1% FBS with either rat ant-mouse E-selectin (Clone

10E9.6, 5μg/mL; BD Pharmingen) or rat anti-mouse PECAM-1 (Clone MEC 13.3, 5μg/mL; BD Pharmingen) for 1h at room temperature followed by 3 brief washes in TBS-FBS. The cremasters were then incubated with the secondary antibody Alexa Fluor® 488 Donkey Anti-Rat IgG (4μg/mL in TBS-FBS, Invitrogen) for 30 min at room temperature in the dark before another 3 washes as before. The cremasters were subsequently stained again in TBS-FBS with either PE-conjugated rat anti-mouse ICAM-1 (clone YN1/1.7.4, 1μg/mL; eBioscience) or PE-conjugated PE-conjugated rat anti-mouse VCAM-1 (429 (clone MVCAM.A), 1μg/mL; BD Pharmingen) for 30 min at room temperature in the dark before another 3 washes as before. Control cremasters were stained with secondary anti-Rat IgG only or the isotype controls PE-conjugated IgG2a (clone eBR2a, 1μg/mL; eBiosciences) or PE-conjugated IgG2b k (1μg/mL; eBioscience), alongside the test cremasters. Finally, they were mounted on microscopy slides with 4',6-diamidino-2-phenylindole (DAPI) mounting medium (Vectasheild) and imaging using the Zeiss LSM 510 (Mark 4) Laser Scanning Confocal Microscope.

2.4 Murine endothelial cell culture

2.4.1 Immortalised murine cardiac endothelial cells (MCECs)

MCECs (donated by Dr Egle Solito, QMUL, London) were cultured on tissue culture plasticware in Dulbecco's modified Eagle's medium (DMEM; Gibco) with 5% fetal calf serum (FCS; Sigma), penicillin (100U/mL; Sigma), streptomycin (100μg/mL; Sigma) and HEPES (4-(2-hydroxyethyl)-1-piperazineethanesulfonic acid) buffer (10μM; Sigma).

Cells were stored in a humidified chamber with 5% CO2 at 37°C and passaged once they reached 95% confluence.

2.4.2 Primary murine lung endothelial cells (MLECs)

MLECs were isolated from the lungs of wild type or Gal-3$^{-/-}$ mice (Reynolds *et al*., 2004). Tissue culture flasks and plates were coated with 10mL 0.1% Gelatin in PBS containing bovine collagen (30μg/mL, 97% Type I 3% type III; Nutacon) and bovine plasma fibronectin (10μg/mL; Sigma) for a minimum of 2h at 37°C. Care was taken to aspirate all remaining solution, as collagen solution is highly acidic. MLEC media was prepared using equal parts low glucose DMEM and Ham's F12 (Gibco) before adding heparin (100μg/mL; Sigma), penicillin (100U/mL), streptomycin (100μg/mL) and L-Glutamine (2mM; Sigma) and filter sterilising using a 0.4μm disposable filter (Nalgene). Finally, endothelial cell growth supplement (25μg; AbD Serotech) and 100mL FCS was added. Cells were stored in a humidified chamber with 5% CO2 at 37°C and passaged once they reached 95% confluence.

2.4.3 MLEC isolation

Lungs from three mice were collected for each genotype; mice were euthanised by cervical dislocation before being transferred to a sterile cell culture hood and sprayed with 70% EtOH (Sigma). Being careful to avoid the peritoneal cavity, the lungs were excised and placed in Ham's F12 media (Gibco) on ice. Connective tissue, fat and blood clots were removed from the lungs, which were briefly rinsed in 70% EtOH, followed

by MLEC media and then chopped into small pieces using two scalpel blades. Tissue was further digested in 10mL 1mg/mL collagenase Type I-S for 2h at 37°C in a rocking waterbath. The digest was diluted in 10mL MLEC media and passed through a 19.5G needle five times followed by a 70μm cell-strainer (BD Falcon). The cell suspension was centrifuged at 3000 *g* for 5min and resuspended in 15mL MLEC media before transfer to pre-coated T75 flasks.

Endothelial cells were first purified by removal of contaminating macrophages using magnetic Dynabeads (Dynal Biotech). The flasks were removed from the incubator and the media replaced with fresh MLEC media before being stored at 4°C for 20min. The MLEC media was replaced with primary antibody solution, purified rat anti-mouse CD16/32 (5μg/3mL; BD Biosciences) diluted in PBS and incubated at 4°C for 30min with occasional swirling to ensure even coating of the antibody. The antibody solution was removed and the cells washed gently with PBS before the secondary antibody-conjugated dynabeads were added. Flasks were incubated with PBS containing approximately $4x10^6$ sheep anti-rat IgG magnetic dynabeads (10μL/3mL) for 30min at 4°C, with occasional swirling. The solution was aspirated and the cells were washed three times with PBS before checking that the beads had attached to the macrophages. Cells were trypsinised with 1x Trypsin (Sigma) and MLEC media was added to stop the reaction, the cell suspension was then transferred to a 15mL falcon and placed in a magnetic holder (Invitrogen). The cells were allowed to attach to the side

of the falcon for 5min before the medium was carefully pipetted off and transferred to a new culture flask. The cells were cultured until colonies of approximately 20 endothelial cells could be seen.

The culture was then purified further by positive selection for the endothelial cells using ICAM-2/CD102 [Clone 3C4(mIC2/4); BD Pharmingen] as a cell marker. The flasks were removed from the incubator and the media replaced with fresh MLEC media before being stored at 4°C for 20min. The MLEC media was replaced with primary antibody solution, purified rat anti-mouse CD102 (10μg/3mL) diluted in PBS and incubated at 4°C for 30min with occasional swirling to ensure even coating of the antibody. The antibody solution was removed and the cells washed gently with PBS before the secondary antibody-conjugated dynabeads were added. Flasks were incubated with PBS containing approximately $4x10^6$ sheep anti-rat IgG magnetic dynabeads (10μL/3mL) for 30min at 4°C, with occasional swirling. The cells were checked to ensure that the beads had attached to the endothelial cells before the bead solution was aspirated and the cells washed three times with PBS. Cells were trypsinised with 1x Trypsin (Sigma) and MLEC media was added to stop the reaction: the cell suspension was then transferred to a 15mL falcon and placed in the magnetic holder. The cells were allowed to attach to the side of the falcon for 5min before the medium was carefully pipetted off and discarded. 10mL MLEC media was used to resuspend the cells, which were then cultured until they

reached 50% confluence, at which point the positive sort was repeated to enhance the culture.

2.5 Flow cytometric analysis of vascular endothelial cells

Flow cytometry was used to analyse cellular expression of Gal-3 as well as various proteins of interest found intra- or extracellularly. Flow cytometry is a valuable tool based on the principle that light will either be absorbed or scattered when it is directed at an object. In this case, cell suspensions are aspirated through a narrow chamber, which allows for only one cell to pass through at any one time. The cells are illuminated by lasers emitting light of varying wavelengths, which may excite fluorochromes present on the surface or within the cell. These fluorochromes may be naturally occurring (autofluorescence) or attached to the cell by the addition of fluorochrome-labelled antibodies. The subsequent light scatter is assessed from different angles of viewpoint; the forward scattered light (FSC) at small angles (0.5-5°) and the side scattered light (SSC) at larger angles (15-150°). The FSC is a measure of the size of the cell or particle to pass through the light whilst the SSC is a measure of the internal granularity of the cell; in some cases these measurements alone are enough to distinguish between different cell types in the sample. FSC and SSC can also be plotted against the amount of fluorescence emitted from the cells due to binding of one or more fluorochromes linked to cell surface or intracellular antigens, thousands of which are available today. Antibodies conjugated to Phycoerythrin (PE) were analysed in the yellow FL2 channel, those

conjugated to fluorescein isothiocyanate (FITC) or Alexa Fluor® 488 were analysed in the green FL1 channel and those conjugated to Allophycocyanin (APC) were analysed in the red FL4 channel.

2.5.1 Flow cytometry using HUVEC

HUVEC were grown to confluence in gelatin-coated 6-well plates and were-treated with cytokines as described in section 2.1.2. Once ready for staining, the cells were detached using trypsin (Sigma) or Accutase solution (Millipore) and plated in a 96-well plate at a density of approximately $2x10^5$ cells per well. Cells were washed by centrifuging at 350 *g* for 30sec followed by resuspension in PBS containing bovine serum albumin (0.02% PBS-BSA; Sigma). Cells were then incubated with primary antibodies in the presence of human blocking IgG (16mg/mL) for 45min on ice in the dark. Antibodies were used as follows: PE-conjugated rat anti-human Gal-3 (clone M3/83, 8μg/mL; eBiosciences), PE-conjugated rat anti-human IgG2a isotype control (clone eBR2a, 8μg/mL; eBiosciences), FITC-conjugated mouse anti-human VCAM-1 (clone 1.G11B1, 2μg/mL; AbD Serotech), FITC-conjugated mouse anti-human IgG1 (2μg/mL; AbD Serotech), PE-conjugated rat anti-human ICAM-1 (clone HA58, 0.25μg/test; eBiosciences), PE-conjugated rat anti-human IgG1κ (0.25μg/test; eBiosciences).

Cells were washed twice with PBS-BSA and those stained for cell surface antigens only were transferred to flow cytometry tubes. Wells stained for

intracellular antigens were fixed using 1X fixation buffer (eBioscience) for 20min in the dark at room temperature followed by addition of 1X permeabilisation buffer (eBioscience). Cells were washed twice in 1X permeabilisation buffer before incubation with primary antibodies at the same concentration as for the cell surface stains. The cells were washed twice more in permeabilisation buffer before a final wash in PBS-BSA and transfer to flow cytometry tubes. The samples were fixed in 2% paraformaldehyde (w/v; Sigma) in PBS-BSA and stored until analysis using the FACSCalibur Flow Cytometer (BD Biosciences) and data acquisition using Cell Quest software (BD Biosciences). Unstained and isotype control wells were used for calibration. Fluorescence was expressed as median fluorescence intensity (MFI) units in the relevant fluorescence channel for each fluorochrome.

2.5.2 Murine endothelial cell adhesion molecule expression

WT and Gal-3$^{-/-}$ MLEC or MCEC cells were treated for 4 hours or overnight with PBS (sham), murine IL-1β (1-100ng/mL), murine TNF-α (10-200ng/mL; Gibco) or rGal-3 (200-1000ng/mL); supernatants were collected for analysis by ELISA and cells were detached using Accutase. Cells were plated into a 96-well plate at a density of approximately 2x10^5 cells per well and were washed twice with PBS-BSA by centrifuging at 350 *g* for 30sec before 10 min pre-incubation with murine Fc Block (0.5μg/mL; eBiosciences) on ice. The following rat anti-mouse primary antibodies were added directly to the cells with Fc Block and incubated for 45min on ice in the dark: PE-conjugated Gal-3 (clone M3/83, 8μg/mL;

eBiosciences), PE-conjugated IgG2a isotype control (clone eBR2a, 8μg/mL; eBiosciences), PE-conjugated PECAM-1 (CD31 clone MEC 13.3, 4μg/mL; BD Pharmingen), PE-conjugated ICAM-1 (CD54 clone YN1/1.7.4, 2μg/mL; eBioscience), PE-conjugated IgG2bκ (2μg/mL; eBioscience), FITC-conjugated ICAM-2 (CD102 clone 3C4, 10μg/mL; BD Pharmingen), purified E-selectin (CD62E clone 10E9.6, 5μg/mL; BD Pharmingen). Cells to be surface stained only were washed twice in PBS-BSA and either transferred to flow cytometry tubes in 2% PFA or incubated with secondary antibody FITC-conjugated F(ab')2 rabbit anti-rat IgG (1:200; AbD Serotech) for 30min on ice in the dark. Those cells were washed twice more before transfer to flow cytometry tubes in 2% PFA. Cells stained for intracellular antigens were fixed for 10 min at room temperature and permeabilised (eBioscience) before subsequent staining as for cell surface antigens, with the exception that antibodies and washes were carried out in 1x permeabilisation buffer. Samples were analysed on the FACSCalibur using the FL1 and FL2 channels.

2.5.3 Murine endothelial cell surface lectin binding assay

A validated panel of lectins was chosen to assess cell surface glycosylation patterns on WT and Gal-3$^{-/-}$ MLEC, which were treated and then plated as in section 2.7.4. The cells were incubated with the following biotinylated lectins in lectin buffer (dH_2O containing 0.26% HEPES sodium salt and 0.88% NaCl) for 45 min at room temperature: *Helix pomatia* agglutinin (HPA; 20μg/mL; Sigma), *Sambucus nigra* lectin (SNA; 166ng/mL), Peanut agglutinin (PNA; 20μg/mL), *Maackia*

amurensis lectin II (MAL II; 3.3μg/mL) and *Lycopersicon esculentum* lectin (LEL; 400ng/mL) (all Vector Labs). The cells were washed twice in lectin buffer followed by incubation for 30 min at room temperature with a streptavidin PE-conjugated secondary antibody (120ng/mL in PBS-BSA; Invitrogen) before a final two washes in PBS-BSA and transfer to flow cytometry tubes in 2% PFA for analysis on the FACSCalibur using the FL1 channel.

2.6 Flow cytometry using murine whole blood

2.6.1 Collection of murine blood by cardiac puncture

Gal-3$^{-/-}$ or WT mice were deeply anaesthetised and up to 900μL of blood was collected by cardiac puncture into heparin-coated syringes (100μL of 100U/mL). Once complete, the blood was carefully expelled into a microcentrifuge tube and inverted twice to mix. The mice were then euthanised by cervical dislocation. Leukocytes were stained with Turk's solution (0.01% crystal violet in 3% acetic acid) with a dilution factor of 20 (25μL blood with 475μL Turk's solution). Differential counts were performed using a Neubauer haemocytometer viewed under a light microscope.

2.6.2 Antibody staining of white blood cells

Murine whole blood was treated for 15min at 37°C with PBS (Sham), murine IL-1β (1-100ng/mL) or murine TNF-α (10-200ng/mL; Gibco) before centrifuging at 300 *g* for 5 min and aspiration of the supernatant. Cells were resuspended in murine FC Block (0.5μg/mL; eBiosciences)

and incubated for 10min on ice. The following rat anti-mouse primary antibodies were added directly to the wells and incubated for 45min on ice in the dark: PE-conjugated Gal-3 (clone M3/83, 8μg/mL; eBiosciences), PE-conjugated IgG2a isotype control (clone eBR2a, 8μg/mL; eBiosciences), FITC-conjugated Ly-6G (clone 1A8, 5μg/mL; BD Pharmingen), PE-conjugated CD11b (clone M1/70, 2μg/mL; eBioscience), PE-conjugated IgG2b k (2μg/mL; eBioscience), APC-conjugated L-selectin (CD62L) (clone MEL-14, 1μg/mL; eBioscience), APC-conjugated IgG2a κ (1μg/mL; eBioscience), Alexa Fluor® 488 Ly-6C (clone HK1.4, 2.5μg/mL; BioLegend). The blood was washed twice in PBS-BSA before the addition of lysis buffer. Multi species 10x red blood cell lysis buffer (eBioscience) was brought to room temperature before dilution in dH_2O and addition of 250μL per well with gentle pipetting to mix, followed by incubation for 10 min until the suspension had lost turbidity. The plate was washed twice in PBS-BSA before samples were transferred to flow cytometry tubes in 2% PFA and analysed on a FACSCalibur using the FL1, FL2 and FL4 channels.

2.6.3 Lectin binding assay on murine leukocytes

Approximately 1mL murine whole blood was collected as in section 2.8.1 and immediately underwent red cell lysis in 10mL 1x multi species red cell lysis buffer for 10 min. The cells were centrifuged at 300 *g* for 5mins then resuspended in 1mL lysis buffer for a further 5 min before two washes in PBS-BSA and transfer to 96-well plate for staining. They were incubated with 25μL lectin buffer containing FC Block (0.5μg/mL) for 10

min before the addition of the following antibodies and biotinylated lectins in lectin buffer for 45 min at room temperature: FITC-conjugated Ly-6G (clone 1A8, 5μg/mL), Alexa Fluor® 488 Ly-6C (clone HK1.4, 2.5μg/mL), HPA (20μg/mL), SNA (166ng/mL), PNA (20μg/mL), MAL II (3.3μg/mL) and *Phaseolus vulgaris* leucoagglutinin (L-PHA; 4μg/mL; Vector Laboratories). The cells were washed twice in lectin buffer followed by incubation for 30 min at room temperature with a streptavidin PE-conjugated secondary antibody (120ng/mL in PBS-BSA; Invitrogen) before a final two washes in PBS-BSA. Following transfer to flow cytometry tubes in 2% PFA, the cells were analysed on a FACSCalibur using the FL1 and FL2 channels.

2.7 *Ex vivo* flow chamber assay

This assay was used to assess leukocyte behaviour under conditions of flow, which were generated using an automated syringe pump (Harvard Apparatus) connected to small-diameter tubing and chamber slides allowing observation of the leukocytes over a monolayer of recombinant protein or live cells. The flow chamber slides were viewed using a Nikon Eclipse TE3000 microscope fitted with x10 and x20 phase contrast objectives (Nikon). Six 10s frames were collected for each well using a Q-Imaging Retiga EXi Digital Video Camera (Q-Imaging) and videos were analysed using Image Pro-Plus software (Media cybernetics).

2.7.1 Murine whole blood flow over E-selectin

Ibidi μ-Slide VI0.4 cell microscopy chambers were coated with recombinant mouse E-selectin Fc Chimera (2μg/mL: R&D Systems) in 100μL PBS/well for 2h at room temperature. The wells were blocked using 0.5% Tween-20 in PBS for 1h at room temperature. Murine whole blood was collected by cardiac puncture, diluted 1:10 in Hank's balanced salt solution (HBSS; Gibco) and flowed through the chamber at 1.010mL/min for 3min. This was followed by HBSS at the same rate for 1min before image acquisition and subsequent offline analysis. In some experiments the whole blood was pre-treated for 15min at 37°C with human recombinant Gal-3 (hrGal-3; 10ng/mL) prior to flow. In other experiments WT and Gal-$3^{-/-}$ whole blood was collected, centrifuged for 8 min at 200 *g* to collect the platelet-rich plasma, which was then spun again for 5 min at 1000 g. The remaining platelet-poor plasma was then added back to the leukocytes from the opposite genotype donor, for example the WT leukocytes received the Gal-$3^{-/-}$ platelet-poor plasma and *vice versa* before they were flowed over E-selectin for 3 min at 1.010mL/min and leukocyte capture was quantified.

During analysis the number of firmly adherent leukocytes was assessed and these were further classified according to their appearance under the phase contrast objective. Those that were phase dark were deemed to be leukocytes showing a more activated phenotype. Experiments were repeated at least three times and statistical significance was assessed using one-way ANOVA with an appropriate post hoc test.

2.8 Enzyme-linked immunosorbent assays (ELISA) for Gal-3

An enzyme-linked immunosorbent assay (ELISA) was used to determine the quantity of Gal-3 in murine platelet-poor plasma using the murine Gal-3 DuoSet® ELISA development Kit (R&D Systems). Whole blood was collected from the animals as described in section 2.6.1, the platelet-poor plasma was isolated as described in section 2.7.1 and used directly or stored at -80°C until analysis by ELISA assay.

2.8.1 ELISA protocol

Certified high binding, flat-bottomed clear 96-well plates (Costar) were coated overnight at room temperature with capture antibody (2.0μg/mL) diluted in PBS without carrier protein. It was then washed three times by submersion in wash buffer (0.05% Tween-20 in PBS, pH7.4; Sigma) and then aspirating each well, after the final wash the plate was blotted on clean paper towels to ensure complete removal of wash buffer. Blocking was carried out for a minimum of 1h at room temperature using reagent diluent [1% low endotoxin bovine serum albumin (BSA; Sigma) in PBS, 0.2μm sterile filtered]. The plate was washed once more before samples and standards were added in duplicate, a seven-point standard curve with 2-fold serial dilutions in reagent diluent and a high standard of 1000pg/mL was used. Samples were added neat or diluted in reagent diluent to an appropriate expected concentration range. The samples and standards were incubated for 2h at room temperature before undergoing the washing procedure once more. Detection antibody at a

final concentration of 200ng/mL in reagent diluent was added and the plate incubated for a further 2h at room temperature. The wash step was once more carried out and the plate incubated for 20min at room temperature with streptavidin-horseradish peroxidase diluted 1:200 in reagent diluent, avoiding direct light. The wash step was repeated for a final time before substrate solution was added; substrate solution A (stabilised H_2O_2; R&D Systems) was mixed with an equal volume of substrate solution B (stabilised tetramethylbenzidine; R&D Systems) and delivered to each well. The plate was observed periodically and once the standard curve displayed an appropriate intensity range the reaction was stopped using sulphuric acid (2N; Sigma) and the plate gently tapped to mix the reagents, typically after 10min. The absorbance values were collected by scanning with a Multiskan plate reader (LabSystems) set to 450nm with wavelength correction set to 540nm.

2.8.2 Determination of unknown Gal-3 concentrations

GraphPad Prism 4 (GraphPad) software was used. Absorbance values for standards were averaged and plotted against the known logarithmic concentration of Gal-3 using a sigmoidal dose-response (variable slope) equation for best curve fit. From this the unknown concentrations of Gal-3 in each sample could be calculated using their averaged absorbance values. Levels of Gal-3 were plotted and statistical significance was assessed using one-way analysis of variance (ANOVA) and an appropriate post hoc test.

2.9 Assessment of murine tissue mRNA

2.9.1 Total RNA isolation from murine cremaster muscle samples

Murine cremaster muscles were dissected and snap frozen in LN_2 following intrascrotal treatment for 4 hours with PBS (sham, 400μL), TNFα (300ng) or varying concentrations of rGal-3 (200-1000μg) as described in section 2.6.1. Frozen cremasters were weighed and quickly transferred to soft tissue homogenising tubes containing 1.4mm ceramic beads (Bertin Technologies) before disruption in 600μL buffer RLT (Qiagen) using the Precellys 24 tissue homogeniser set to 5500 *g* for 20 sec three times with 20 sec pauses. The tubes were centrifuged at 8000 *g* and the supernatant further disrupted by passage through a 27G syringe at least ten times before RNA isolation with the RNeasy kit (Qiagen) and on-column DNase according to manufacturer guidelines. Briefly, 600μL 70% EtOH was added to the supernatants and mixed well by pipetting, the sample was transferred in 700μL volumes to a spin column and centrifuged at 8000 *g* for 15 sec to allow adsorption of RNA onto the spin column silica membrane. Flow though was discarded, 350μL of buffer RW1 was added and the column was centrifuged at 8000 *g* for 15 sec before 80μL of DNase I incubation mix was added directly to the membrane, which was incubated at room temperature for 15 min. 350μL buffer RW1 followed by 500μL buffer RPE was added before centrifugation at 8000 *g* for 15 sec after each addition. An extended 2 min centrifugation step at 8000 *g* was carried out after addition of 500μL buffer RPE to further dry the membrane. The column was placed in a new collection tube and 40μL dH_2O was added directly to the membrane,

the tubes were centrifuged for 1 min at 10000 *g* before the eluate was collected and added back to the membrane for a final repeat centrifugation followed by storage on ice.

The quality and concentration of RNA was assessed using a Nanodrop ND-1000 Spectrophotometer (NanoDrop Technologies) following manufacturer guidelines. The spectral measurement was made with 1μL sample, the concentration was measured in ng/μL from the absorbance at 260nm. The ratio of absorbencies at 260/280nm and 230/260nm were used to assess protein and salt contamination, where pure samples have a ratio of approximately 2.

2.9.2 cDNA synthesis

RNA was reverse transcribed into cDNA using a thermal cycler (Abgene) and a mastermix composed as follows; 2μg RNA in 7μL dH_20, 1μL 40mM dNTP mix (10mM of each component; dATP, dGTP, dCTP and dTTP; Promega), 1μL oligo $(dT)_{15}$ and 4μL dH_20. The initial mastermix was incubated at 65°C for 5 min to denature RNA secondary structure then placed on ice for 2 min to allow the oligos to anneal. A second mastermix was prepared; 4μL 5x first strand buffer, 1μL 0.1M dithioreitol (DTT), 1μL RNaseOUT and 1μL Superscript™ III reverse transcriptase (200U/μL, all Invitrogen) and added to each sample before brief mixing. Samples were incubated at 55°C for 1 h for cDNA extension and then heated at 70°C for 15 min to halt the reaction.

2.9.3 Real-time PCR

Quantitative real time PCR was performed using a mastermix prepared as follows; 1μL gene-specific primer (Qiagen), 5.2μL 2x Power SYBR Green Mastermix (Applied Biosystems) and 1.8μL dH_20 and dispensed into each well of a 384-well plate (Applied Biosystems). Primers included those for *Lgals3*, *Gapdh*, *Rpl32*, *Il-1b*, *tnf*, *Il-6*, *Ccl2*, *Cxcl1*, *Cxcl12*, *Ly-6G*, *Csf1r*, *Pecam1*, *Icam1* and *Sele*. Diluted cDNA was added to each well to the equivalent of approximately 50ng/2μL of the original RNA that was reverse transcribed, each sample was tested in duplicate. Thermal cycling was carried out using the ABI Prism® 7900 Real Time PCR system according to manufacturer recommendations; 50°C for 2 min, 95°C for 15 min, then 40 cycles of 94°C for 15 s, 55°C for 30 s and 72°C for 30 s. SYBR green binds and emits fluorescence upon binding to newly synthesised double-stranded DNA thus reflecting the number of amplicons generated, the cycle threshold (Ct) value was defined as the cycle at which the sample reached a set threshold level of fluorescence. The comparative Ct method (Pfaffl, 2001) was used to measure gene transcription, where the Ct values were first normalised with an endogenous housekeeping gene and then to the control samples, which were used as a calibrator and given a value of 1 and the results were expressed as relative units based on $2^{-\Delta\Delta Ct}$.

2.9.4 Genotyping of Gal-$3^{-/-}$ mouse colony

Standard PCR was carried out to ensure the knockout mouse colony was intact using the REDExtract-N-amp™ Tissue PCR kit (Sigma) which

enables genomic DNA extraction from murine tail clippings. Briefly, tail clippings of approximately 0.5cm in length were incubated for 10 min at room temperature in 50μL extraction solution containing 12.5μL tissue preparation solution before a subsequent incubation at 95°C for 3 min. The reaction was halted by the addition of 50μL neutralisation solution and vortexing. Wild type reverse, common and mutant primers for the detection of the *Lgals3* gene (The Jackson Laboratory) were diluted to 10μM with dH_2O to make one primer mix; the reaction mix was prepared in a 384 well plate with 4μL sample, 10μL REDExtract-N-amp™ 2x reaction mix and 6μL primer mix to give a final concentration of 0.3μM per primer. Thermal cycling (Abgene) was carried out according to manufacturer recommendations; 94°C for 3 min, then 35 cycles of 94°C for 30 s, 65°C for 30 s and 72°C for 30 s with a final incubation at 72°C for 2 min. The amplified DNA (15μL) and low molecular weight marker (8μL; New England Biolabs) was directly loaded onto a 2% agarose gel for separation by electrophoresis, which was prepared using Tris-acetate-EDTA (TAE) buffer and Gel Red nucleic acid stain (1:10000; Biotium) and run at 100V until the lanes approached the end of the gel before product size was examined using a UV light box.

2.10 Assessment of murine cremaster protein content

Murine cremaster muscles were dissected and snap frozen in LN_2 following intrascrotal treatment for 4 hours with PBS (sham, 400μL) or rGal-3 (1000μg) as described in section 2.6.1. Frozen cremasters were weighed and quickly transferred to soft tissue homogenising tubes

containing 1.4mm ceramic beads (Bertin Technologies) before disruption in 600μL PBS containing protease inhibitors Aprotinin, Leupeptin and Pepstatin (all 10μg/mL; Sigma) at 600 *g* for 2 × 30 s cycles with one 30 s break. The supernatant was collected and 1% Triton-X-100 was added before the samples were stored at -80°C overnight. After thawing the samples were centrifuged at 10,000 *g* for 5 min and the protein content assed using the Pierce® BCA (Bicinchoninic Acid) assay following manufacturer guidelines. Briefly, 25μL of prepared albumin standard (25-2000μg/mL) or unknown sample was incubated at 37°C with 200μL working reagent and the absorbance at 562nm was measured on a Multiskan FC plate reader (Thermo Scientific). A final protein quantity of 200μg was then assessed using the mouse cytokine array panel A Proteome Profiler™ (R&D Systems) according to manufacturer instructions. Briefly, the membranes were blocked for 1 hour at room temperature in a rocking platform while the samples were incubated with the biotinylated detection antibody cocktail also for 1 hour at room temperature. The block buffer was aspirated from the well, the sample/antibody mix was added and the membranes incubated overnight at 4°C. The membranes were washed thoroughly before addition of streptavidin-HRP conjugated secondary antibody for 30 min at room temperature and a final wash step was carried out. The membranes were imaged using the supplied chemi-reagent mix and exposure to X-ray film as well as using the FluorChem E (Protein Simple), which increases exposure until the desired intensity is reached, in this case approximately 10 min. Pixel densitometry was carried out using Fiji

imaging software (ImageJ) and subtracting an averaged background reading from each duplicate antibody spot.

2.11 Statistical analysis

All data were analysed using GraphPad Prism 4 software. Data are expressed as mean±standard error of the mean (SEM) of n experiments. All data were tested for normal distribution. Statistical significance was assessed using unpaired students t-tests, one-way analysis of variance (ANOVA) or two-way ANOVA with the appropriate post hoc test, commonly Dunnett's post-test or the Tukey range test. In all cases a P value of ≤0.05 was considered significant.

Chapter 3: Examining the role of endogenous Gal-3 in leukocyte recruitment to the inflamed microvasculature

3.1 Maintenance of Gal-3$^{-/-}$ colony

Heterozygote breeding pairs of Gal-3$^{-/-}$ founders and C57BL/6 wild type mice were set up and their pups genotyped using tail clippings and the primer sequences shown (Figure 3.1A). Gal-3$^{-/-}$ pups of the F1 generation, which display only one band at 150 base pairs (Figure 3.1B, arrows) were selected and homozygote Gal-3$^{-/-}$ breeding pairs set up. The F2 generation were therefore all homozygote Gal-3$^{-/-}$ and could be used in further studies.

.

A

Primer Type	5'→3' Sequence
Wild type reverse	GAG GAG GGT CAA AGG GAA AG
Common	GAC TGG AAT TGC CCA TGA AC
Mutant	TCG CCT TCT TGA CGA GTT CT

B

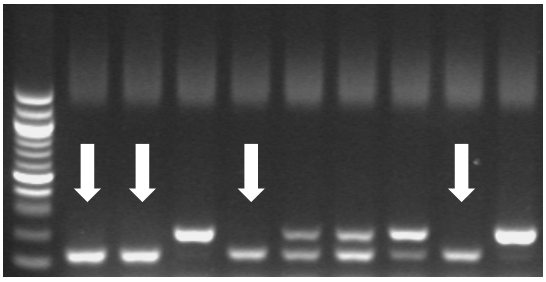

220bp: Wild type

150bp: Gal-3$^{-/-}$

Double band: Heterozygote

Figure 3.1 Gal-3$^{-/-}$ breeding pairs were selected from heterozygote crosses
Tail clippings from pups of Gal-3$^{-/-}$/ C57BL/6 crosses were genotyped as described in methods and using the primer sequences shown (A). Homozygote Gal-3$^{-/-}$ mice (B, arrows) were then selected and Gal-3$^{-/-}$/ Gal-3$^{-/-}$ breeding pairs set up for further experiments.

3.2 Analysis of the inflamed cremasteric microcirculation in wild type mice by intravital microscopy

The cremasteric microcirculation of C57BL/6 mice was visualised by intravital microscopy 2 or 4h after intrascrotal injection with PBS (400μL), IL-1β (30ng in 400μL PBS) or TNFα (300ng in 400μL PBS). Leukocyte flux, rolling velocity, adhesion and emigration was investigated in segments of 100μm in 3-5 vessels per mouse and results are expressed as mean±SEM of 3-4 mice per group. Statistical significance was assessed by one-way ANOVA and Tukey's multiple comparison post-test.

3.2.1 Response to TNFα treatment

The microcirculation was found to be strongly inflamed after 4h but not 2h treatment with TNFα. The average leukocyte rolling velocity (μm/s) was significantly reduced in TNFα-treated animals at 4h when compared to sham-treated animals (Figure 3.2B; 4h TNFα 4.8±1.1 *vs.* sham 31.8±6.3, $P<0.01$, n=4). The number of rolling leukocytes in 2h or 4h-treated animals was not significantly different from sham animals, however there was a significant decrease at 4h when compared to the 2h-treated mice (Figure 3.2A; 2h TNFα 62.0±18.6 *vs.* 4h TNFα 11.1±2.7, $P<0.05$, n=3-4). Both the number of adherent cells (per 100μm segment) and those found to have emigrated (per 100μm^2) either side of the vessel was significantly increased in TNFα-treated animals at 4h (Figure 3.2C, D; Adherent 4h TNFα 8.4±0.9 *vs.* sham 3.4±0.5, $P<0.01$, n=4; Emigration 4h TNFα 10.4±2.0 *vs.* sham 3.1±1.0, $P<0.05$, n=4).

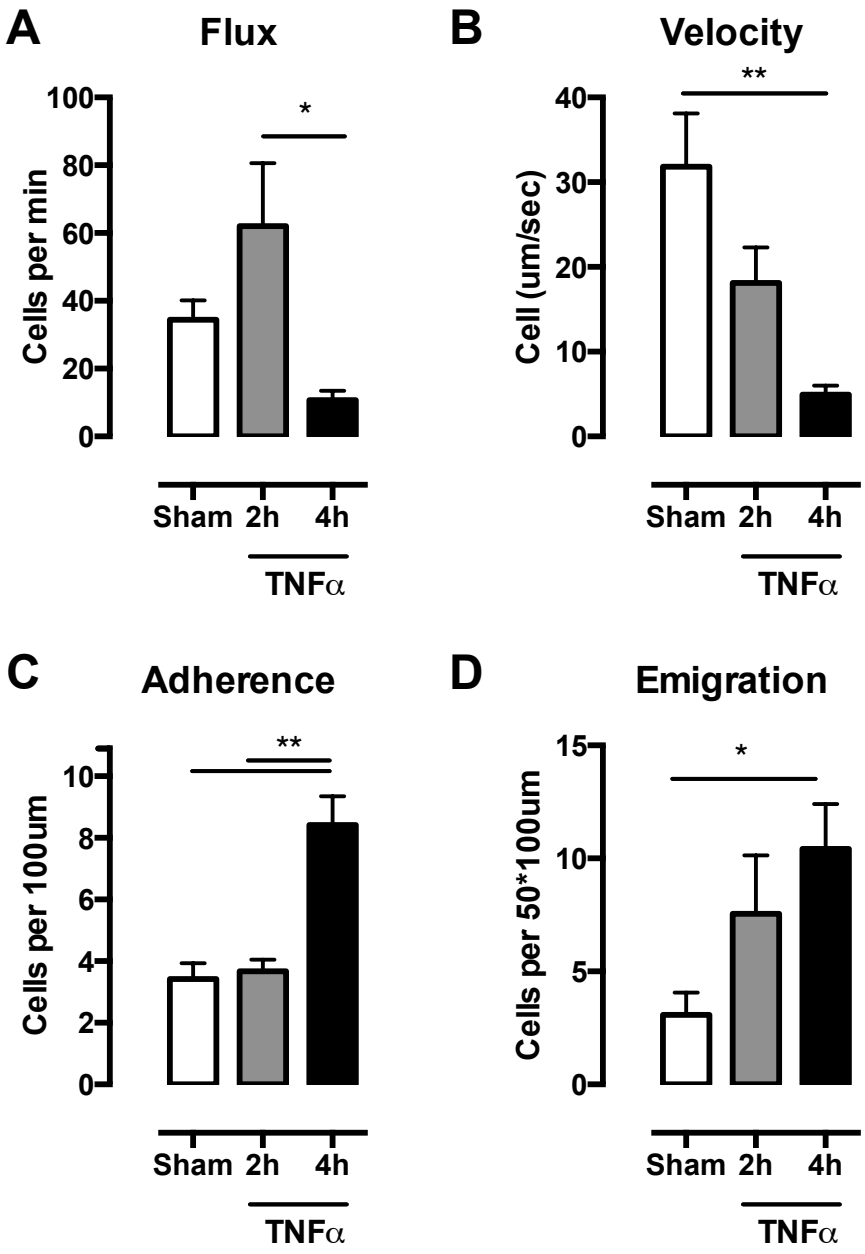

Figure 3.2 Fixed-time profile of TNF-α-induced leukocyte recruitment in the mouse cremasteric microcirculation

IVM was performed as detailed in Methods. Briefly, the cremasteric microcirculation in C57BL/6 mice was assessed 2 or 4h after intrascrotal injection of PBS (400μL) or murine recombinant TNF-α (300ng in 400μL PBS). Leukocyte flux (**A**), rolling velocity (**B**), adhesion (**C**) and emigration (**D**) was investigated in segments of 100μm in 3-5 vessels per mouse and results are expressed as mean±SEM of 3-4 mice per group. Statistical significance was assessed by one-way ANOVA and Tukey's multiple comparison post-test; denoted by asterisks *P<0.05 and **P<0.01

3.2.2 Response to IL-1β treatment

The leukocyte recruitment seen after treatment with IL-1β was similar to that seen with TNFα, whereby the vessels were strongly inflamed after 4h treatment but not after a shorter time of 2h. Again rolling velocities were significantly reduced from those seen in sham-treated animals, though at 4h they were not reduced to the same extent as seen in TNFα-treated animals (Figure 3.3B; 4h IL-1β 12.7±3.8 *vs.* sham 31.8±6.3, $P<0.05$, n=4). A significant increase in the number of adherent and emigrated cells was observed at 4h (Figure 3.3C, D; Adherent 4h IL-1β 6.6±1.2 *vs.* sham 3.4±0.5, $P<0.05$, n=4; emigration 4h IL-1β 10.3±2.5 *vs.* sham 3.1±1.0, $P<0.05$, n=4). The leukocyte rolling flux was unchanged by IL-1β treatment (Figure 3.3A; sham 34.5±5.7 *vs.* 4h IL-1β 47.6±5.7, ns, n=4). It was important to characterise these responses to IL-1β and TNFα to establish that after 4h treatment the vessels would be adequately inflamed in order that we could compare responses in the Gal-$3^{-/-}$ mice.

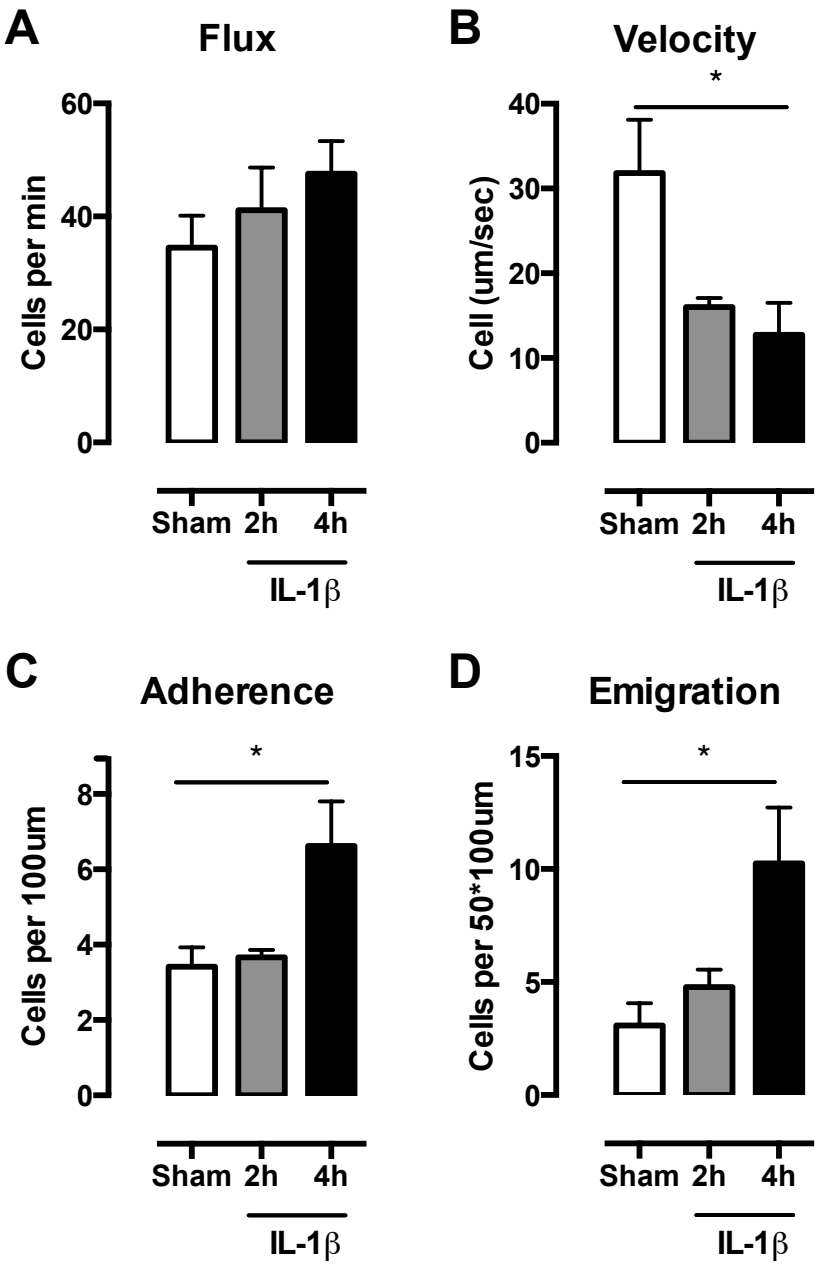

Figure 3.3 FIxed-time profile of IL-1β-induced leukocyte recruitment in the mouse cremasteric microcirculation

IVM was performed as detailed in Methods. Briefly, the cremasteric microcirculation in C57BL/6 mice was assessed 2 or 4h after intrascrotal injection of PBS (400μL) or murine recombinant IL-1β (30ng in 400μL PBS). Leukocyte flux (**A**), rolling velocity (**B**), adhesion (**C**) and emigration (**D**) was investigated in segments of 100μm in 3-5 vessels per mouse and results are expressed as mean±SEM of 3-4 mice per group. Statistical significance was assessed by one-way ANOVA and Tukey's multiple comparison post-test; denoted by asterisks *P<0.05.

3.3 Analysis of the inflamed cremasteric microcirculation in Gal-3$^{-/-}$ mice by intravital microscopy

The cremasteric microcirculation of Gal-3$^{-/-}$ mice was then assessed after 4h treatment with inflammogen, reflecting the time taken to see changes in leukocyte recruitment in wild type mice. Leukocyte flux, rolling velocity, adhesion and emigration was investigated in segments of 100μm in 3-5 vessels per mouse and results are expressed as mean±SEM of 3-5 mice per group. Statistical significance was assessed by two-way ANOVA and with Bonferroni's multiple comparison post-test.

3.3.1 Response to TNFα treatment

Leukocyte recruitment was first analysed after treatment with TNFα (300ng in 400μL PBS) for 4h. There were no differences in leukocyte flux, rolling velocity, adhesion and emigration in sham-treated Gal-3$^{-/-}$ animals compared to their wild type counterparts. The mice were found to display similar levels of leukocyte adhesion after TNFα treatment (Figure 3.4C; WT 8.4±0.9 *vs.* KO 7.8±1.3, not significant) as well as leukocyte emigration (Figure 3.4D; WT 10.4±2.0 *vs.* KO 13.25±4.4, not significant). However, the Gal-3$^{-/-}$ mice lacked the reduction in rolling velocity observed in wild type animals in response to TNFα treatment (Figure 3.4B; WT 4.8±1.1 *vs.* KO 34.8±11.1, $P<0.05$, n=4). In addition to this, Gal-3$^{-/-}$ mice displayed increased leukocyte flux in response to TNFα treatment when compared to wild type animals (Figure 3.4A; WT 11.1±2.7 *vs.* KO 30.8±7.1, $P<0.05$, n=4).

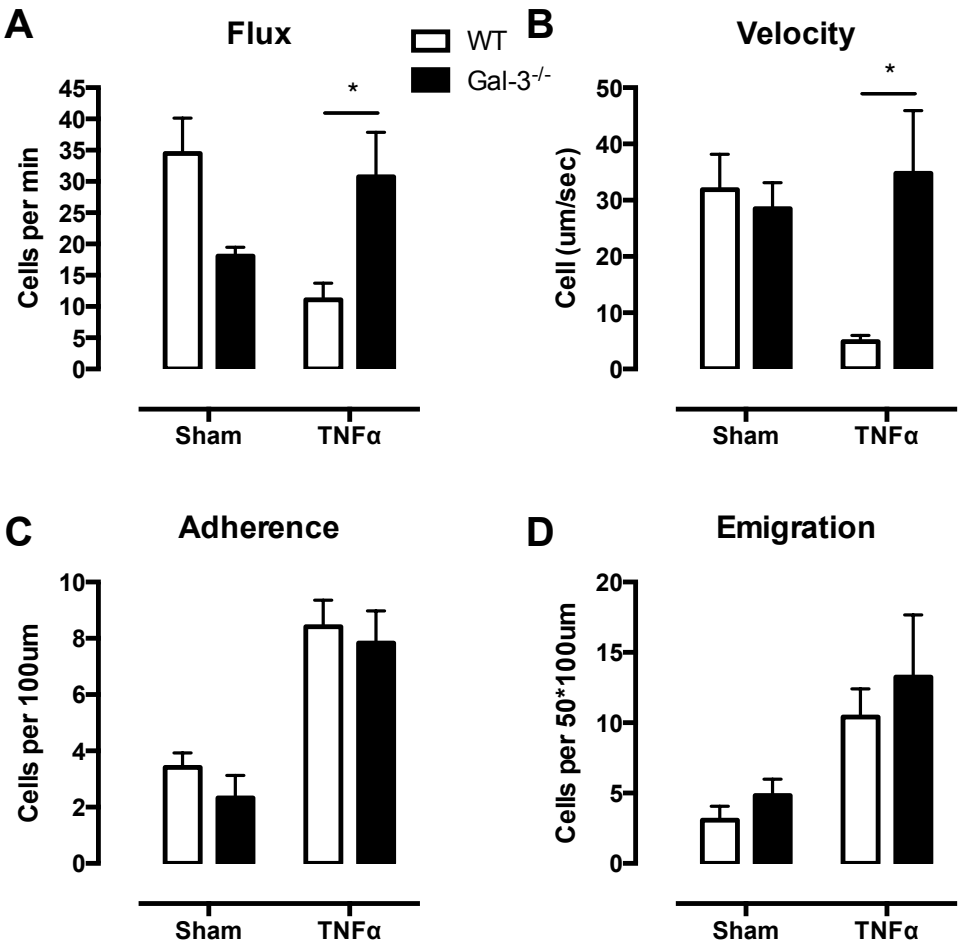

Figure 3.4 Rolling velocities are not reduced in inflamed post-capillary venules of Gal-3$^{-/-}$ mice treated with TNFα

IVM was performed as detailed in Methods. Briefly, the cremasteric microcirculation in C57BL/6 or Gal-3$^{-/-}$ mice was assessed 4h after intrascrotal injection of PBS (400μL) or murine recombinant TNFα (300ng in 400μL PBS). Leukocyte flux (**A**), rolling velocity (**B**), adhesion (**C**) and emigration (**D**) was investigated in segments of 100μm in 3-5 vessels per mouse and results are expressed as mean±SEM of 3-5 mice per group. Statistical significance was assessed by two-way ANOVA and with Bonferroni's multiple comparison post-test; denoted by asterisks * $P<0.05$.

3.3.2 Response to IL-1β treatment

Treatment with IL-1β (30ng in 400μL PBS) also induced differing responses between wild type and Gal-3$^{-/-}$ mice, which again exhibited a lack in reduction of rolling velocities as well as reduced leukocyte emigration to the tissue. Average rolling velocity was reduced after IL-1β treatment in wild type mice, though this was not the case in the Gal-3$^{-/-}$ mice (Figure 3.5B; WT 12.1±3.0 *vs.* KO 35.3±10.5, $P<0.05$, n=4-5). In contrast to the increased emigration recorded after treatment with TNFα compared to sham-treated animals, there were significantly fewer leukocytes that emigrated in the Gal-3$^{-/-}$ mice after IL-1β treatment (Figure 3.5D; WT 10.0±1.9 *vs.* KO 4.5±0.5, $P<0.05$, n=4-5). In contrast, the number of adherent leukocytes in response to IL-1β treatment was comparable in wild type and Gal-3$^{-/-}$ animals (Figure 3.5C; WT 6.7±0.9 *vs.* KO 5.7±1.2, not significant) as were levels of leukocyte flux (Figure 3.5A; WT 38.6±8.8 *vs.* 46.0±16.8, not significant).

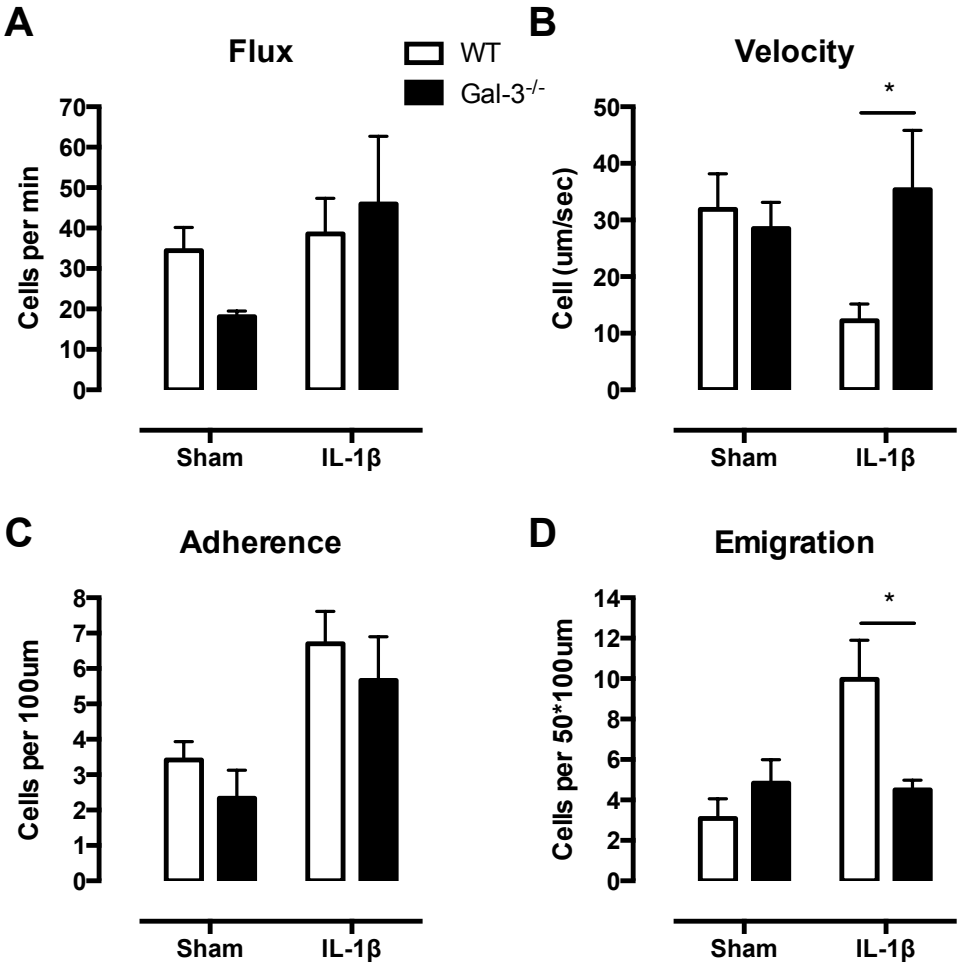

Figure 3.5 Rolling velocities are not reduced in inflamed post-capillary venules of Gal-3$^{-/-}$ mice treated with IL-1β in addition to reduced leukocyte emigration in these animals

IVM was performed as detailed in Methods. Briefly, the cremasteric microcirculation in C57BL/6 or Gal-3$^{-/-}$ mice was assessed 4h after intrascrotal injection of PBS (400μL) or murine recombinant IL-1β (30ng in 400μL PBS). Leukocyte flux (**A**), rolling velocity (**B**), adhesion (**C**) and emigration (**D**) was investigated in segments of 100μm in 3-5 vessels per mouse and results are expressed as mean±SEM of 3-5 mice per group. Statistical significance was assessed by one-way ANOVA and with Bonferroni's multiple comparison post-test; denoted by asterisks * $P<0.05$.

3.4 Analysis of murine Gal-3$^{-/-}$ whole blood under conditions of flow

The parallel plate flow chamber enables the investigation of cells *ex vivo* under conditions that - as closely as possible - mimic those found in mammalian blood vessels. In this case flow chamber slides were coated with E-selectin (2µg/mL) and murine whole blood from C57BL/6 or Gal-3$^{-/-}$ mice was collected by cardiac puncture using heparin (10U/mL) as an anti-coagulant. The blood was diluted and flown through the E-selectin coated chambers at a rate of 1.010mL/min for 3min; this was followed by 1min of HBSS alone at the same rate before image acquisition. Results are expressed as mean±SEM and significance was assessed using unpaired student's t-tests.

3.4.1 Wild type and Gal-3$^{-/-}$ leukocyte capture to E-selectin in parallel flow chambers

Under conditions of flow, Gal-3$^{-/-}$ leukocytes exhibit a reduced capacity to adhere to E-selectin when compared to wild type cells (Figure 3.6A, C; total cell count WT 25.7±3.3 *vs.* KO 12.3±1.1, P=0.0183, n=3). In addition to this the leukocytes that adhere can be classified as phase light or phase dark, where phase dark cells are those displaying a more active phenotype, which in the presence of a cell monolayer would attempt to transmigrate through it. A much smaller proportion (percentage of total cells) of Gal-3$^{-/-}$ cells displayed phase dark morphology when compared to wild type cells (Figure 3.6B, C; WT 33.3±6.3 *vs.* KO 11.7±3.0, P=0.0371, n=3).

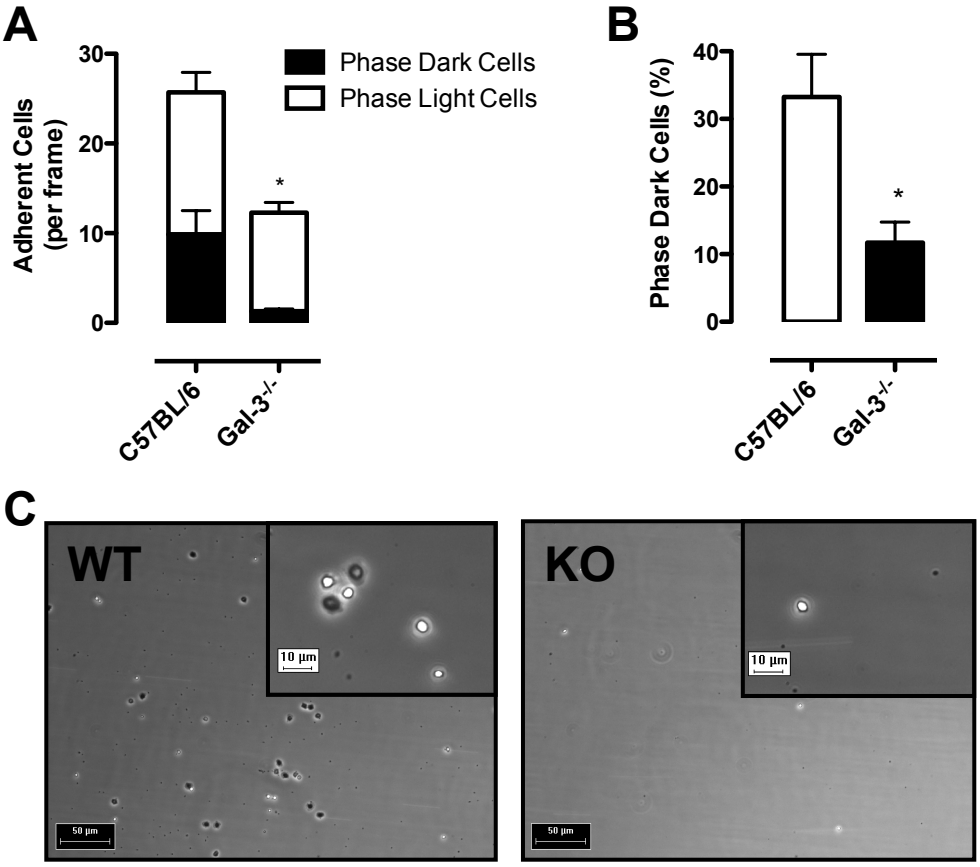

Figure 3.6 Gal-3$^{-/-}$ whole blood displays reduced leukocyte capture to E-selectin under conditions of flow

Ibidi flow chamber μ-slides were coated with recombinant E-selectin (2μg/ml) and blocked using 0.5% Tween-20. C57BL/6 or Gal-3$^{-/-}$ whole blood was collected by cardiac puncture using heparin (10U/mL) and subsequently diluted 1:10 in HBSS. Blood was flown for 3mins at 1.010mL/min, followed by 1min HBSS. Videos of 10s were captured for a total of 4-6 frames per mouse and 3 mice per group. **A)** Captured leukocytes in each frame were quantified and classified as phase dark or phase light; results are expressed as mean±SEM. Total cells captured for the two genotypes were compared and significance was assessed using an unpaired t-test, denoted by asterisk * $P<0.05$. **B)** Percentage phase dark cells of total leukocytes captured were calculated and results are expressed as mean±SEM. Significance was assessed using an unpaired student's t-test, denoted by asterisks * $P<0.05$. **C)** Representative images are stills taken from C57BL/6 (left panel) or Gal-3$^{-/-}$ (right panel) experiments with higher magnification shown in the insets.

3.4.2 Wild type and Gal-3$^{-/-}$ leukocyte capture to E-selectin after fluorescent labelling in the same volume

In addition to investigating the number of adherent leukocytes in separate chambers, the whole blood was collected and fluorescently labelled before flow over E-selectin in the same chamber. The wild type blood was labelled with carboxyfluorescein succinimidyl ester (CFSE; 20µg/mL) and the Gal-3$^{-/-}$ whole blood was labelled with Rhodamine-6G (20µg/mL) for 15 minutes at 37°C before mixing the two genotypes and dilution 1:10 in HBSS directly before flow and image capture. Results are expressed as mean±SEM and significance was assessed using an unpaired student's t-test. As seen in separate chambers, the Gal-3$^{-/-}$ whole blood exhibited significantly fewer adherent cells in comparison to wild type whole blood (Figure 3.7A; WT 4.0±0.7 *vs.* KO 2.1±0.3, P=0.0327, n=7 frames).

3.4.3 White blood cell counts of wild type and Gal-3$^{-/-}$ mice

When carrying out these experiments, a small volume of whole blood was collected and a white blood cell count carried out using a haemocytometer. There was found to be no significant difference in white blood cell count (cells/µL) between wild type and Gal-3$^{-/-}$ mice (WT 29.92±0.17 *vs.* KO 28.00±3.41, n.s).

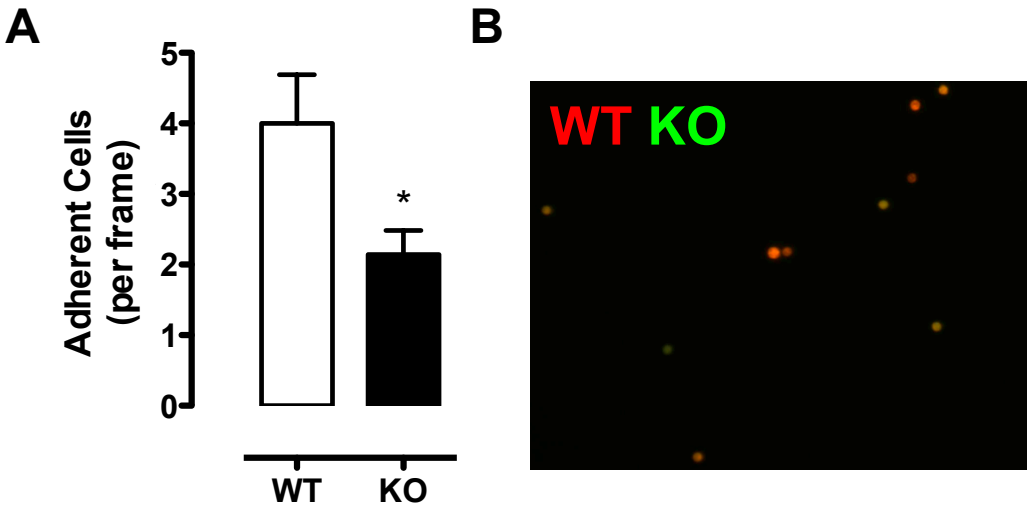

Figure 3.7 Fluorescently labelled Gal-3$^{-/-}$ whole blood displays reduced leukocyte capture to E-selectin under conditions of flow
Ibidi flow chamber μ-slides were coated with recombinant E-selectin (2μg/ml) and blocked using 0.5% Tween-20. C57BL/6 or Gal-3$^{-/-}$ whole blood was collected by cardiac puncture using heparin (10U/mL) and labeled separately with CFSE (20μg/ml, Gal-3$^{-/-}$) or R-6G (2μg/ml, C57BL/6) for 15min at 37°C before mixing and diluting 1:10 in HBSS. The blood was flown through one chamber for 3mins at 1.010mL/min, followed by 1min HBSS. Videos of 10s were captured for a total of 7 frames per experiment and N=1. **A)** Captured leukocytes in each frame were quantified and classified as CFSE or R-6G positive. Results are expressed as mean±SEM and significance was assessed using an unpaired student's t-test, denoted by asterisks * P<0.05. **B)** Representative still taken from recordings, red R-6G positive cells are from C57BL/6 and green CFSE positive cells are from Gal-3$^{-/-}$ mice.

3.5 Analysis of murine Gal-3$^{-/-}$ whole blood by flow cytometry

3.5.1 E-selectin ligand expression on Gal-3$^{-/-}$ neutrophils

Wild type or Gal-3$^{-/-}$ whole blood was collected by cardiac puncture using heparin (10U/mL) and treated for 10min at 37°C with vehicle (PBS), TNFα (50ng/mL) or IL-1β (50ng/mL) before cell staining with antibodies against CD44 and PSGL-1 (CD162) as well as the neutrophil marker Ly-6G (Clone 1A8). Data are shown as mean±SEM and significance was assessed by two-way ANOVA and Bonferroni's multiple comparison post-test. Gal-3$^{-/-}$ neutrophils displayed comparative basal expression of both CD44 (Figure 3.8A; WT 2137.2±149.6 *vs.* KO 2394.4±88.1, ns, n=3) and PSGL-1 (Figure 3.8A; WT 378.1±36.2 *vs.* KO 431.2±69.8, ns, n=3). Expression after treatment with IL-1β or TNFα was calculated as fold change from vehicle. There were no differences from wild type cells in CD44 expression on Gal-3$^{-/-}$ neutrophils after IL-1β (Figure 3.8C; WT 104.2±14.2 *vs.* KO 93.6±6.7, not significant) or TNFα (Figure 3.8C; WT 111.8±10.2 *vs.* KO 100.4±9.6, not significant) treatment. In contrast, when compared to wild type cells Gal-3$^{-/-}$ neutrophils displayed reduced PSGL-1 expression after treatment with TNFα (Figure 3.8C; WT 115.7±2.2 *vs.* KO 98.9±2.5, $P<0.01$, n=3) but not IL-1β (Figure 3.8C; WT 99.9±3.6 *vs.* KO 109.7±3.8, not significant).

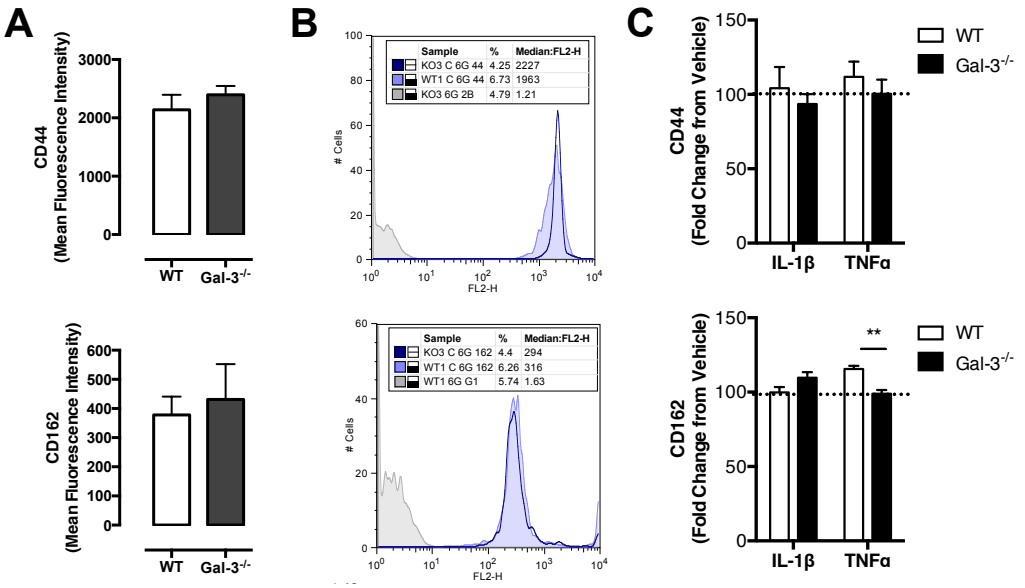

Figure 3.8 Gal-3$^{-/-}$ neutrophils display reduced PSGL-1 after treatment with TNFα

Wild type or Gal-3$^{-/-}$ whole blood was collected by cardiac puncture using heparin (10U/mL) and treated for 10min at 37°C with vehicle (PBS), TNFα (50ng/mL) or IL-1β (50ng/mL). Murine Fc Receptors were blocked before cell staining with antibodies against CD44 and PSGL-1 (CD162) as well as the neutrophil marker Ly-6G (Clone 1A8); analysis was carried out with the FACSCalibur Flow cytometer and FlowJo software, as detailed in Methods. **A**) Basal expression of CD44 and PSGL-1 on wild type and Gal-3$^{-/-}$ neutrophils. **B**) Representative histogram plots showing basal CD44 (top) and PSGL-1 (bottom) expression on wild type (filled blue) and Gal-3$^{-/-}$ (dark blue line) monocytes, with isotype control (grey). **C**) Ligand expression after IL-1β and TNFα treatment. MFI values were plotted as fold change from vehicle treated; the data are shown as mean±SEM of 3-4 mice per group, significance was assessed by two-way ANOVA and Bonferroni's multiple comparison post-test.

3.5.2 E-selectin ligand expression on Gal-3$^{-/-}$ monocytes

Wild type or Gal-3$^{-/-}$ whole blood was collected by cardiac puncture using heparin (10U/mL) and treated for 10min at 37°C with vehicle (PBS), TNFα (50ng/mL) or IL-1β (50ng/mL) before cell staining with antibodies against CD11b and L-selectin as well as the monocyte marker Ly-6C. Data are shown as mean±SEM and significance was assessed by two-way ANOVA and Bonferroni's multiple comparison post-test. Gal-3$^{-/-}$ monocytes displayed comparative basal expression of both CD44 (Figure 3.9A; WT 117.9±21.8 *vs.* KO 111.0±18.3, ns, n=3) and PSGL-1 (Figure 3.9A; WT 347.3±39.0 *vs.* KO 310.1±61.4, ns, n=3). Expression after treatment with IL-1β or TNFα was calculated as fold change from vehicle. In contrast to those seen on neutrophils, there were no differences from wild type cells in PSGL-1 expression on Gal-3$^{-/-}$ monocytes after IL-1β (C; WT 85.0±9.0 *vs.* KO 111.3±11.0, not significant) or TNFα (C; WT 78.7±8.3 *vs.* KO 106.3±12.5, not significant) treatment. However, the expression of CD44 on Gal-3$^{-/-}$ monocytes was increased from that seen on wild type cells in response to IL-1β (C; WT 84.0±10.6 *vs.* KO 126.5±7.7, P<0.01, n=3) but not TNFα (C; WT 95.5±10.7 *vs.* KO 95.4±8.4, not significant) treatment.

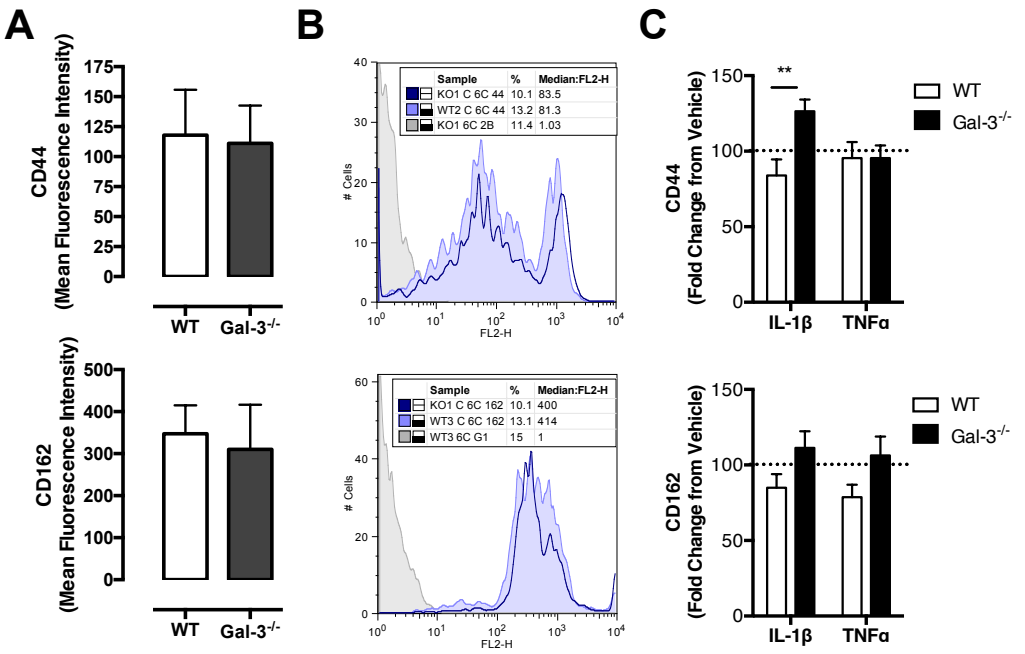

Figure 3.9 Gal-3$^{-/-}$ monocytes display increased CD44 after treatment with IL-1β

Wild type or Gal-3$^{-/-}$ whole blood was collected by cardiac puncture using heparin (10U/mL) and treated for 10min at 37°C with vehicle (PBS), TNFα (50ng/mL) or IL-1β (50ng/mL). Murine Fc Receptors were blocked before cell staining with antibodies against CD44 and PSGL-1 (CD162) as well as the monocyte marker Ly-6C; analysis was carried out with the FACSCalibur Flow cytometer and FlowJo software, as detailed in Methods. **A**) Basal expression of CD44 and PSGL-1 on wild type and Gal-3$^{-/-}$ monocytes. **B**) Representative histogram plots showing basal CD44 (top) and PSGL-1 (bottom) expression on wild type (filled blue) and Gal-3$^{-/-}$ (dark blue line) monocytes, with isotype control (grey). **C**) Ligand expression after IL-1β and TNFα treatment. MFI values were plotted as fold change from vehicle treated; the data are shown as mean±SEM of 3-4 mice per group, significance was assessed by two-way ANOVA and Bonferroni's multiple comparison post-test.

3.5.3 Lectin binding on Gal-3$^{-/-}$ neutrophils

Wild type or Gal-3$^{-/-}$ whole blood was collected by cardiac puncture using heparin (10U/mL); the cells were stained with antibodies against the neutrophil marker Ly-6G (Clone 1A8) as well as a validated panel of lectins before analysis by flow cytometry. Data are shown as mean±SEM of MFI and significance was assessed using an unpaired student's t-test. When compared to their wild type counterparts, Gal-3$^{-/-}$ neutrophils were found to display comparable binding of the lectins SNA (Figure 3.10C; WT 4.4±0.7 *vs.* KO 4.4±1.0, not significant), L-PHA (Figure 3.10C; WT 249.3±66.0 *vs.* KO 248.1±81.7, not significant) and MAL II (Figure 3.10C; WT 19.5±3.3 *vs.* KO 29.9±2.7, not significant). In contrast, Gal-3$^{-/-}$ neutrophils displayed reduced capability to bind the lectins PNA (Figure 3.10A,C; WT 17.6±2.2 *vs.* KO 7.0±1.0, $P<0.05$, n=3) and HPA (Figure 3.10B,C; WT 32.6±4.5 *vs.* KO 18.9±3.2, $P<0.05$, n=6) when compared to wild type cells.

3.5.4 Lectin binding on Gal-3$^{-/-}$ monocytes

Wild type or Gal-3$^{-/-}$ whole blood was collected by cardiac puncture using heparin (10U/mL); the cells were stained with antibodies against the monocyte marker Ly-6C as well as a validated panel of lectins before analysis by flow cytometry. Data are shown as mean±SEM of MFI and significance was assessed using an unpaired student's t-test. When compared to their wild type counterparts, Gal-3$^{-/-}$ monocytes were found to display similar binding of the lectins SNA (Figure 3.11C; WT 12.9±1.5 *vs.* KO 11.5±1.4, not significant), L-PHA (Figure 3.11C; WT 64.5±11.8 *vs.*

KO 59.5±16.1, not significant) and MAL II (Figure 3.11C; WT 27.1±3.3 *vs.* KO 33.4±5.4, not significant). Though not significant, it is possible that Gal-3$^{-/-}$ monocytes display reduced binding of the lectins HPA (Figure 3.11B,C; WT 2.5±0.3 *vs.* KO 1.7±0.3, P=0.1304, n=5-6) and PNA (Figure 3.11A,C; WT 15.0±1.6 *vs.* KO 8.6±0.7, P=0.0606, n=2-3) when compared to wild type cells.

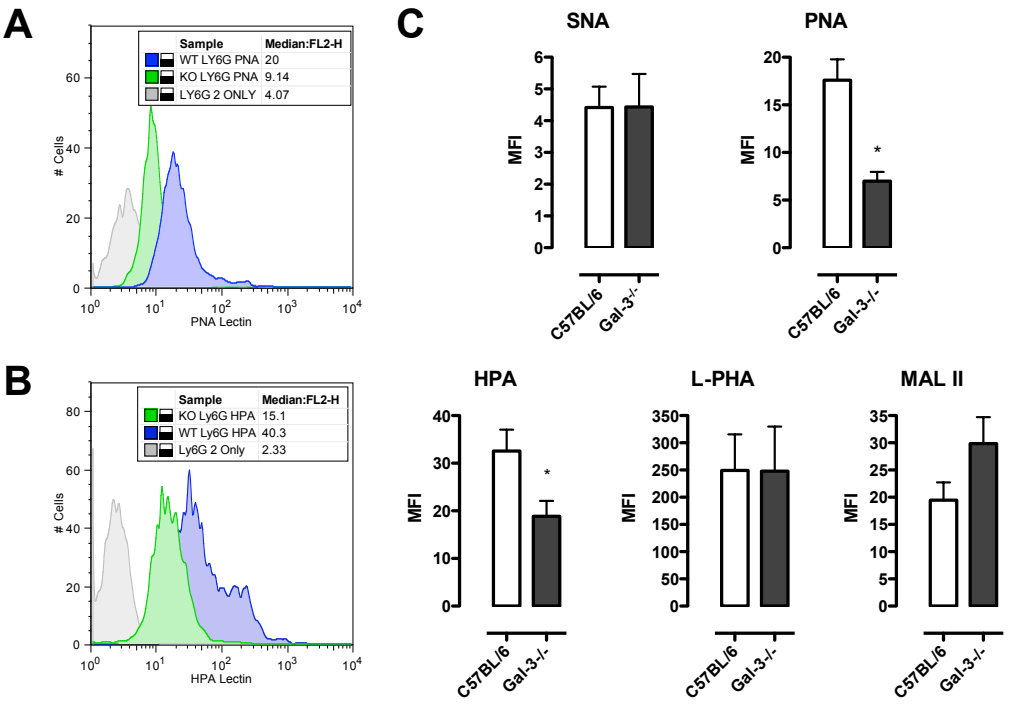

Figure 3.10 Murine neutrophils display reduced PNA and HPA lectin binding sites on their cell surface

Wild type or Gal-3$^{-/-}$ whole blood was collected by cardiac puncture using heparin (10U/mL). Murine Fc Receptors were blocked before cell staining with antibodies against the neutrophil marker Ly-6G (Clone 1A8) as well as a validated panel of lectins; analysis was carried out with the FACSCalibur Flow cytometer and FlowJo software, as detailed in Methods. **A**) Representative histogram plots showing PNA lectin binding on wild type (blue) and Gal-3$^{-/-}$ (green) neutrophils, with isotype control (grey). **B**) Representative histogram plots showing HPA lectin binding on wild type (blue) and Gal-3$^{-/-}$ (green) neutrophils, with isotype control (grey). **C**) MFI values were plotted for all the lectins tested and the data are shown as mean±SEM of 3-6 mice per group, significance was assessed using an unpaired student's t-test.

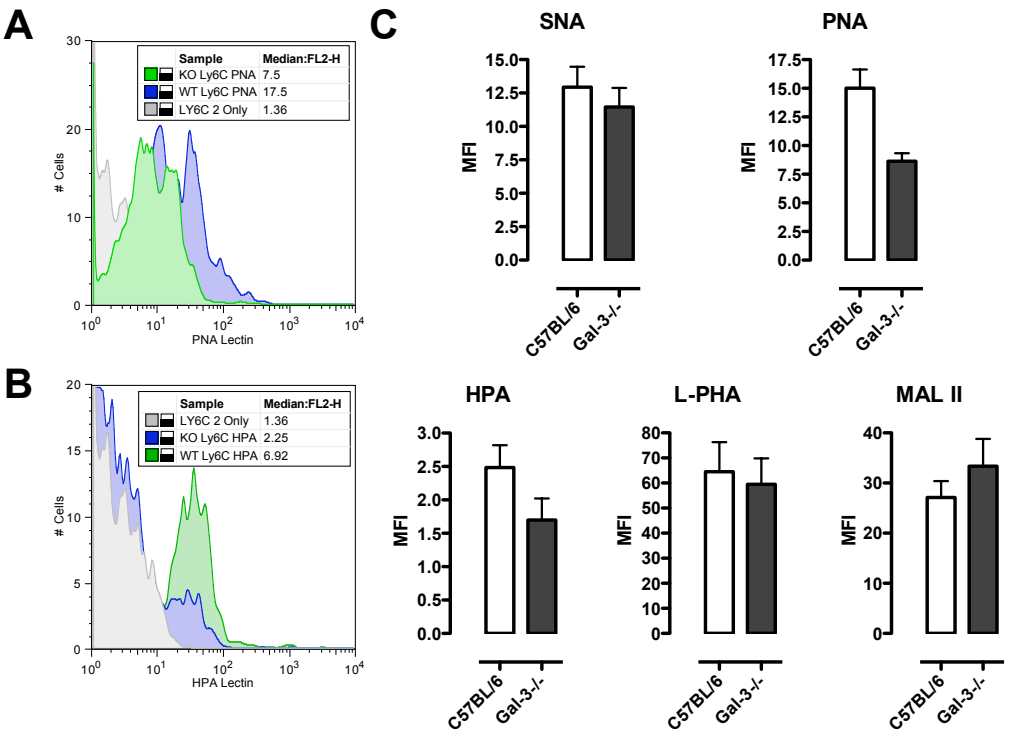

Figure 3.11 Murine monocytes display a trend for reduced PNA and HPA lectin binding sites on their cell surface

Wild type or Gal-3$^{-/-}$ whole blood was collected by cardiac puncture using heparin (10U/mL). Murine Fc Receptors were blocked before cell staining with antibodies against the monocyte marker Ly-6C as well as a validated panel of lectins; analysis was carried out with the FACSCalibur Flow cytometer and FlowJo software, as detailed in Methods. **A**) Representative histogram plots showing PNA lectin binding on wild type (blue) and Gal-3$^{-/-}$ (green) monocytes, with isotype control (grey). **B**) Representative histogram plots showing HPA lectin binding on wild type (blue) and Gal-3$^{-/-}$ (green) monocytes, with isotype control (grey). **C**) MFI values were plotted for all the lectins tested and the data are shown as mean±SEM of 3-6 mice per group, significance was assessed using an unpaired student's t-test.

3.5.6 CD11b and L-selectin expression on Gal-3$^{-/-}$ neutrophils

Wild type or Gal-3$^{-/-}$ whole blood was collected by cardiac puncture using heparin (10U/mL) and treated for 10min at 37°C with vehicle (PBS), TNFα (50ng/mL) or IL-1β (50ng/mL) before cell staining with antibodies against CD11b and L-selectin as well as the neutrophil marker Ly-6G (Clone 1A8). Data are shown as mean±SEM and significance was assessed by two-way ANOVA and Bonferroni's multiple comparison post-test. In contrast to treatment with IL-1β, which did not alter expression from vehicle treated cell levels; treatment with TNFα increased neutrophil expression of CD11b in wild type cells (Figure 3.12C; vehicle 828.4±226.6, IL-1β 982.8±218.6 *vs.* TNFα 1616.2±84.4). Furthermore, when compared to their wild type counterparts, Gal-3$^{-/-}$ neutrophils exhibited significantly reduced levels of CD11b basally (Figure 3.12C; WT 828.4±226.6 *vs.* KO 191.0±28.3, $P<0.05$, n=3-5) and after treatment with IL-1β and TNFα (Figure 3.12C; WT 1616.2±84.4 *vs.* KO 918.0±34.0, $P<0.01$, n=3-5).

In a similar fashion to CD11b expression patterns in wild type neutrophils, treatment with TNFα induced L-selectin shedding though IL-1β did not (Figure 3.13C; vehicle 187.6±66.0, IL-1β 198.58±58.2 *vs.* TNFα 44.1±7.9). However, L-selectin shedding was unaltered in the Gal-3$^{-/-}$ neutrophils basally (Figure 3.13C; WT 187.6±66.0 *vs.* KO 137.1±63.3, ns, n=5) and after TNFα treatment (Figure 3.13C; WT 44.1±7.9 *vs.* KO 43.2±18.3, ns, n=5).

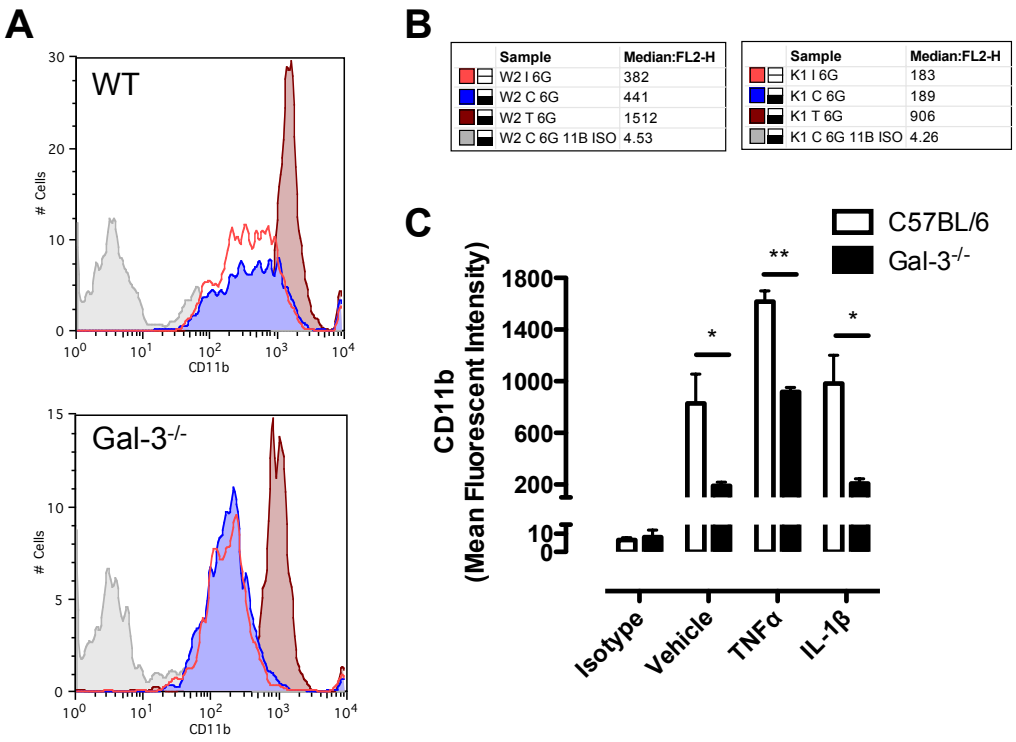

Figure 3.12 Gal-3$^{-/-}$ neutrophils display reduced levels of CD11b basally and after treatment with TNFα and IL-1β

Wild type or Gal-3$^{-/-}$ whole blood was collected by cardiac puncture using heparin (10U/mL) and treated for 10min at 37°C with vehicle (PBS), TNFα (50ng/mL) or IL-1β (50ng/mL). Murine Fc Receptors were blocked before cell staining with antibodies against CD11b as well as the neutrophil marker Ly-6G (Clone 1A8); analysis was carried out with the FACSCalibur Flow cytometer and FlowJo software, as detailed in Methods. **A**) Representative histogram plots of wild type and Gal-3$^{-/-}$ neutrophils stained for isotype control (grey) or CD11b after treatment with vehicle (blue), IL-1β (red line) or TNFα (dark red). **B**) Tables show matching MFI values for the representative histogram plots, wild type on the left and Gal-3$^{-/-}$ cells on the right. **C**) MFI values were plotted and the data are shown as mean±SEM of 3-4 mice per group, significance was assessed by two-way ANOVA and Bonferroni's multiple comparison post-test, denoted by asterisks * P<0.05 and ** P<0.01.

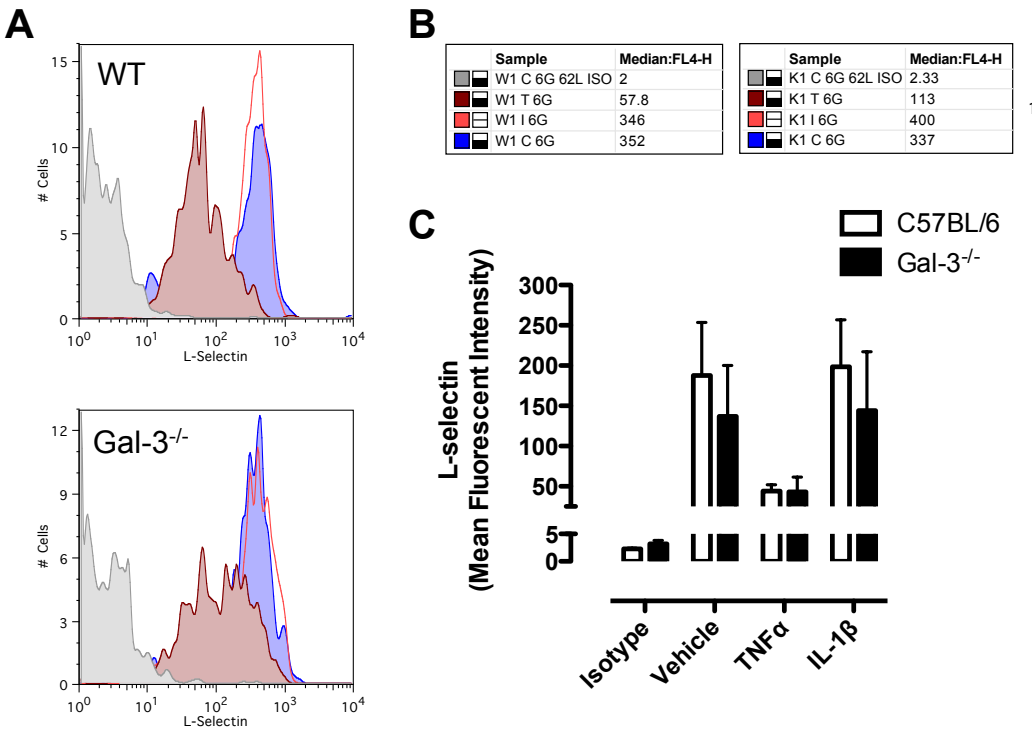

Figure 3.13 Gal-3$^{-/-}$ neutrophils display normal levels of L-selectin basally and after treatment with TNFα and IL-1β

Wild type or Gal-3$^{-/-}$ whole blood was collected by cardiac puncture using heparin (10U/mL) and treated for 10min at 37°C with vehicle (PBS), TNFα (50ng/mL) or IL-1β (50ng/mL). Murine Fc Receptors were blocked before cell staining with antibodies against L-selectin as well as the neutrophil marker Ly-6G (Clone 1A8); analysis was carried out with the FACSCalibur Flow cytometer and FlowJo software, as detailed in Methods. **A**) Representative histogram plots of wild type and Gal-3$^{-/-}$ neutrophils stained for isotype control (grey) or L-selectin after treatment with vehicle (blue), IL-1β (red line) or TNFα (dark red). **B**) Tables show matching MFI values for the representative histogram plots, wild type on the left and Gal-3$^{-/-}$ cells on the right. **C**) MFI values were plotted and the data are shown as mean±SEM of 3-4 mice per group, significance was assessed by two-way ANOVA and Bonferroni's multiple comparison post-test.

3.5.7 CD11b and L-selectin expression on Gal-3$^{-/-}$ monocytes

Wild type or Gal-3$^{-/-}$ whole blood was collected by cardiac puncture using heparin (10U/mL) and treated for 10min at 37°C with vehicle (PBS), TNFα (50ng/mL) or IL-1β (50ng/mL) before cell staining with antibodies against CD11b and L-selectin as well as the monocyte marker Ly-6C. Data are shown as mean±SEM and significance was assessed by two-way ANOVA and Bonferroni's multiple comparison post-test. The variation in the monocyte populations was much greater than in the neutrophil population. In a similar fashion to the neutrophil expression pattern, treatment with TNFα but not IL-1β increased monocyte expression of CD11b (Figure 3.14C; vehicle 310.4±107.8, IL-1β 418.2±149.5 *vs.* TNFα 562.8±144.8) and induced L-selectin shedding (Figure 3.15C; vehicle 195.5±42.6, IL-1β 193.4±48.2 *vs.* TNFα 92.0±28.3).

In contrast to expression on neutrophils, CD11b expression on Gal-3$^{-/-}$ monocytes was comparable to wild type cells, both in vehicle (Figure 3.14C; WT 310.4±107.8 *vs.* KO 325.2±153.8) and TNFα treated cells (Figure 3.14C; WT 562.8±144.8 *vs.* KO 523.4±159.6). L-selectin shedding was also unchanged in the Gal-3$^{-/-}$ monocytes after TNFα treatment (Figure 3.15C; WT 92.0±28.3 *vs.* KO 62.7±23.7), though its possible that their basal expression of the selectin showed a trend to be reduced when compared to their wild type counterparts (Figure 3.15C; WT 197.5±42.6 *vs.* KO 116.6±50.3).

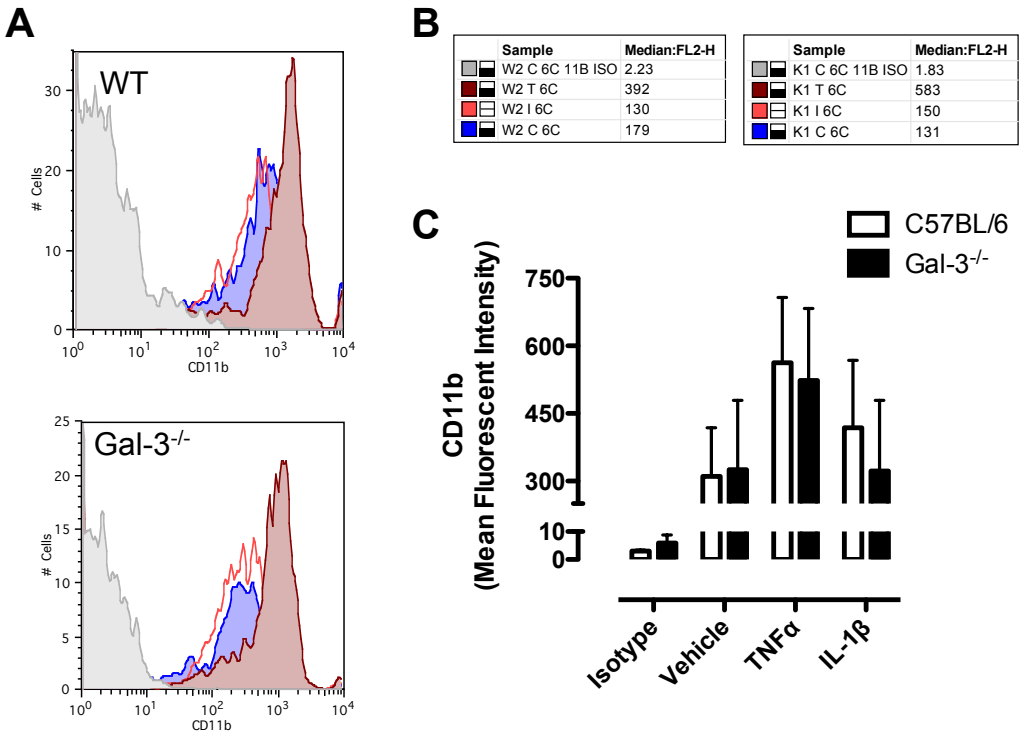

Figure 3.14 Gal-3$^{-/-}$ monocytes display normal levels of CD11b basally and after treatment with TNFα and IL-1β

Wild type or Gal-3$^{-/-}$ whole blood was collected by cardiac puncture using heparin (10U/mL) and treated for 10min at 37°C with vehicle (PBS), TNFα (50ng/mL) or IL-1β (50ng/mL). Murine Fc Receptors were blocked before cell staining with antibodies against CD11b as well as the monocyte marker Ly-6C; analysis was carried out with the FACSCalibur Flow cytometer and FlowJo software, as detailed in Methods. **A**) Representative histogram plots of wild type and Gal-3$^{-/-}$ neutrophils stained for isotype control (grey) or L-selectin after treatment with vehicle (blue), IL-1β (red line) or TNFα (dark red). **B**) Tables show matching MFI values for the representative histogram plots, wild type on the left and Gal-3$^{-/-}$ cells on the right. **C**) MFI values were plotted and the data are shown as mean±SEM of 3-4 mice per group, significance was assessed by two-way ANOVA and Bonferroni's multiple comparison post-test.

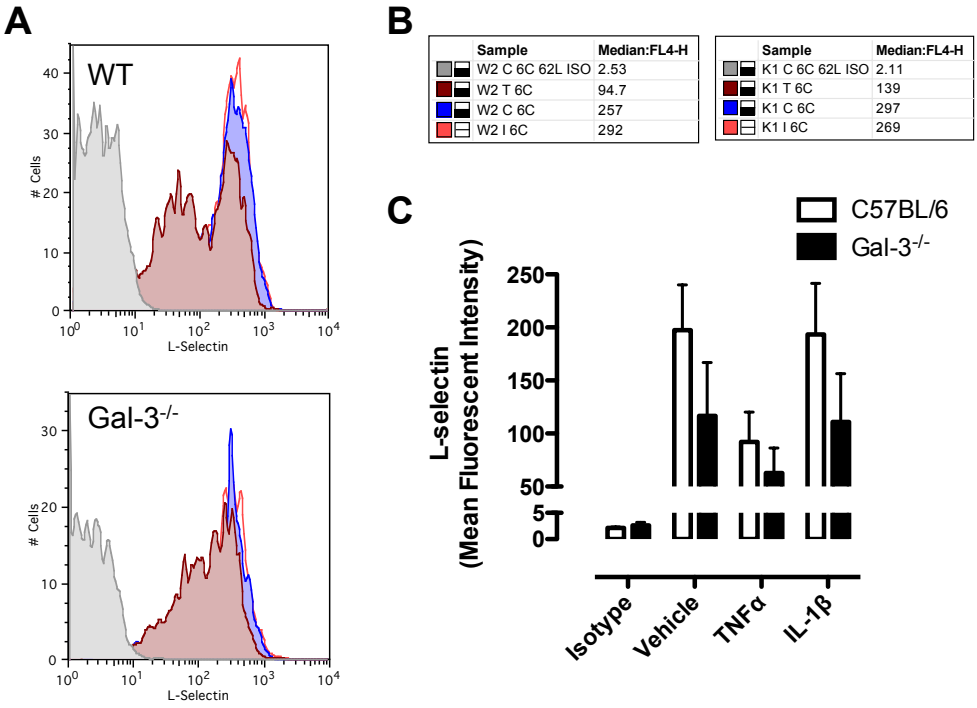

Figure 3.15 Gal-3$^{-/-}$ monocytes display normal levels of L-selectin basally and after treatment with TNFα and IL-1β

Wild type or Gal-3$^{-/-}$ whole blood was collected by cardiac puncture using heparin (10U/mL) and treated for 10min at 37°C with vehicle (PBS), TNFα (50ng/mL) or IL-1β (50ng/mL). Murine Fc Receptors were blocked before cell staining with antibodies against L-selectin as well as the monocyte marker Ly-6C; analysis was carried out with the FACSCalibur Flow cytometer and FlowJo software, as detailed in Methods. **A**) Representative histogram plots of wild type and Gal-3$^{-/-}$ neutrophils stained for isotype control (grey) or L-selectin after treatment with vehicle (blue), IL-1β (red line) or TNFα (dark red). **B**) Tables show matching MFI values for the representative histogram plots, wild type on the left and Gal-3$^{-/-}$ cells on the right. **C**) MFI values were plotted and the data are shown as mean±SEM of 3-4 mice per group, significance was assessed by two-way ANOVA and Bonferroni's multiple comparison post-test.

3.6 Characterisation of isolated murine lung endothelial cells from Gal-3$^{-/-}$ mice

Murine lung endothelial cells were isolated from C57BL/6 or Gal-3$^{-/-}$ mice and first characterised by flow cytometric analysis of cell surface expression of Gal-3 and the endothelial cell marker, ICAM-2. There were no morphological differences between the wild type and Gal-3$^{-/-}$ MLEC (Figure 3.16B,C) when viewing by bright field microscopy in addition to by forward-side scatter flow cytometry plots (Figure 3.16A). The gated cellular events were plotted on a histogram for MFI of Gal-3 (blue) or its isotype control IgG2a (grey), the wild type cells were found to moderately express Gal-3 on their surface under basal conditions and the Gal-3$^{-/-}$ cell were found to have no Gal-3 expression (Figure 3.16A, middle panel). Over 90% of the total events in both C57BL/6 and Gal-3$^{-/-}$ mice expressed cell surface ICAM-2 (green), confirming that the isolated cell populations were of high purity for endothelial cells (Figure 3.16A, right panel).

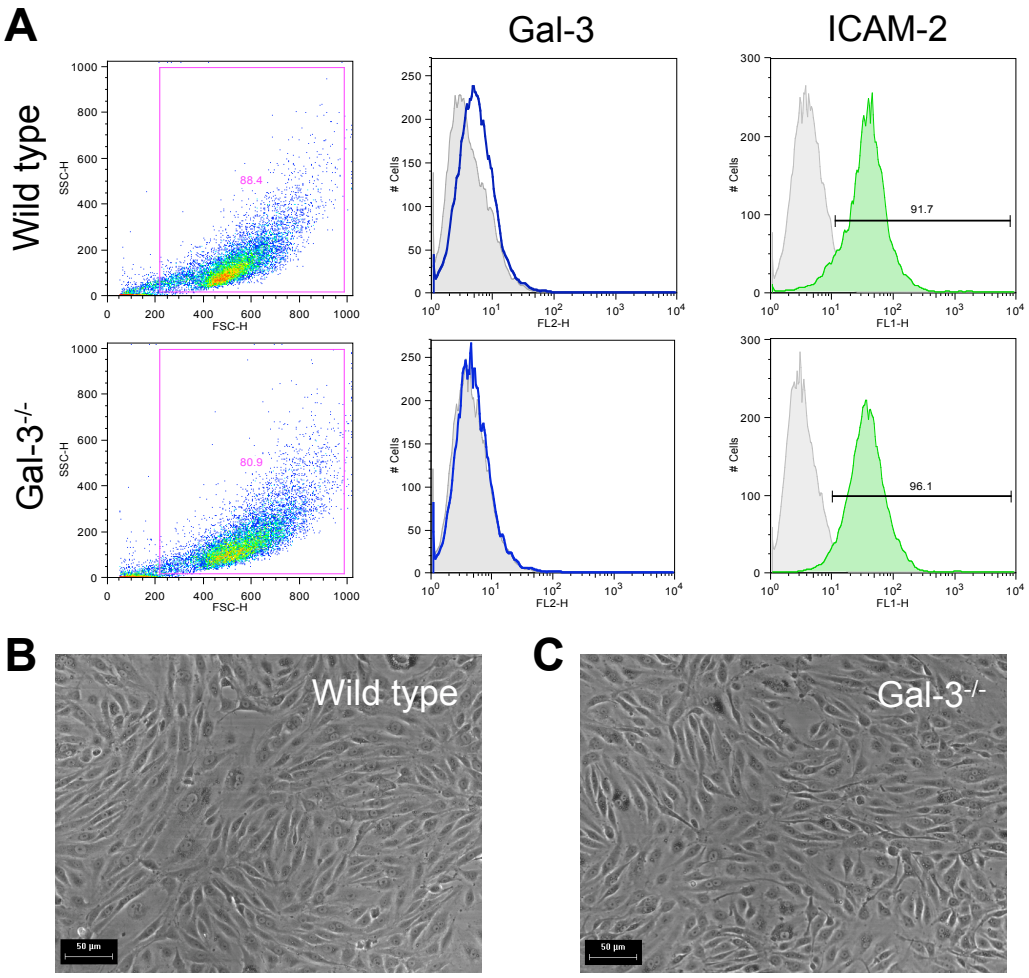

Figure 3.16 Characterisation of wild type and Gal-3$^{-/-}$ murine primary endothelial cells

Confluent MLEC were collected and stained on ice for cell surface antigens before analysis with the FACSCalibur Flow cytometer and FlowJo software, as detailed in Methods. **A)** Representative forward/side scatter plot for the MLEC populations, gated for >80% of the total events. **B)** Histogram showing mean fluorescent intensity of gated MLEC population for IgG2a isotype control (grey) or Gal-3 (blue) stained wild type (top) and Gal-3$^{-/-}$ (bottom) cells. **C)** Histogram showing mean fluorescent intensity of gated MLEC population for unlabelled control (grey) or ICAM-2 (green) stained wild type (top) and Gal-3$^{-/-}$ (bottom) cells.

3.6.1 Basal surface expression of E-selectin and ICAM-1 on wild type and Gal-3$^{-/-}$ MLEC

Confluent wild type and Gal-3$^{-/-}$ MLEC were collected and murine Fc receptors were blocked before cell staining for surface ICAM-1 and E-selectin and their isotype controls before analysis by flow cytometry. MFI was expressed as mean±SEM of 3 mice sets and statistical significance was assessed using an unpaired student's t-test. When compared to their wild type counterparts, Gal-3$^{-/-}$ MLEC express significantly reduced basal ICAM-1 (Figure 3.17 lower panel; WT 623.7±110.0 *vs.* KO 121.6±106.2, $P<0.05$, n=3). Though slightly reduced, the levels of surface E-selectin on Gal-3$^{-/-}$ MLEC were comparable to wild type (Figure 3.17 upper panel; WT 8.7±2.8 *vs.* KO 5.3±0.6, not significant).

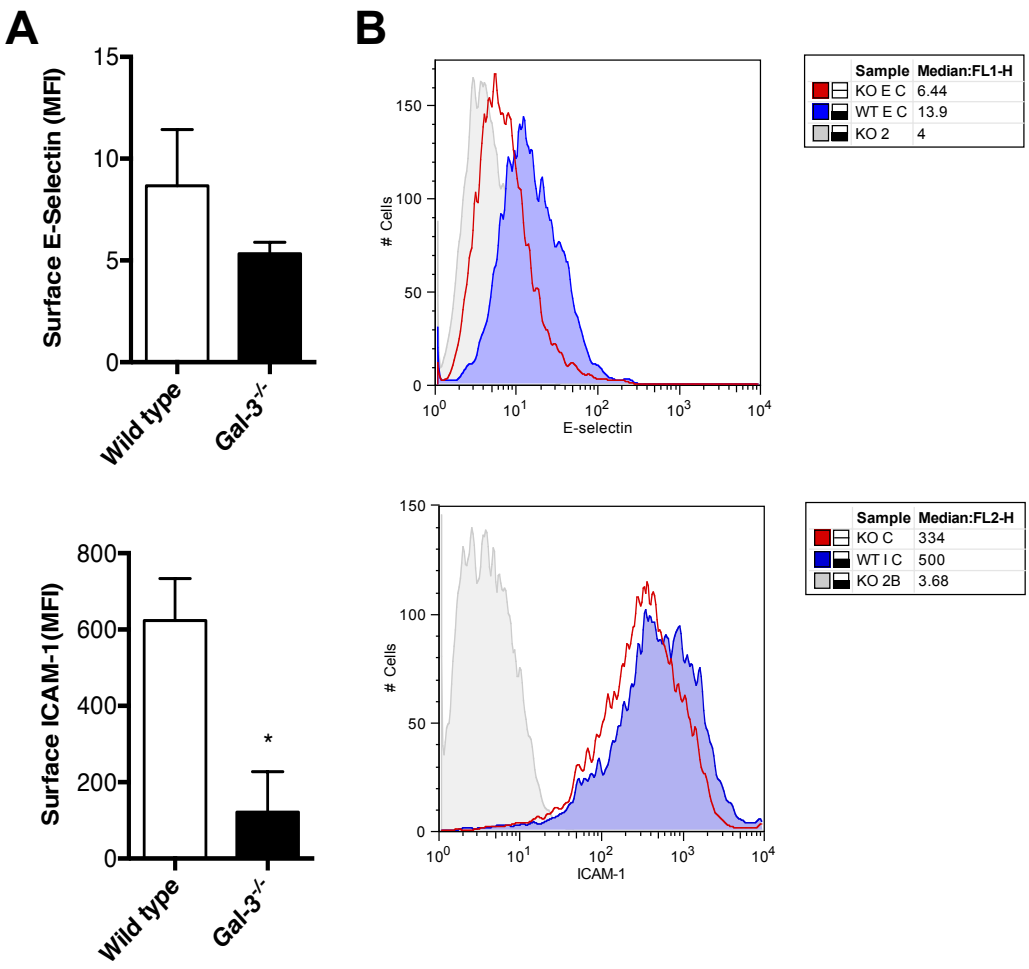

Figure 3.17 Basal surface expression of E-selectin and ICAM-1 on wild type and Gal-3$^{-/-}$ MLEC

Confluent wild type and Gal-3$^{-/-}$ MLEC were collected and murine Fc receptors were blocked before cell staining for surface ICAM-1 and E-selectin and their isotype controls before analysis with the FACSCalibur Flow cytometer and FlowJo software, as detailed in Methods. **A)** MFI was expressed as mean±SEM of 3 mice sets for E-selectin (upper panel) and ICAM-1 (lower panel). Statistical significance was assessed using an unpaired student's t-test and is denoted by asterisks * $P<0.05$. **B)** Representative histogram plots showing isotype control (grey tinted), wild type cells (blue) and Gal-3$^{-/-}$ cells (red line) stained for E-selectin (upper panel) and ICAM-1 (lower panel).

3.6.2 Surface expression of E-selectin and ICAM-1 on wild type and Gal-3$^{-/-}$ MLEC after TNFα treatment

Confluent wild type and Gal-3$^{-/-}$ MLEC were treated for 4h with vehicle (PBS) or TNFα in varying concentrations (10, 100, 200ng/mL). The MLEC were collected and murine Fc receptors were blocked before cell staining for surface ICAM-1 and E-selectin and their isotype controls and analysis by flow cytometry**.** MFI was expressed as mean±SEM of 3 mice sets and statistical significance was assessed using two-way ANOVA followed by Bonferroni's multiple comparison post-test. There were no significant differences in the levels of E-selectin expression on wild type and Gal-3$^{-/-}$ MLEC in response to treatment with TNFα though the variation within mice sets was extremely large (Figure 3.18A, upper panel,). In contrast, the Gal-3$^{-/-}$ MLEC expressed much-reduced ICAM-1 on their surface after treatment with 100ng/mL TNFα (Figure 3.18A, lower panel; WT 1070.3±245.0 *vs.* KO 280.3±262.9, $P<0.05$, n=3). Additionally, though the interaction of gene and treatment did not cause significant variation in the results, the effect of gene overall was considered significant (Figure 3.18A, lower panel, $P=0.0002$, n=3)

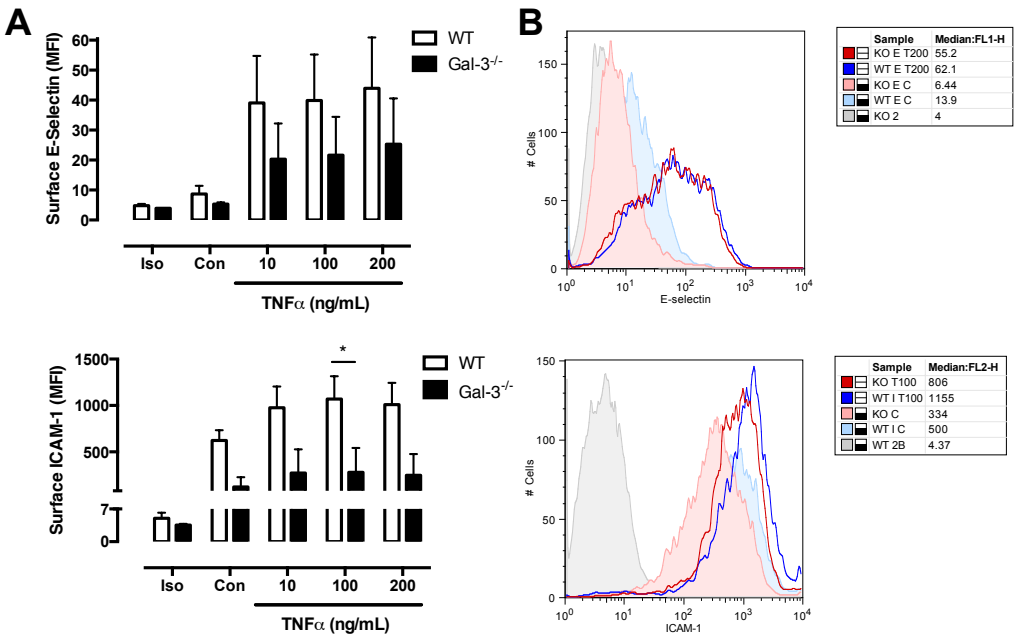

Figure 3.18 Surface expression of E-selectin and ICAM-1 on wild type and Gal-3$^{-/-}$ MLEC after TNFα treatment

Confluent wild type and Gal-3$^{-/-}$ MLEC were treated for 4h with vehicle (PBS) or TNFα in varying concentrations (10, 100, 200ng/mL). The MLEC were collected and murine Fc receptors were blocked before cell staining for surface ICAM-1 and E-selectin and their isotype controls before analysis with the FACSCalibur Flow cytometer and FlowJo software, as detailed in Methods. **A)** MFI was expressed as mean±SEM of 3 mice sets for E-selectin (upper panel) and ICAM-1 (lower panel). Statistical significance was assessed using two-way ANOVA followed by Bonferroni's multiple comparison post-test and is denoted by asterisks * P<0.05. **B)** Representative histogram plots showing isotype control (grey tinted), vehicle (PBS) treated wild type cells (filled pale blue), TNFα (100ng/mL)-treated wild type cells (blue line), vehicle (PBS) treated Gal-3$^{-/-}$ cells (filled pale red) and TNFα (100ng/mL)-treated Gal-3$^{-/-}$ cells (red line) stained for E-selectin (upper panel) and ICAM-1 (lower panel).

3.6.3 Surface expression of E-selectin and ICAM-1 on wild type and Gal-3$^{-/-}$ MLEC after IL-1β treatment

Confluent wild type and Gal-3$^{-/-}$ MLEC were treated for 4h with vehicle (PBS) or IL-1β in varying concentrations (1, 50, 100ng/mL). The MLEC were collected and murine Fc receptors were blocked before cell staining for surface ICAM-1 and E-selectin and their isotype controls and analysis by flow cytometry**.** MFI was expressed as mean±SEM of 3 mice sets and statistical significance was assessed using two-way ANOVA followed by Bonferroni's multiple comparison post-test. When compared to their wild type counterparts, the Gal-3$^{-/-}$ MLEC expressed much reduced E-selectin on their surface after treatment with both 50ng/mL (Figure 3.19A,B, upper panel; WT 58.5±4.7 *vs.* KO 37.0±21.8, P<0.01, n=3) and 100ng/ml (Figure 3.19 A, B, upper panel; WT 37.0±21.8 *vs.* KO ±, P<0.05, n=3) IL-1β. Furthermore, ordinary two-way ANOVA found that the interaction of both gene and treatment caused significant variation in the results at all concentrations (Figure 3.19 A, B, upper panel, interaction P=0.0441, n=3) and the Gal-3$^{-/-}$ MLEC were found to have significantly reduced E-selectin expression overall (Figure 3.19 A, B, upper panel, P=0.0006, n=3).

The Gal-3$^{-/-}$ MLEC expressed much-reduced ICAM-1 on their surface after treatment with 50ng/mL IL-1β (Figure 3.19A A, B, lower panel; WT 1055.7±228.8 *vs.* KO 276.5±257.3, P<0.05, n=3). Additionally, though the interaction of gene and treatment did not cause significant variation in the results, the effect of gene overall was considered significant (Figure 3.19 A, B, lower panel, P=0.0002, n=3).

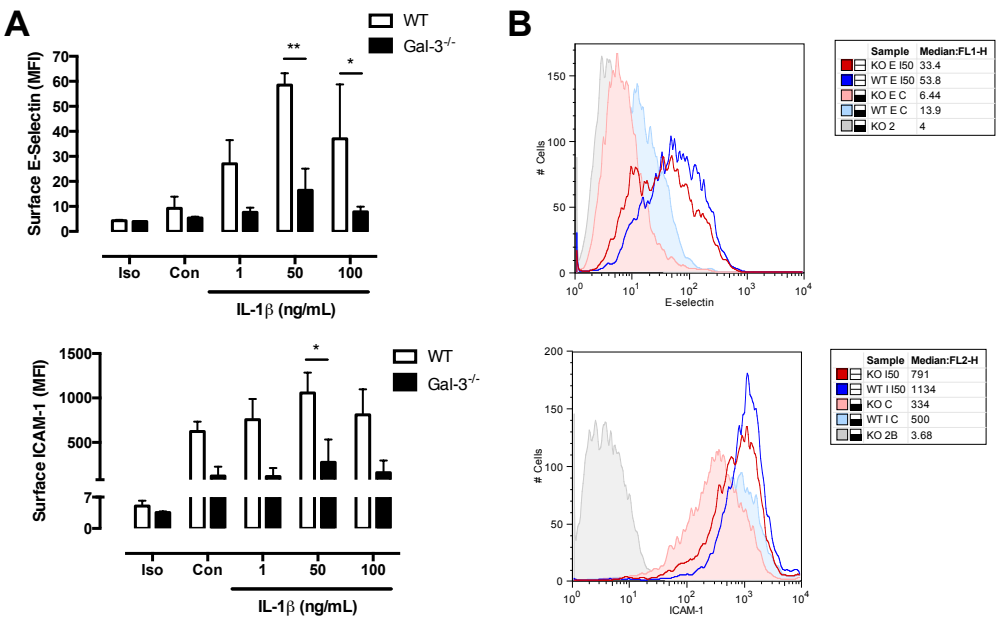

Figure 3.19 Surface expression of E-selectin and ICAM-1 on wild type and Gal-3$^{-/-}$ MLEC after IL-1β treatment

Confluent wild type and Gal-3$^{-/-}$ MLEC were treated for 4h with vehicle (PBS) or IL-1β in varying concentrations (1, 50, 100ng/mL). The MLEC were collected and murine Fc receptors were blocked before cell staining for surface ICAM-1 and E-selectin and their isotype controls before analysis with the FACSCalibur Flow cytometer and FlowJo software, as detailed in Methods. **A)** MFI was expressed as mean±SEM of 2-3 mice sets for E-selectin (upper panel) and ICAM-1 (lower panel). Statistical significance was assessed using two-way ANOVA followed by Bonferroni's multiple comparison post-test and is denoted by asterisks * P<0.05 and ** P<0.01. **B)** Representative histogram plots showing isotype control (grey tinted), vehicle (PBS) treated wild type cells (filled pale blue), IL-1β (50ng/mL)-treated wild type cells (blue line), vehicle (PBS) treated Gal-3$^{-/-}$ cells (filled pale red) and IL-1β (50ng/mL)-treated Gal-3$^{-/-}$ cells (red line) stained for E-selectin (upper panel) and ICAM-1 (lower panel).

3.7 Discussion

The role of endogenous Gal-3 in leukocyte recruitment was examined; Gal-3$^{-/-}$ mice and Gal-3$^{-/-}$ leukocytes were studied in models of inflammation using techniques such as IVM and flow chamber assays, which enable the analysis of aspects of the cascade in isolation. Firstly, the wild type response to fixed-time treatment with TNFα and IL−1β locally was characterised; these cytokines were chosen for a number of reasons. It is well established that these two stimuli are important pro-inflammatory modulators of both the acute inflammatory response (Dinarello, 2011, Dinarello, 2000) and long-term disease pathogeneses where inflammation has become chronic in nature, for example in rheumatoid arthritis (Schiff, 2000, Kollias *et al*., 1999). Initial studies on the effects of these cytokines on endothelial cell function found that *in vitro* they induce increased expression of E-selectin (Bevilacqua *et al*., 1989), VCAM-1 (Osborn *et al*., 1989) and ICAM-1 (Pober *et al*., 1986), thus initiating their state of 'adhesiveness' for leukocytes. Furthermore, the administration of these cytokines *in vivo* results in leukocyte recruitment that may differ in mode; for example, an early study examining responses to both cytokines intradermally in the rabbit found that IL-1β-induced neutrophil extravasation peaked at 3-4h whereas TNFα-induced neutrophil extravasation was much quicker and also associated with protein synthesis-independent oedema formation (Rampart *et al*., 1989). More recently, Thompson *et al.* reported that neutrophil recruitment in cremasteric venules of PECAM-1$^{-/-}$ mice was

reduced when compared to wild type mice treated with IL-1β but not TNFα (Thompson *et al*., 2001).

In this study IVM showed that after 4 - but not 2h - treatment with these cytokines the cremasteric microcirculation was shown to be inflamed and exhibited increased levels of leukocyte adhesion and emigration as well as reduced leukocyte rolling velocity, which is in line with the literature (Young *et al*., 2002, Thompson *et al*., 2001). In terms of endogenous Gal-3, Gal-3$^{-/-}$ mice displayed similar leukocyte recruitment profiles to their wild type counterparts, with the exception of slow rolling in response to both stimuli and emigration after IL-1β, but not TNFα treatment. Though the vessels were inflamed, the leukocyte rolling velocity in response to both TNFα and IL-1β 4h treatment was not reduced in Gal-3$^{-/-}$ animals, suggesting that Gal-3 is a requirement for slow rolling in this experimental system.

Early intravital studies using the cremaster model to investigate leukocyte rolling established that expression of P-selectin at the endothelial cell surface and P-selectin-dependent leukocyte rolling (20-50μm/s) occur within 10 min of surgical trauma and that this is upregulated after 2 h treatment with TNFα. In contrast, baseline E-selectin expression is barely detectable but significantly upregulated after 2 h treatment with TNFα (Jung and Ley, 1997). At 2 hours after TNFα treatment leukocytes in wild type, P- or L-selectin$^{-/-}$ mice were travelling at rolling velocities of 3-7μm/s; however, in E-selectin$^{-/-}$ mice the leukocyte rolling velocity

remained at 12-20μm/s (Kunkel and Ley, 1996). Thus, since leukocyte rolling is carried out by Selectin binding and slow rolling predominantly by E-selectin, it was important to look at Gal-3 roles in E-selectin-dependent rolling in greater depth.

The parallel chamber flow assay was used as this enabled the investigation of both wild type and Gal-$3^{-/-}$ leukocytes in tandem; murine whole blood from wild type or Gal-$3^{-/-}$ mice was flown over E-selectin-coated plates and the number of leukocytes captured was quantified. It was found that the absence of Gal-3 did not affect white blood cell counts and so any differences observed can be attributed to changes in the leukocytes themselves. This is in line with full haematological reports published on the Consortium for Functional Genomics, which find no differences in Gal-$3^{-/-}$ blood components and leukocyte cell counts when compared to wild type mice, excepting a slight but significant reduction in blood glucose concentration (CFG, 2013). Heparin was used to prevent clotting as studies have shown that increasing concentrations of this anti-coagulant does not affect neutrophil-selectin interactions (Reinhardt and Kubes, 1998). Strikingly, Gal-$3^{-/-}$ leukocytes were not captured to the E-selectin and those few that did displayed an inability to enter a more activated phenotype, which was seen in wild type cells when they became phase-dark. This reduced capture of Gal-$3^{-/-}$ cells was replicated even when the cells were flown together in the same chamber, with the use of fluorescent dyes to distinguish the two genotypes. These results suggest that in absence of Gal-3, leukocytes have undergone inherent

changes that cannot be fully rescued by extracellular factors, for example those found in the plasma of wild-type mice. Taken together, the cells lack the machinery needed to bind E-selectin and facilitate the downstream signalling pathways that are initiated once bound; thus, E-selectin and its ligands were studied in greater depth.

All selectins have structurally homologous extracellular domains with amino acid lectin domains, epidermal growth factor domains and complement regulatory repeats; however, they have distinct cytoplasmic domains, resulting in their differing roles (Hu *et al*., 2000). Early selectin studies found that leukocyte adhesion to IL-1β-activated endothelial cells induced clustering of E-selectin near the binding sites and that cross-linking of E-selectin led to its transmembrane linkage to the actin cytoskeleton via its cytoplasmic domain (Yoshida *et al*., 1996). Subsequent serine phosphorylation of this domain suggests that it can transduce signals and thus is highly important in downstream signalling from the receptor (Yoshida *et al*., 1998). Upon E-selectin binding by leukocytes or antibody cross-linking MAPK is activated; specifically, a Ras/Raf/phospho-MEK complex is formed, which is associated with increased expression of an early transcription factor for many pro-inflammatory genes, c-fos (Hu *et al*., 2000). These effects were E-selectin-mediated, as adhesion of JY cells, a human leukocyte cell line that binds predominantly via ICAM-1/LFA-1 interactions, to IL-1β-activated endothelia did not induce MAPK activation (Hu *et al*., 2000). Furthermore, it is now known that rolling on E-selectin leads to LFA-1

activation via syk-dependent pathways, whereby the β_2-integrin enters the extended but not high affinity state to facilitate leukocyte slow rolling on ICAM-1 (Kuwano *et al*., 2010). Zanardo *et al.* found that in C57BL/6 mice treated locally with TNFα for 3h before surgical preparation all rolling was E- and P-selectin- dependent; it was mediated predominantly by PSGL-1 but another ligand was also present, which was down-regulated during systemic, but not local TNFα administration (Zanardo *et al*., 2004). It was unclear whether the ligand was shed or internalised and the authors proposed that it was not L-selectin, CD43, β_2-integrin or CD66-nonspecific cross-reacting antigen, suggesting that there are more E-selectin ligands to be identified (Zanardo *et al*., 2004). In slight contrast, Yang *et al.* found that E-selectin-mediated slow rolling following TNFα treatment was unaffected in PSGL-1$^{-/-}$ mice, confirming that other E-selectin ligands are functionally important and this was in addition to observing low levels of E-selectin-independent rolling (Yang *et al*., 1999).

Since there have been no reports of direct interactions between galectins and selectins, we hypothesised that lack of endogenous Gal-3 may affect availability of separate ligands. The levels of ESL-1, PSGL-1 and other E-selectin ligand expression in Gal-3$^{-/-}$ mice have yet to be reported; however, it has been shown that levels of PSGL-1 are similar in Mgat5$^{-/-}$ and wild type neutrophils though the expression pattern at the cell surface may differ, resulting in altered neutrophil recruitment in these animals (Bahaie *et al*., 2011). In order to address this, the expression of CD44 and PSGL-1 was examined by flow cytometry in wild type and Gal-3$^{-/-}$

leukocytes. Basally, neutrophils and monocytes express comparable levels of both ligands when compared to wild type cells; however, after treatment with TNFα but not IL-1β, Gal-3$^{-/-}$ neutrophils express reduced PSGL-1 in comparison with wild type counterparts. This suggests a possible mechanism behind reduced slow rolling in response to TNFα *in vivo* though, does not explain the reduced IL-1β-induced slow rolling seen in the absence of Gal-3.

All selectin ligands carry sLe^x, commonly on α1,3-fucosylated and α2,3-sialylated O-glycans and though they are less well understood, E-selectin ligands specifically must be modified by a fucosyltransferase such as fucosyltransferase VII or IV to be functional. Recent work has established that the E-selectin ligands ESL-1 and CD44 bind in a similar fashion to galectins, via N-linked glycans whereas PSGL-1 uses O-glycans to bind (Block *et al*., 2012). The importance of post-translational modification of E-selectin ligands to their functionalilty was recently demonstrated using mice lacking the polypeptide GalNAc transferase-1, which generates core-type O-glycan structures from GalNAc binding to threonine or serine residues in their protein backbone. GalNt-1$^{-/-}$ mice display reduced P- and E-selectin-mediated rolling, which in turn reduces adhesion and emigration of leukocytes in these animals; signalling through syk and thus integrin activation was unaffected, confirming that it is the ability of ligands to bind rather than downstream pathways, which are impaired (Block *et al*., 2012). Of particular importance, Saravanan *et al.* (2009) found that some glycogenes were differentially expressed in

Gal-3$^{-/-}$ mice undergoing a corneal model of wound-healing; these included glycosyltransferases and glycosidases that were down- or upregulated in order to produce less N-glycans and more O-glycans. For example, an enzyme involved in Gal-3 ligand synthesis, β3-galactotransferase 5 (β3GalT5), was downregulated whereas N-acetylgalactosaminyltransferases-3 and -7 (ppGalNAcTs-3 and -7) which initiate O-glycosylation, were upregulated (Saravanan *et al*., 2009a). Hence the glycosylation pattern of Gal-3$^{-/-}$ leukocytes was assessed, as any inherent changes would greatly affect the ability of E-selectin ligands such as ESL-1, PSGL-1 and CD44 to bind. This was carried out using a validated panel of biotinylated lectins, which each bind glycans of different structures. As untreated Gal-3$^{-/-}$ leukocytes exhibited reduced capture to E-selectin under conditions of flow, basal levels of lectin binding by neutrophils and monocytes was analysed by flow cytometry. When compared to wild type cells, Gal-3$^{-/-}$ neutrophils exhibited reduced levels of PNA and HPA lectin binding, yet comparable levels of SNA, L-PHA and MAL II binding. This was also apparent for the Gal-3$^{-/-}$ monocytes, though the levels were not quite significant.

HPA selectively binds to α-N-acetylgalactosamine residues and has been extensively studied as a marker of cancer cell metastasis; one study found that HPA recognises integrin-α_6 in breast and colorectal cancer cells (Rambaruth *et al*., 2012). Another study hypothesised that as it is similar in structure to sLe^x, they may have similar but not identical glycotopes (Kohler *et al*., 2010); supporting the idea put forward here that

reduced HPA binding indicates reduced selectin ligand binding. PNA lectin has specificity for terminal β-galactose residues, it is inhibited by lactose and displays enhanced binding of sialidase-treated glycoproteins, which have no terminal sialic acid structures. The so-called PNA receptor in keratinocytes is CD44, an E-selectin ligand; suggesting that though CD44 levels are not reduced in Gal-3$^{-/-}$ leukocytes, they may display reduced binding capacity due to altered glycosylation (Hudson *et al*., 1995). In fact Gal-3$^{-/-}$ monocytes displayed slightly increased CD44 in response to IL-1β perhaps as result of a compensatory mechanism due to reduced binding, which warrants further investigation. Of the unchanged lectins, both SNA and MAL II bind sialic acid, though SNA prefers to bind to terminal residues in an α2,6 linkage and MAL II prefers those in an α2,3 linkage; L-PHA binds β1,8-branches on complex N-glycans and thus may indicate the presence of galectin and specifically Gal-3 ligands. It is interesting to note that these were not changed, especially as Saravanan *et al.* (2009) found that N-glycans in general were reduced in Gal-3$^{-/-}$ mice; however, this study was carried out in corneal cells and so there may be cell type-specific differences in differential gene expression of the Gal-3$^{-/-}$ animals, which should be further investigated.

The two classical stimuli TNFα and IL-1β were used throughout this study since they are known to have differing roles on both the leukocytes and endothelial cells. For example, IL-1β activates the endothelia directly whereas wild type neutrophils respond to TNFα by increasing their

expression of β_2-integrin (CD18) and initiating L-selectin shedding, this is in contrast to cells treated with IL-1β which do not (Young *et al*., 2002). It was therefore interesting to examine whether endogenous Gal-3 affected this response and to do so flow cytometry using wild type and Gal-$3^{-/-}$ whole blood was carried out. Since Gal-3 is not thought to affect β_2-integrin-dependent leukocyte recruitment (Nieminen *et al*., 2008), CD11b, also known as αM-integrin, which forms Mac-1 with the β_2-integrin CD18, was investigated. L-selectin is involved in the initial fast rolling stage of leukocyte recruitment, though is important for secondary leukocyte capture whereby leukocytes bind L-selectin before strengthening interactions on P-and E-selectin (Ley *et al*., 2007). It was found that Gal-$3^{-/-}$ neutrophils exhibited reduced CD11b expression basally and a reduced capacity to increase expression of this integrin in response to TNFα though the monocytes did not. Additionally, L-selectin expression in the Gal-$3^{-/-}$ neutrophils and monocytes were unchanged from wild type cells, both basally and after stimulation, suggesting that their ability to initiate the rolling stages of leukocyte recruitment might be unimpaired.

The predominant role of CD11b is during the intravascular crawling stage of leukocyte recruitment where Mac-1 binds to its ligand ICAM-1 (Green *et al*., 2004, Phillipson *et al*., 2006). To investigate CD11b biology, studies often compare Mac-$1^{-/-}$ mice to LFA-$1^{-/-}$ mice, which lack the integrin CD18/CD11a. Mac-$1^{-/-}$ neutrophils adhere to post-capillary venules in similar numbers to LFA-$1^{-/-}$ neutrophils, however they fail to crawl towards areas of preferential transmigration and though they

eventually transmigrate in similar numbers to wild type neutrophils, this process requires a much longer length of time compared to their wild type counterparts (Petri *et al*., 2008). Of particular importance to our finding that Gal-3$^{-/-}$ leukocytes express reduced CD11b basally and fail to reduce their rolling velocity in response to TNFα treatment of the cremaster, are studies which report that Mac-1 binding to ICAM-1 is involved in slow leukocyte rolling in response to this cytokine (Dunne *et al*., 2003).

To complement these studies carried out on the leukocytes, murine lung endothelial cells (MLECs) were isolated from wild type and Gal-3$^{-/-}$ mice and analysed by flow cytometry. Firstly, basal levels of E-selectin and ICAM-1 were examined, as these CAMs both have roles in leukocyte slow rolling and their expression is upregulated by IL-1β and TNFα stimulation (Pober *et al*., 1986, Bevilacqua *et al*., 1989). Levels of E-selectin in the two MLEC genotypes were comparable; however, Gal-3$^{-/-}$ MLEC exhibited much-reduced ICAM-1 under basal conditions. Furthermore, the effect of gene was considered to significantly reduce ICAM-1 expression on endothelial cells after treatment with TNFα and IL-1β. Similarly, after IL-1β but not TNFα treatment, Gal-3$^{-/-}$ MLECs also expressed reduced E-selectin overall; a finding that would have direct consequences for IL-1β-induced slow rolling and possibly subsequent transmigration. Furthermore, if Gal-3$^{-/-}$ neutrophils are unable to increase CD11b expression upon incubation with these classical stimuli and Gal-3$^{-/-}$ endothelial cells express reduced ICAM-1, this may explain why Gal-3$^{-/-}$ leukocytes do not reduce their rolling velocity *in vivo*. It is worth noting

here that despite this altered endothelial cell surface cell adhesion molecule expression, levels of adhesion were unchanged in the Gal-3$^{-/-}$ mice, both basally and after stimulation. However, Kubes *et al.* demonstrated that rolling needs to be reduced by approximately 90% to affect levels of leukocyte adhesion; these authors used a high dose of fucoidin, a sulphated homopolymer of fucose, to attain this level of reduction and determined the ensuing attenuation of reperfusion-induced leukocyte adhesion (Kubes *et al*., 1995). Furthermore, in wild type mice treated with TNFα approximately 90% of rolling leukocytes progress to become adherent and in E-selectin$^{-/-}$ mice where rolling velocities remain high, 50% of the rolling leukocytes are still able to adhere (Kunkel *et al*., 2000). These studies and data presented here highlight the complex yet distinct nature of each step in the leukocyte recruitment cascade.

In addition to its role in slow rolling, Gal-3$^{-/-}$ mice examined using intravital microscopy exhibited a significantly reduced level of emigrated leukocytes in response to 4h IL-1β treatment when compared to the wild type response. This effect was absent in TNFα-treated mice and thus it is particularly interesting to note that there may be stimulus-specific roles for Gal-3. Furthermore, since IL-1β activates the endothelia directly (Young *et al*., 2002) the differences in leukocyte emigration observed between TNFα and IL-1β-treated Gal-3$^{-/-}$ mice suggest that endothelial function may be compromised in these mice, possibly in terms of their expression of CAMs and junctional adhesion molecules involved in transmigration. More recently, it was found that neutrophil transmigration

elicited by IL-1β but not TNFα is protein-synthesis dependent and requires ICAM-2, JAM-A then PECAM-1 in distinct but sequential steps (Woodfin *et al*., 2009, Young *et al*., 2002). In future the expression of these molecules in Gal-3$^{-/-}$ endothelial cells should be assessed as well as their glycosylation pattern, since all three contain N-glycosylation sites (Koenen *et al*., 2009, Feduska *et al*., 2013, Newton *et al*., 1999). Also of interest to this study, IL-1β but not TNFα-induced neutrophil transmigration is dependent on α_6-integrin (Dangerfield *et al*., 2005), which is recognised by HPA lectin, one of those found to exhibit reduced binding in Gal-3$^{-/-}$ cells. In future, expression of α_6-integrin in the IL-1β-treated Gal-3$^{-/-}$ cremasters should be assessed as this would account for the stimulus specific roles. Another possibility is that similar to observations in Mac-1$^{-/-}$ mice, Gal-3$^{-/-}$ cells take longer to emigrate in response to IL-1β and that, given the IVM time course used here this translates as an overall reduction. In future, different fixed time protocols should be used, such as recruitment to the murine air-pouch in response to these classical stimuli to establish whether transmigration is impaired in the long-term.

Gal-3 roles in leukocyte recruitment have been studied in *in vivo* models of inflammation, albeit using different tissues and inflammatory stimuli; the findings presented here are in keeping with published results, which are summarised in Table 1.1. Many investigations report reduced leukocyte infiltration of the affected tissue in Gal-3$^{-/-}$ mice; lower numbers of lymphocytes and eosinophils were recruited to OVA-challenged

airways (Ge *et al*., 2010), there was reduced monocyte, macrophage and neutrophil recruitment to the CNS in a model of EAE (Jiang *et al*., 2009) and despite slightly conflicting reports using a thioglycollate broth model of peritonitis, two studies found reduced infiltration of neutrophils at either day 1 or 4 after insult (Hsu *et al*., 2000, Colnot *et al*., 1998). Farnworth *et al.* found that Gal-3$^{-/-}$ mice exhibited more severe lung injury associated with reduced neutrophil recruitment at 15 h after *S. pneumoniae* infection, which is β_2-integrin-independent (Farnworth *et al*., 2008). This reduction in extravasated neutrophils at 12-24 h was also reported by Nieminen *et al.,* who found that recruitment was unaffected in β_2-integrin-dependent *E. Coli*-driven lung infection in Gal-3$^{-/-}$ animals (Nieminen *et al*., 2008). This is in slight contrast to the reduction in rolling velocity in Gal-3$^{-/-}$ mice presented here as slow rolling in TNFα-treated cremaster venules is dependent on β_2-integrins; since leukocyte velocities in CD18$^{-/-}$ mice treated with TNFα were approximately 3-fold higher than those in wild type mice (Jung *et al*., 1998). However, as these findings have been reported when investigating different vascular beds and responses to varied stimuli, they would involve different phenotypes such as adhesion molecule profiles and ultimately, distinct outcomes (Rao *et al*., 2007a). Indeed, taken together these investigations further suggest that Gal-3 is a multi-faceted molecule capable of interacting with and acting *via* different receptors in different cells and tissues.

Chapter 4: Examining the effect of exogenous Gal-3 on leukocyte recruitment to the inflamed microvasculature

4.1 Analysis of the murine cremasteric microcirculation in response to treatment with exogenous Gal-3

4.1.1 Local Gal-3 treatment results in increased leukocyte recruitment in a time-dependent manner

In order to establish whether exogenous Gal-3 was capable of initiating leukocyte recruitment to the cremasteric microcirculation in the absence of a classical inflammogen, a time-course using rGal-3 was carried out. Intravital microscopy was first performed using wild type C57BL/6 mice, which were injected i.s. with rGal-3 (500ng in 400μL PBS) 2 or 4h before subsequent analysis. Leukocyte flux, rolling velocity, adhesion and emigration was investigated in segments of 100μm in 3-5 vessels per mouse and results are expressed as mean±SEM of 3-4 mice per group. Statistical significance was assessed by one-way ANOVA and Dunnett's multiple comparison post-test. Leukocyte recruitment overall was increased at the 4h but not the 2h time-point with no significant differences observed between sham-treated animals and those treated with Gal-3 for 2h (Figure 4.1C,D). In comparison, at 4h the microcirculation displayed significantly reduced leukocyte rolling velocities (Figure 4.1B; Sham 25.2±7.2 *vs.* 4h 8.8±0.5, $P<0.05$, n=3-4) as well as significant increases in both adhesion (Figure 4.1C; sham 3.7±0.9 *vs.* 4h 6.5±0.5, $P<0.05$, n=3-4) and emigration (Figure 4.1D; sham 3.4±1.3 *vs.* 4h 8.3±1.2, $P<0.05$, n=3-4). In contrast, the levels of leukocyte flux were comparable between all treatments (Figure 4.1A).

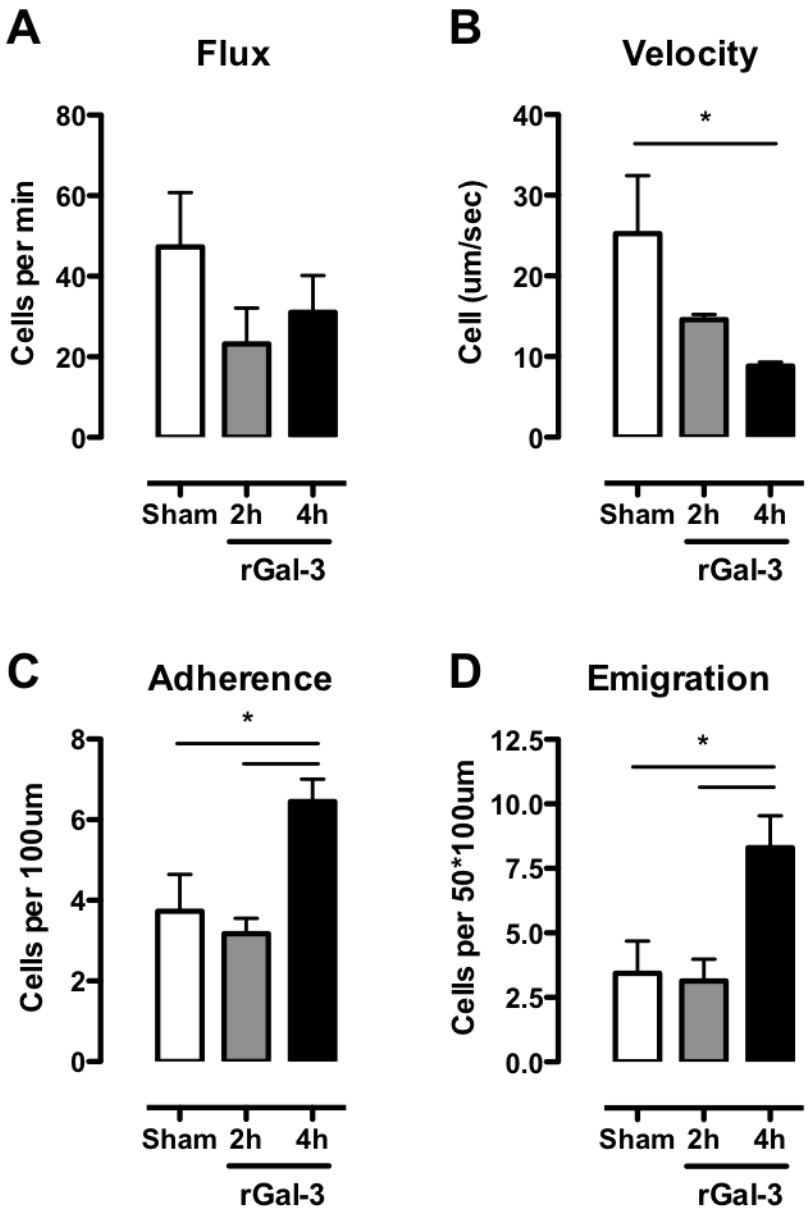

Figure 4.1 Treatment of the mouse cremasteric microcirculation with recombinant Gal-3 results in increased leukocyte recruitment in a time-dependent manner

IVM was performed as detailed in Methods. Briefly, the cremasteric microcirculation of C57BL/6 mice was assessed 2 or 4h after intrascrotal injection of PBS (sham, 400µL) or recombinant rGal-3 (500ng in 400µL PBS). Leukocyte flux (**A**), rolling velocity (**B**), adhesion (**C**) and emigration (**D**) was investigated in segments of 100µm in 3-5 vessels per mouse and results are expressed as mean±SEM of 3-5 mice per group. Statistical significance was assessed by one-way ANOVA and Tukey's multiple comparison post-test; denoted by asterisks *P<0.05.

4.1.2 Validation of the use of anti-Ly-6G to label murine neutrophils

In addition to assessing total leukocyte recruitment, the extravasation of neutrophils specifically can be visualised using fluorescently labelled antibodies against murine Ly-6G, which are administered *via* the tail vein (10μg in 200μL saline) immediately prior to administration of a local stimulus to the cremaster by i.s. injection. Firstly, it was important to establish whether the antibody itself would affect the leukocyte recruitment recorded in this system, in particular the ability of the neutrophils to emigrate into the tissue. In order to do this leukocyte recruitment was assessed in C57BL/6 mice that had been administered anti-Ly-6G, IgG2a (isotype control, 10μg in 200μL saline) or vehicle (200μL saline) i.v. as well as TNFα (300ng in 400μL PBS) i.s. in all cases. The average total (Ly-6G positive plus negative cells) leukocyte flux, rolling velocity, adhesion and emigration in each group was analysed and assessed for significance using two-way ANOVA and Tukey's multiple comparison post-test.

When compared to vehicle treated mice, administration of anti-Ly-6G or its isotype control did not cause significant differences in the responses to i.s. TNFα with respect to leukocyte flux (Figure 4.2A; Veh 45.9±7.9, IgG2a 15.8±2.0 *vs.* Ly-6G 26.9±9.7, not significant), rolling velocity (Figure 4.2B; Veh 12.8±4.6, IgG2a 22.7±4.8 *vs.* Ly-6G 7.1±2.1, not significant), adhesion (Figure 4.2C; Veh 5.5±0.6, IgG2a 5.7±0.8 *vs.* Ly-6G 9.3±1.3, not significant) or emigration (Figure 4.2D; Veh 16.3±1.1, IgG2a 16.4±1.0 *vs.* Ly-6G 23.6±2.5, not significant).

In addition to assess leukocyte recruitment, it was also important to confirm that the antibody was specifically labelling neutrophils. After vessel recording, whole blood was collected by cardiac puncture and analysed by flow cytometry after red cell lysis. The leukocyte cell populations could be distinguished by forward side scatter (Figure 4.2E, upper panel) and showed that the neutrophil population was 90.9% positive for Ly-6G, with no staining of lymphocytes or monocytes (Figure 4.2E, lower panel).

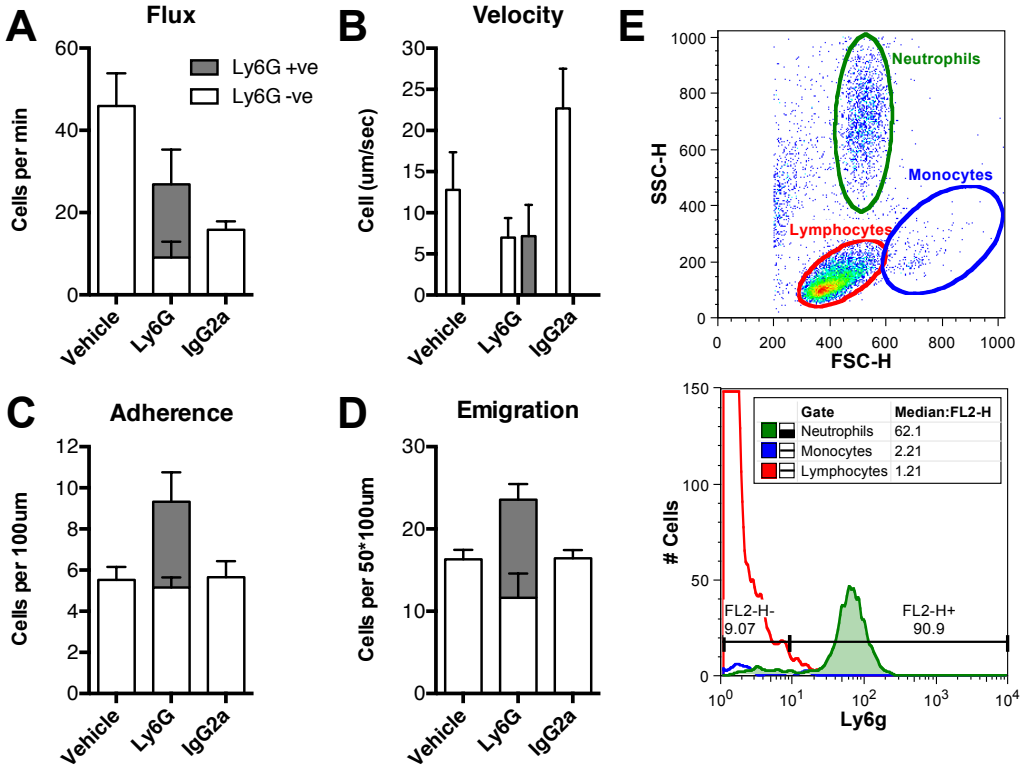

Figure 4.2 Validation of the anti-mouse Ly-6G antibody used to label neutrophils in the murine cremasteric microcirculation

IVM was performed as detailed in Methods. Briefly, the cremasteric microcirculation in C57BL/6 mice was assessed 4h after intrascrotal injection of murine recombinant TNFα (300ng in 400µL PBS) and i.v. administration of saline (200µL), anti-mouse Ly-6G (2µg in 200µL saline) or anti-mouse IgG2a (2µg in 200µL saline). Leukocyte flux (**A**), rolling velocity (**B**), adhesion (**C**) and emigration (**D**) was investigated in segments of 100µm in 2-3 vessels per mouse and results are expressed as mean±SEM of 2-3 mice per group. Ly-6G positive cells are shown in the filled (grey) columns and Ly-6G negative cells in the empty columns. Statistical significance was assessed by two-way ANOVA and Tukey's multiple comparison post-test. **E**) After vessel recording, whole blood was collected by cardiac puncture and analysed by flow cytometry after red cell lysis. Upper panel shows the forward-side scatter plot of a representative sample and lower panel shows the fluorescence intensity of the gated cell populations.

4.1.3 Investigating neutrophil recruitment to the cremasteric microcirculation in response to rGal-3

Following validation, the anti-Ly-6G antibody was used to label neutrophils recruited to the cremaster after C57BL/6 mice were-treated i.s. with vehicle (PBS, 400uL) or rGal-3 (200ng-1000ng in 400uL PBS). Vessels were recorded using the brightfield and PE channels before offline analysis and image stills are shown (Figure 4.3) from representative sham-treated (top panel) or rGal-3-treateted mice (1000ng; lower panel).

In contrast to the vessels of sham animals shown in the upper panel, it is clear that many Ly-6G positive neutrophils as well as unlabelled leukocytes are present in and closely surrounding the vessels of the rGal-3-treated animals. A dose-response was therefore performed in C57BL/6 mice at the 4h time-point with varying doses of rGal-3 (200ng, 500ng, 1000ng in 400μL PBS).

The average Ly-6G positive and negative leukocyte flux, rolling velocity, adhesion and emigration in each group was analysed in segments of 100μm in 3-5 vessels per mouse and results are expressed as mean±SEM of 3-4 mice per group. Significance was assessed using two-way ANOVA and Tukey's multiple comparison post-test.

Though there may be a slight trend for reduced flux in 1000ng-treated mice, levels of leukocyte flux remained comparable between all treatment

groups for both Ly-6G -ve (Figure 4.4A; sham 18.9±5.0 *vs.* 1000ng 11.8±4.7, not significant) and Ly-6G +ve (Figure 4.4A; sham 47.5±3.7 *vs.* 1000ng 23.1±11.6, not significant) cell populations. However, rolling velocities were significantly reduced from sham levels in both 500ng and 1000ng-treated mice and this reduction was similar for Ly-6G -ve (Figure 4.4B; Sham 69.8±24.2 *vs.* 500ng 14.0±5.1, 1000ng 5.1±1.1, $P<0.01$, n=3-4) and Ly-6G +ve (Figure 4.4B; Sham 55.0±18.1 *vs.* 500ng 13.6±4.7, 1000ng 5.2±1.2, $P<0.05$, n=3-4) cells.

The numbers of adherent cells recorded after treatment with lower does of rGal-3 were not increased from numbers seen in sham-treated animals and were comparable between Ly-6G -ve (Figure 4.4C; Sham 1.3±0.4, 200ng 1.9±0.9, 500ng 2.4±0.1, not significant) and Ly-6G +ve (Figure 4.4C; Sham 0.6±0.4, 200ng 1.4±0.9, 500ng 2.0±0.5, not significant) cells at all treatment groups. However, at the highest treatment of 1000ng, adhesion was significantly increased from sham for both Ly-6G -ve (Figure 4.4C; sham 1.3±0.4 *vs.* 1000ng 4.8±0.3, $P<0.05$, n=3) and Ly-6G +ve (Figure 4.4C; sham 0.6±0.4 *vs.* 1000ng 5.5±1.8, $P<0.01$, n=3) cells, which accounted for approximately half of the total cells seen.

In a similar pattern to that seen with the adherent cells, the numbers of emigrated cells recorded after treatment with lower does of rGal-3 were also not increased from numbers seen in sham-treated animals and were comparable between Ly-6G -ve (Figure 4.4D; Sham 4.4±1.1, 200ng 2.9±0.8, 500ng 3.743±0.8, not significant) and Ly-6G +ve (Figure 4.4D;

Sham 2.5±0.5, 200ng 2.7±1.8, 500ng 3.738±0.8, not significant) cells at all treatment groups. Once again, at the highest treatment of 1000ng, emigration was significantly increased from sham for both Ly-6G -ve (Figure 4.4D; sham 4.4±1.1 *vs.* 1000ng 12.1±1.3, $P<0.05$, n=3) and Ly-6G +ve (Figure 4.4D; sham 2.5±0.5 *vs.* 1000ng 12.3±4.4, $P<0.01$, n=3) cells, which accounted for approximately half of the total cells in the tissue.

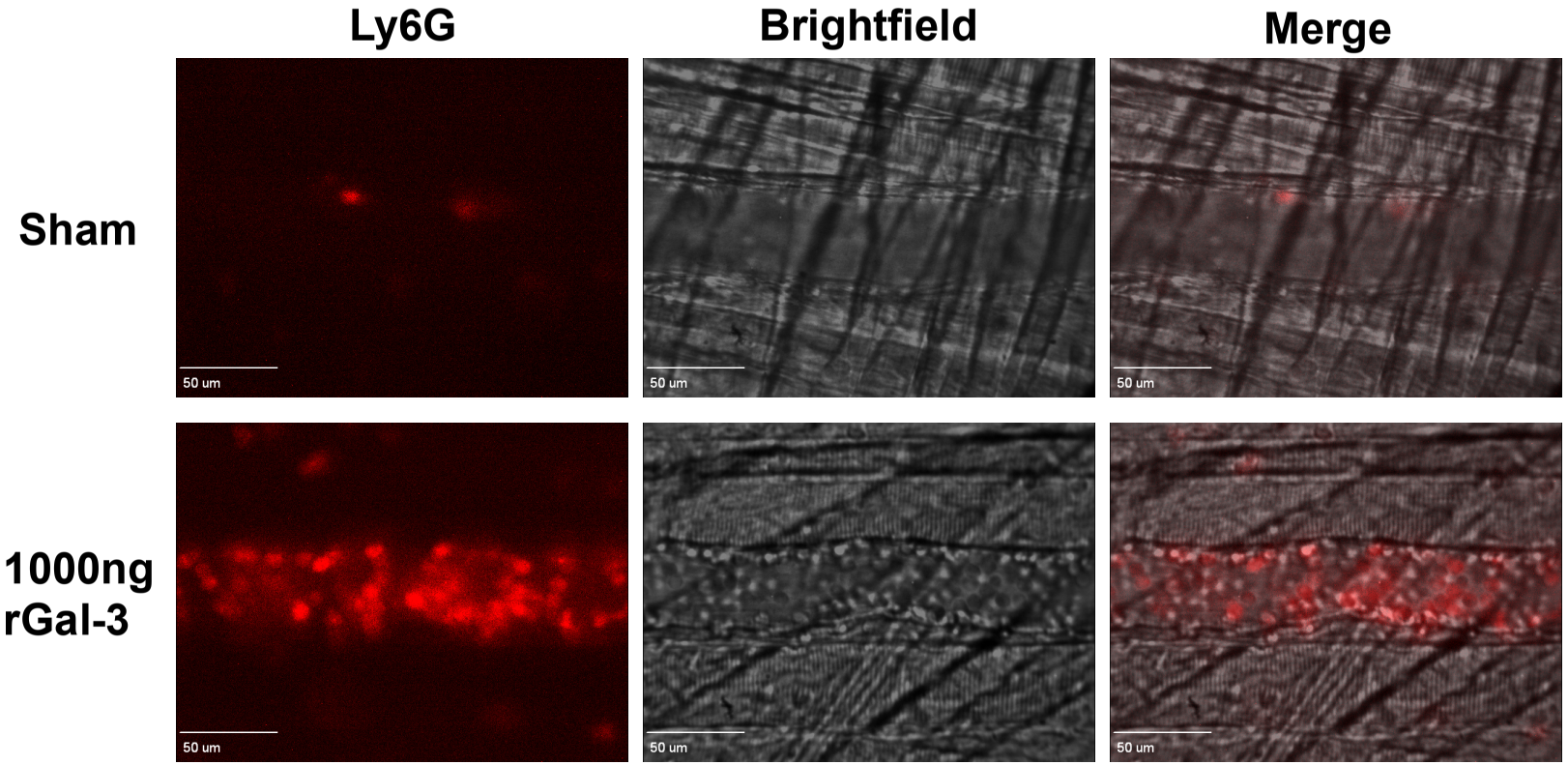

Figure 4.3 Treatment of the mouse cremasteric microcirculation with rGal-3 results in increased leukocyte recruitment, including neutrophils

IVM was performed as detailed in Methods. Briefly, the cremasteric microcirculation in C57BL/6 mice was assessed 4h after intrascrotal injection of PBS (400µL) or recombinant rGal-3 (1000ng in 400µL PBS) and i.v. administration of anti-mouse Ly-6G (2µg in 200µL saline) to label murine neutrophils. Leukocyte recruitment was investigated in segments of 100µm in 3-5 vessels per mouse and 3-5 mice per group. Images are representative stills taken from vessel recordings.

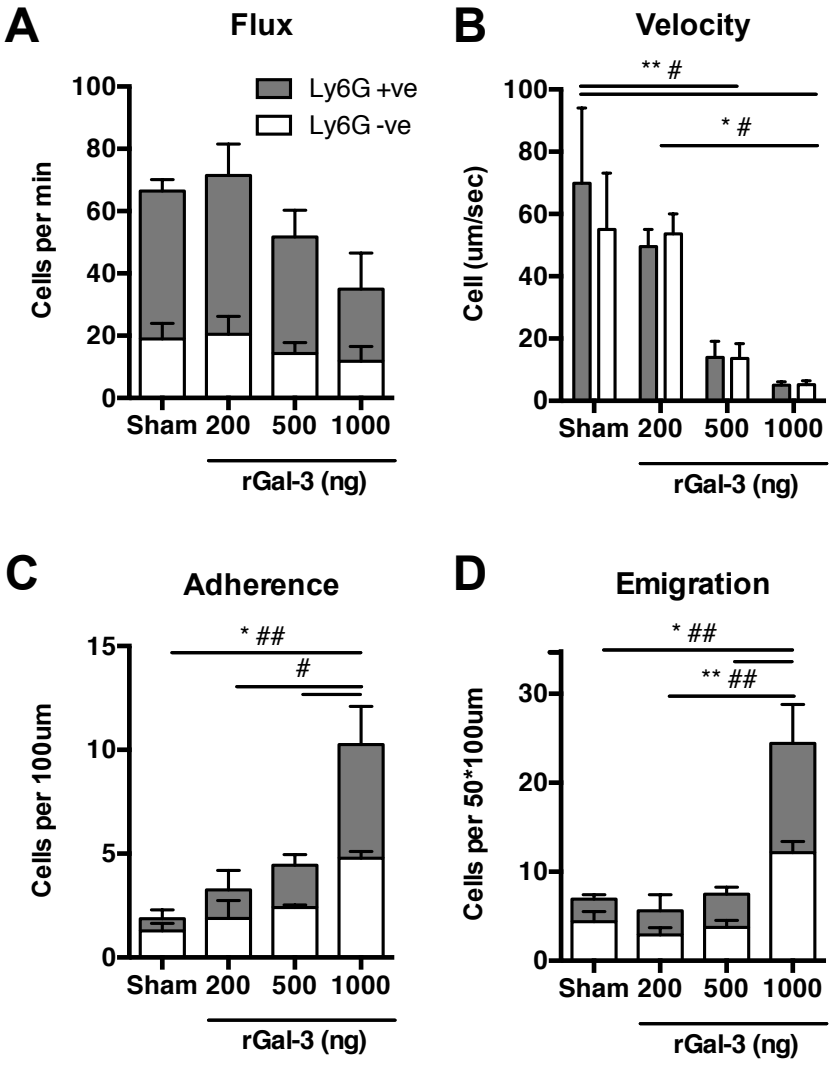

Figure 4.4 Treatment of the mouse cremasteric microcirculation with rGal-3 results in increased neutrophil recruitment in a dose-dependent manner

IVM was performed as detailed in Methods. Briefly, the cremasteric microcirculation in C57BL/6 mice was assessed 4h after intrascrotal injection of PBS (sham, 400µL) or recombinant rGal-3 (200-1000ng in 400µL PBS) and i.v. administration of anti-mouse Ly-6G (2µg in 200µL saline) to label murine neutrophils. Leukocyte flux (**A**), rolling velocity (**B**), adhesion (**C**) and emigration (**D**) was investigated in segments of 100µm in 3-5 vessels per mouse and results are expressed as mean±SEM of 3-4 mice per group. Ly-6G positive cells are shown in the filled (grey) columns and Ly-6G negative cells in the empty columns. Statistical significance was assessed by two-way ANOVA and Tukey's multiple comparison post-test; denoted by asterisks * $P<0.05$ and ** $P<0.01$ between Ly-6G-ve bars and # $P<0.05$ and ## $P<0.01$ between Ly-6G+ve bars.

4.1.4 Investigating monocyte recruitment to the cremasteric microcirculation in response to rGal-3 using IVM

IVM was performed as detailed in Methods. Briefly, the cremasteric microcirculation in $CX_3CR1^{gfp/+}$ mice was assessed 4h after intrascrotal injection of PBS (sham) or recombinant rGal-3 (1000ng). GFP positive and negative leukocyte rolling velocity, adhesion and emigration was investigated in segments of 100μm in 3-5 vessels per mouse and results are expressed as mean±SEM of 3 mice per group. Statistical significance was assessed using an unpaired students t-test.

In response to rGal-3 treatment, there was no difference in the leukocyte rolling velocity of GFP +ve and GFP -ve cells (Figure 4.5A; +ve 27.6±11.1 *vs.* –ve 43.3±11.2, not significant). This was also the case for levels of adhesion (Figure 4.5B; +ve 1.3±0.3 *vs.* –ve 2.0±0.6, not significant) and emigration (Figure 4.5C; +ve 2.6±0.6 *vs.* –ve 7.6±2.6, not significant), where GFP positive cells accounted for approximately half of the total cells recruited. When comparing levels of GFP positive monocytes alone, rGal-3 treatment significantly increased recruitment of these cells when compared to sham-treated animals. Monocyte rolling velocity was significantly reduced after rGal-3 treatment (Figure 4.6A; sham 62.7±9.2 *vs.* rGal-3 27.6±6.4, $P<0.05$, n=3). This was in addition to increased adhesion (Figure 4.6A; sham 0.4±0.03 *vs.* rGal-3 1.3±0.2, $P<0.01$, n=3) and (Figure 4.6A; sham 0.8±0.06 *vs.* rGal-3 2.6±0.4, $P<0.01$, n=3) emigration of monocytes to the inflamed rGal-3-treated area.

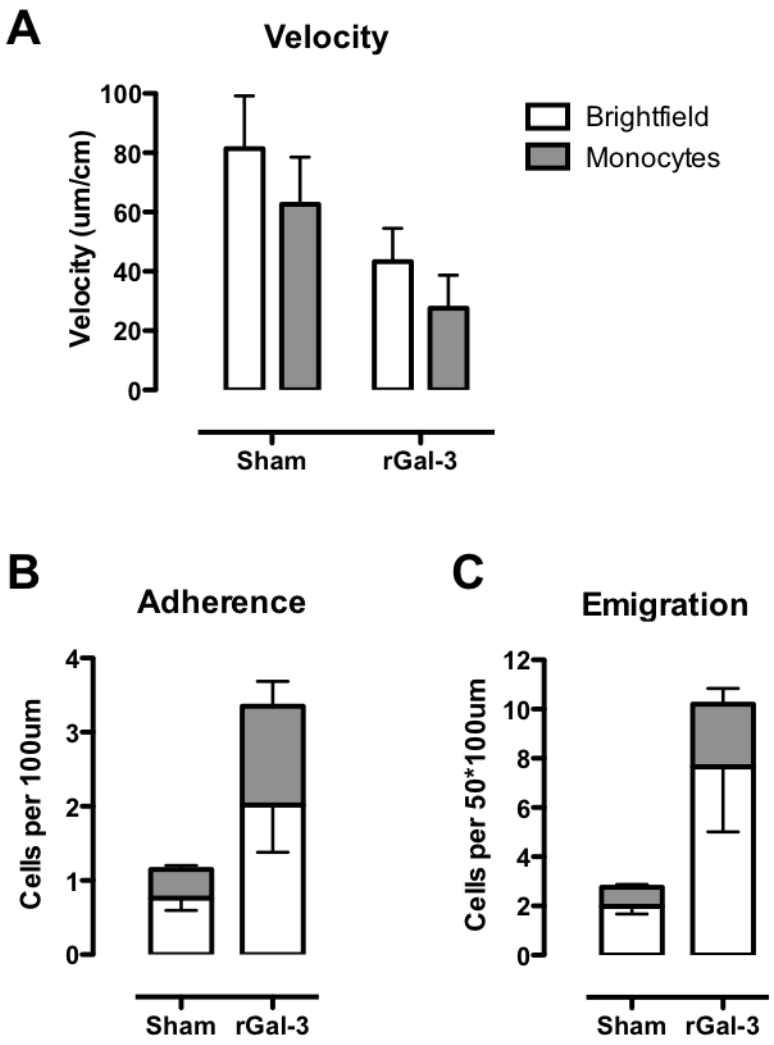

Figure 4.5 Local treatment with rGal-3 induces leukocyte recruitment to the area, including monocytes

IVM was performed as detailed in Methods. Briefly, the cremasteric microcirculation in mice bearing GFP under their CX_3CR1 promoter was assessed 4h after intrascrotal injection of PBS (400µL) or recombinant rGal-3 (1000ng in 400µL PBS). Leukocyte rolling velocity (**A**), adhesion (**B**) and emigration (**C**) was investigated in segments of 100µm in 3-5 vessels per mouse and results are expressed as mean±SEM of 3 mice per group. GFP positive cells are shown in the filled (grey) columns and GFP negative cells in the empty columns.

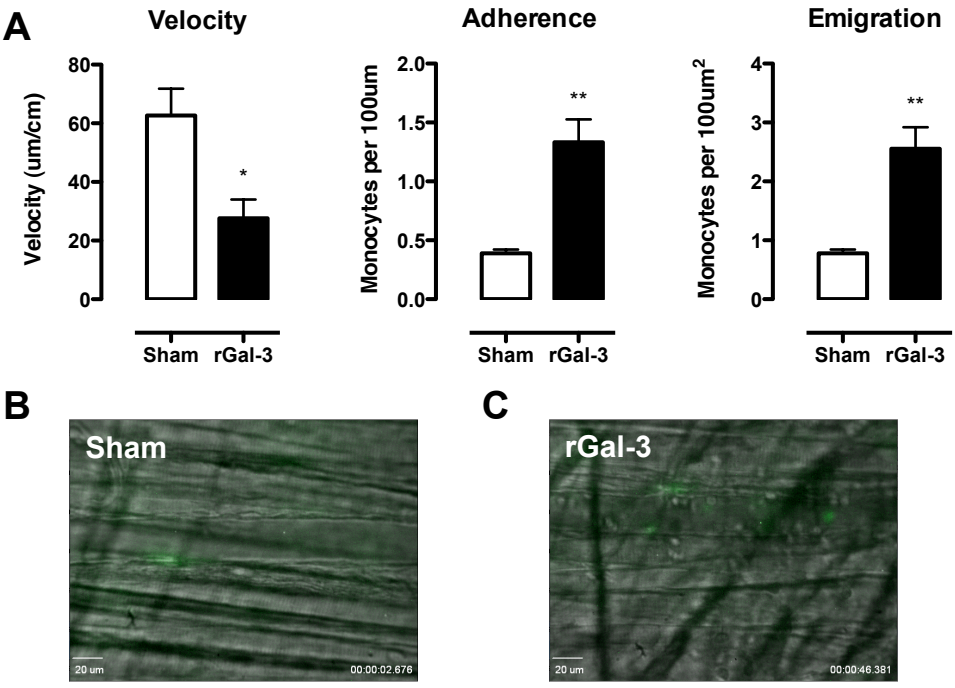

Figure 4.6 Local rGal-3 treatment results in reduced monocyte rolling velocity as well as increased monocyte adhesion and emigration

IVM was performed as detailed in Methods. Briefly, the cremasteric microcirculation in mice bearing GFP under their CX_3CR1 promoter was assessed 4h after intrascrotal injection of PBS (400µL) or recombinant rGal-3 (1000ng in 400µL PBS). **A**) GFP positive leukocyte rolling velocity, adhesion and emigration was investigated in segments of 100µm in 3-5 vessels per mouse and results are expressed as mean±SEM of 3 mice per group. Statistical significance was assessed using an unpaired students t-test, denoted by asterisks * $P<0.05$ and ** $P<0.01$. **B**) Representative still taken from recording of a sham-treated mouse, GFP positive cells are shown in green. **C**) Representative still taken from recording of a rGal-3-treated mouse, GFP positive cells are shown in green.

4.1.5 Investigating monocyte recruitment to the cremasteric microcirculation in response to rGal-3 using confocal microscopy

Cremasters from sham or rGal-3-treated (1000ng) $CX_3CR1^{gfp/+}$ mice were exteriorised and stained as detailed in section 2.6. Emigrated neutrophils and monocytes per frame were quantified and results are expressed as mean±SEM of 4-5 vessels per mouse and 4 mice per group. Significance was assessed using an unpaired students t-test. Similarly to the vessels analysed by IVM, mice treated with rGal-3 exhibited increased emigration of neutrophils when compared to sham-treated animals (Figure 4.7A; sham 1.4±0.7 *vs.* rGal-3 9.7±4.5). Furthermore, monocytes were present in the rGal-3-treated cremasters in similar numbers to neutrophils (Figure 4.7A; Neutrophils 9.7±4.5 *vs.* monocytes 5.2±1.3). Finally, the number of emigrated monocytes was significantly increased in rGal-3-treated vessels when compared to their PBS-treated counterparts (Figure 4.7A; sham 1.2±0.7 *vs.* rGal-3 5.2±1.3, $P<0.05$, n=4).

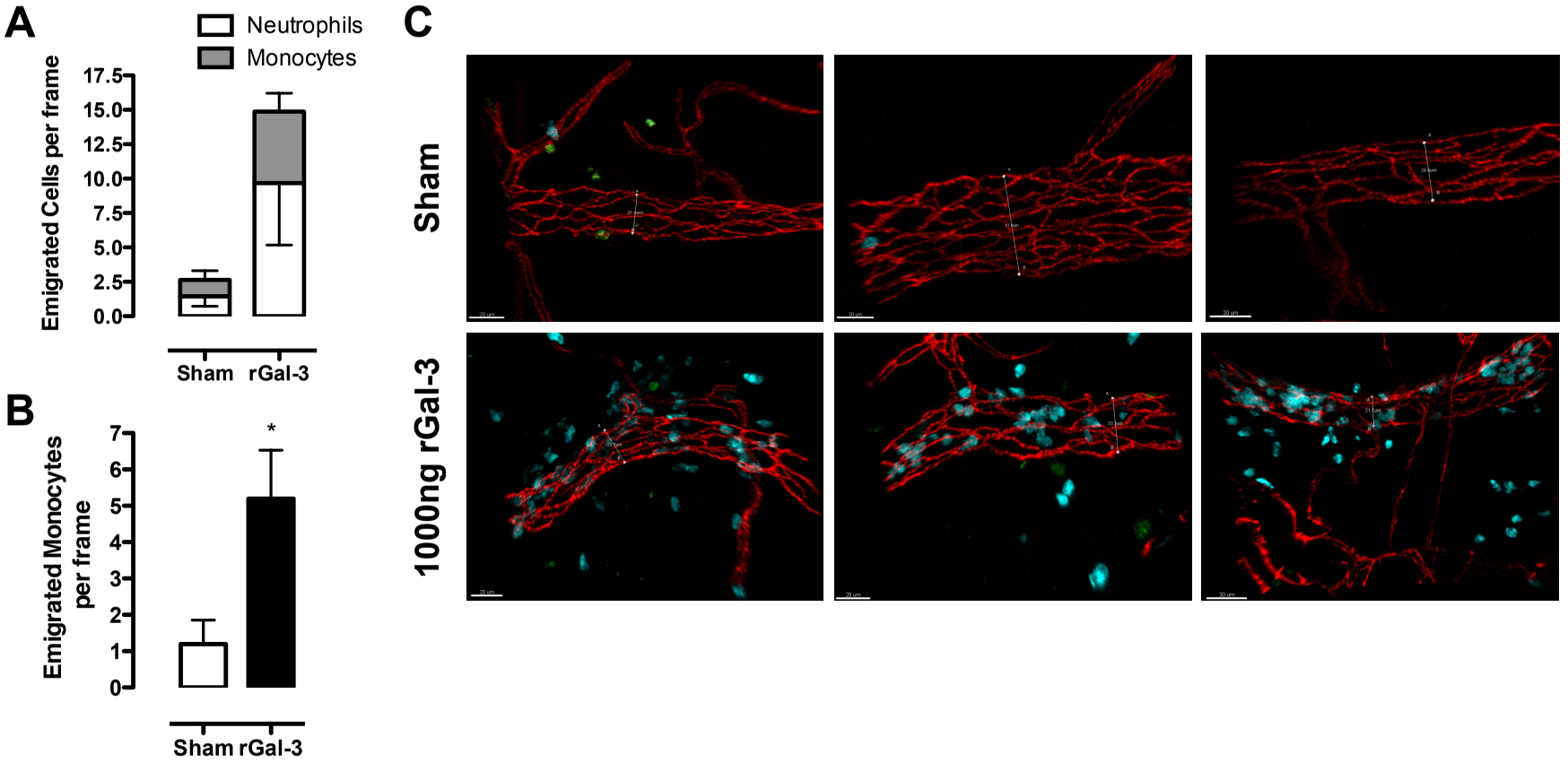

Figure 4.7 rGal-3 induces monocyte recruitment to the murine cremasteric microcirculation

Cremasters from $CX_3CR1^{gfp/+}$ mice treated intrascrotally for 4h with sham PBS (400μL) or rGal-3 (1000ng in 400μL PBS) were exteriorised and fixed flat on wax sheets in 4% PFA before permeabilisation and blocking, as detailed in Methods. Antibodies against VE-Cadherin and MRP14 were used to stain the cremasters before viewing by confocal microscopy. **A**) Emigrated neutrophils (empty bars) and monocytes (grey bars) were quantified; results are expressed as mean±SEM of 4-5 vessels per mouse and 4 mice per group. **B**) Emigrated monocytes per frame were quantified and significance was assessed using an unpaired students t-test, denoted by asterisk * $P<0.05$. **C**) Representative images from sham (upper panels) and rGal-3 (Lower panels)-treated mice; vessels are stained using VE-Cadherin (Red), MRP14 positive neutrophils are blue and GFP positive monocytes are green.

4.1.6 Analysis of murine cremaster mRNA content after treatment with rGal-3

In order to further examine the effects of rGal-3 on the tissue after i.s. injection, the cremasters were collected and immediately snap frozen in liquid nitrogen, before subsequent RNA isolation, cDNA synthesis and real-time PCR analysis of expression of various inflammatory genes was carried out. The cremasters from C57BL/6 mice-treated i.s. with vehicle control (PBS) or rGal-3 (1000ng) were analysed. Results were expressed as 2-ΔΔCT where gene expression was normalised to an internal housekeeping gene (GAPDH) and then normalised against the sham cremasters, which were set at one.

When compared to their sham-treated counterparts, cremaster muscle treated with rGal-3 displayed significantly increased mRNA for IL-1β (Figure 4.8; sham 3.0±2.7 *vs.* rGal-3 123.2±46.3, P<0.05, n=3), Keratinocyte-derived chemokine (KC, Figure 4.8; sham 4.7±4.0 *vs.* rGal-3 74.7±5.0, P<0.001, n=3), monocyte chemoattractant protein-1 (MCP-1, Figure 4.8; sham 0.3±0.1 *vs.* rGal-3 63.1±19.4, P<0.05, n=2-3) and IL-6 (Figure 4.8; sham 4.8±3.5 *vs.* rGal-3 169.7±36.2, P<0.01, n=3) and there was a trend for increased TNFα (Figure 4.8; sham 3.0±2.7 *vs.* rGal-3 18.0±9.1, not significant, n=3). In contrast, the expression of SDF-1 was not changed in rGal-3-treated cremaster muscle when compared to sham preparations (Figure 4.8; sham 1.0±0.1 *vs.* rGal-3 0.8±0.2, not significant).

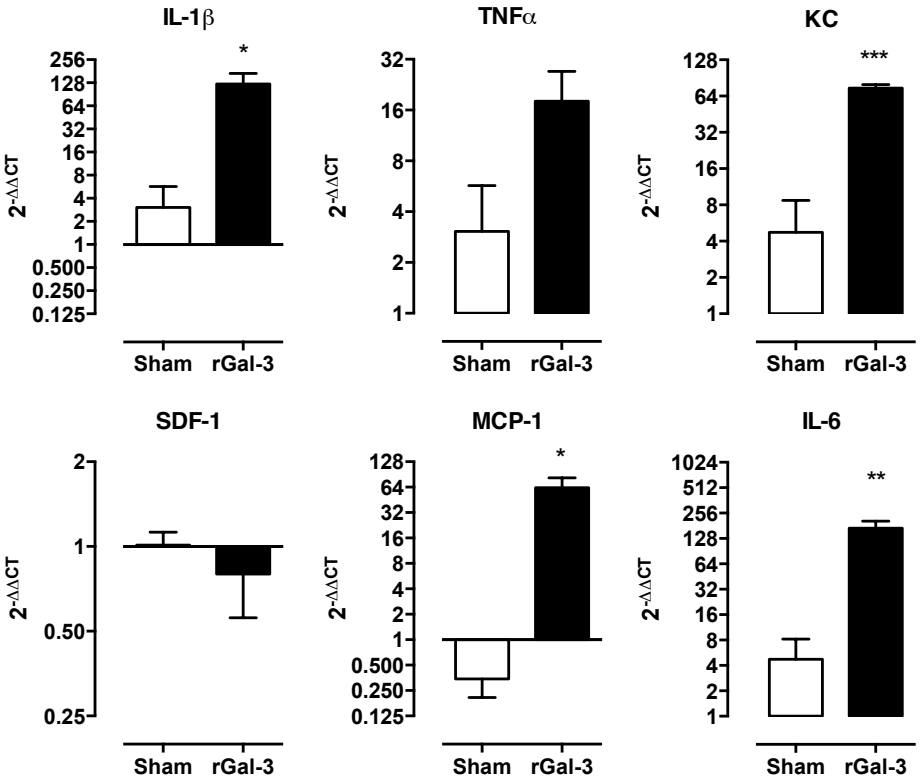

Figure 4.8 Intrascrotal rGal-3 increases levels of local cytokines and chemokines found in the cremaster

The cremasteric microcirculation in C57BL/6 mice was assessed 4h after intrascrotal injection of PBS (400µL) or recombinant rGal-3 (1000ng in 400µL PBS) by IVM. Directly following the vessel recordings, the mice were culled by cervical dislocation and the cremaster muscle collected for immediate snap freezing in liquid Nitrogen and longer storage at -80°C. Tissues were homogenised from frozen and RNA extraction, cDNA synthesis and real-time PCR was then performed for IL-1β, TNFα, KC, SDF-1, MCP-1 and IL-6. Results are expressed as $2^{-\Delta\Delta CT}$ where gene expression is normalised to an internal housekeeping gene (GAPDH) and then normalised once more to the sham cremasters, which were set at one. They are displayed as mean±SEM of 2-3 mice per group. . Significance was assessed using an unpaired student's t-test and is denoted by asterisks * P<0.05, ** P<0.01 and *** P<0.001.

4.1.7 Analysis by proteome array of murine cremaster protein content after treatment with rGal-3

Murine cremaster muscles were dissected and snap frozen following intrascrotal treatment for 4 hours with PBS or rGal-3 (1000ng). Frozen cremasters were homogenised and the protein content assessed before a final protein quantity of 200μg was then assessed using the mouse cytokine array panel A Proteome Profiler™ (R&D Systems) according to manufacturer instructions. The membranes were imaged using the FluorChem E, which increases exposure until the desired intensity is reached, in this case approximately 10 min. Pixel densitometry was carried out using Fiji imaging software (ImageJ) and subtracting an averaged background reading from each duplicate antibody spot.

The proteome array of rGal-3-treated cremaster samples displayed increased binding of many cytokines and chemokines, when compared to sham cremaster arrays (Figure 4.9A). This was semi-quantified for two separate arrays of different cremaster samples using pixel densitometry; however, the variation between these two sets was high.

Cytokines increased after rGal-3 treatment included IFNγ (Figure 4.10; Sham 100% *vs.* 233.1±79), MCP-1 (Figure 4.10; Sham 100% *vs.* 448±171), IL-6 (Figure 4.10; Sham 100% *vs.* 181±45), KC (Figure 4.10; Sham 100% *vs.* 266±80), MIP-1α (Figure 4.10; Sham 100% *vs.* 195±75), MIP-2 (CXCL2) (Figure 4.10; Sham 100% *vs.* 235±137) and TNFα (Figure 4.10; Sham 100% *vs.* 163±33). Crucially, the levels of some

proteins in rGal-3 arrays were comparable to sham arrays, for example MIP-1β (Figure 4.10; Sham 100% *vs.* 96±14) or were reduced after stimulation with the lectin, for example BCA-1 (Figure 4.10; Sham 100% *vs.* 74±0.4).

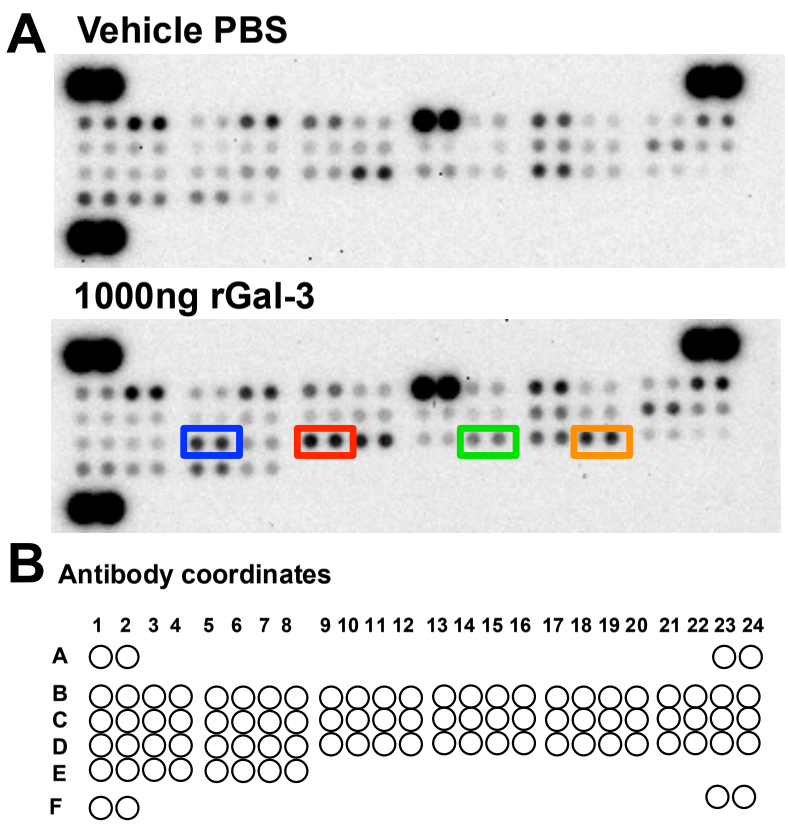

C

Coordinate	Target/Control
A1, A2	Reference Spot
A23, A24	Reference Spot
B1, B2	CXCL13/BCA-1
B3, B4	C5/C5a
B5, B6	G-CSF
B7, B8	GM-CSF
B9, B10	I-309/CCL1
B11, B12	Eotaxin/CCL11
B13, B14	sICAM-1
B15, B16	IFN-γ
B17, B18	IL-1α
B19, B20	IL-1β
B21, B22	IL-1ra
B23, B24	IL-2
C1, C2	IL-3
C3, C4	IL-4
C5, C6	IL-5
C7, C8	IL-6
C9, C10	IL-7
C11, C12	IL-10
C13, C14	IL-13

Coordinate	Target/Control
C15, C16	IL-12
C17, C18	IL-16
C19, C20	IL-17
C21, C22	IL-23
D1, D2	IP-10/CXCL10
D3, D4	I-TAC/CXCL11
D5, D6	**KC/CXCL1**
D7, D8	M-CSF
D9, D10	**CCL2/MCP-1**
D11, D12	MCP-5/CCL12
D13, D14	MIG/CXCL9
D15, D16	**MIP-1α /CCL3**
D17, D18	MIP-1β/CCL4
D19, D20	**MIP-2 CXCL2**
D21, D22	RANTES/CCL5
D23, D24	SDF-1/CXCL12
E1, E2	TARC/CCL17
E3, E4	TIMP-1
E5, E6	TNF-α
E7, E8	TREM-1
F1, F2	Reference Spot
F23, F24	PBS (Neg Control)

Figure 4.9 Proteome profile array analysis of cytokine protein content in murine cremasters after local rGal-3 treatment
Murine cremaster muscles were dissected and snap frozen following intrascrotal treatment for 4 hours with PBS (400μL) or rGal-3 (1000μg). Frozen cremasters were homogenised and the protein content assessed before a final protein quantity of 200μg was then assessed using the mouse cytokine array panel A Proteome Profiler™, as described in Methods. **A**) The membranes were imaged using the FluorChem E, which increases exposure until the desired intensity is reached, in this case approximately 10 min. **B,C**) Each duplicate antibody spot corresponds to a cytokine target, as listed with most relevant highlighted in colour.

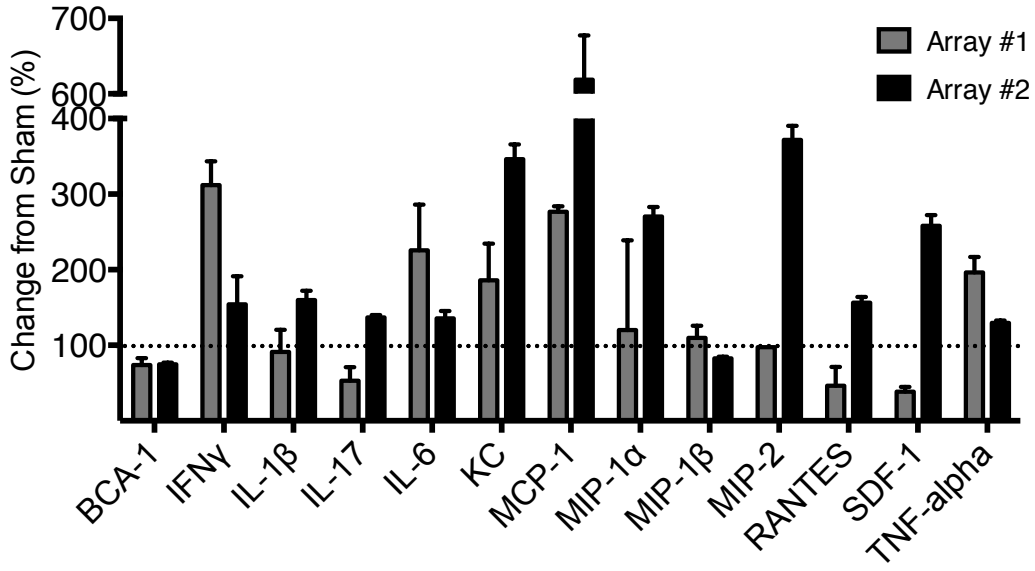

Figure 4.10 Densitometric analysis of cremaster proteome after treatment with rGal-3

Murine cremaster muscles were dissected and snap frozen following intrascrotal treatment for 4 hours with PBS (400μL) or rGal-3 (1000μg). Frozen cremasters were homogenised and the protein content assessed before a final protein quantity of 200μg was then assessed using the mouse cytokine array panel A Proteome Profiler™, as described in Methods. The membranes were imaged using the FluorChem E, which increases exposure until the desired intensity is reached, in this case approximately 10 min. Pixel densitometry was carried out using Fiji imaging software (ImageJ) and subtracting an averaged background reading from each duplicate antibody spot. Results are expressed as mean±SEM of the duplicates, as a percentage of the sham-treated cremaster blot, for two separate arrays.

4.2 Analysis of exogenous Gal-3 under conditions of flow

4.2.1 Treatment with rGal-3 does not increase Gal-3$^{-/-}$ leukocyte capture to E-selectin

The Gal-3 content of wild type platelet-poor plasma was evaluated by ELISA against a known standard curve (Figure 4.11). The plasma was found to contain 9.29ng/mL Gal-3, which was comparable to levels described in the literature. Subsequently, Gal-3$^{-/-}$ whole blood was collected and treated for 15 minutes at 37°C with PBS or rGal-3 (10ng/mL) before dilution 1:10 in HBSS and flow through the chamber. Captured leukocytes in each frame were quantified and classified as phase light or dark and results are expressed as mean±SEM of 6 frames per mouse and 6 mice per group. Significance between total capture was assessed using an unpaired students t-test. However, it was found that the rGal-3 was not able to rescue the phenotype as the cells did not adhere in significantly greater numbers to E-selectin when compared to vehicle treatment (Figure 4.12A; Vehicle 5.9±1.0 *vs.* rGal-3 7.3±1.3, not significant , n=6).

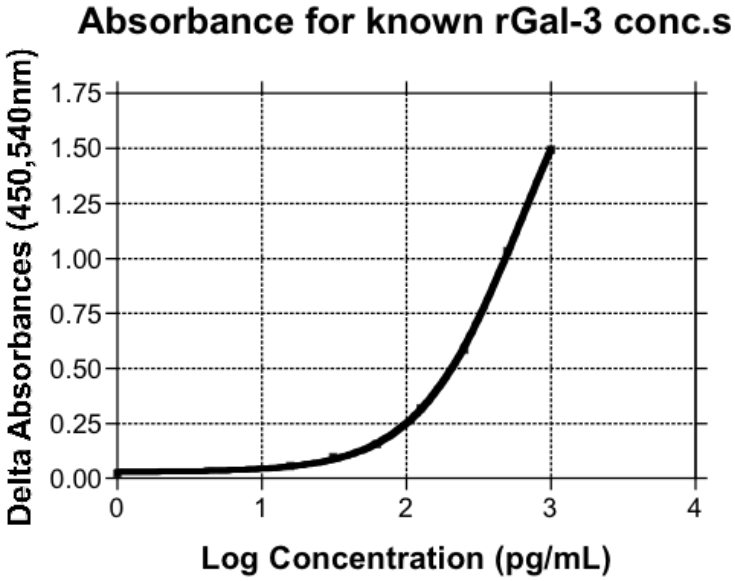

X Labels	Delta Absorbance (450 540nm)	Gal-3 (pg/mL)
C57/BL/6	0.234 ± 0.014	9292.3 ± 873.7
Gal-$3^{-/-}$	0.0192 ± 0.0012	Negligible

Figure 4.11 Wild type murine plasma contains Gal-3
Wild type C57BL/6 or Gal-$3^{-/-}$ whole blood was collected by cardiac puncture using heparin (10U/mL) and immediately centrifuged at 200 *g* for 8min to pellet the white and red blood cells. The platelet-rich plasma was collected and centrifuged again at 1000 *g* for 5min; the platelet-poor plasma was then collected for analysis by ELISA. The plasma was diluted 1:100 in reagent diluent (supplied) and plated in duplicate for comparison to known concentrations of Gal-3 (standard curve shown in the top panel). Gal-3 content in each well was calculated using absorbance at 450nm with wavelength correction set to 540nm. Results are expressed as mean±SEM of 3 mice per group.

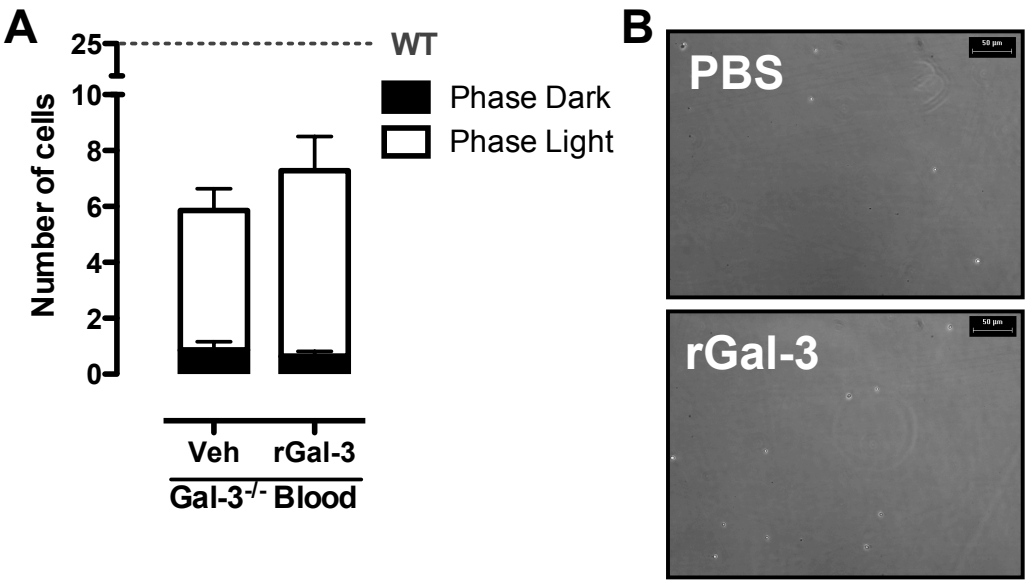

Figure 4.12 rGal-3 is unable to rescue Gal-3$^{-/-}$ leukocyte capture to E-selectin under conditions of flow

Ibidi flow chamber μ-slides were coated with recombinant E-selectin (2μg/ml) and blocked using 0.5% Tween-20. Gal-3$^{-/-}$ whole blood was collected by cardiac puncture using heparin (10U/mL) and treated for 10min at 37°C with vehicle (PBS) or recombinant Gal-3 (10μg/ml). The blood was diluted 1:10 in HBSS and flown for 3mins at 1.010mL/min, followed by 1min HBSS. Videos of 10s were captured for a total of 6 frames per mouse and 6 mice per group. **A)** Captured leukocytes in each frame were quantified and classified as phase light or dark. Results are expressed as mean±SEM and significance was assessed using an unpaired students t-test. **B)** Representative images are stills taken from recordings, the top panel shows Gal-3$^{-/-}$ whole blood treated with vehicle (PBS) and the lower panel shows Gal-3$^{-/-}$ whole blood treated with rGal-3.

4.2.2 Examining the role of Gal-3 in the plasma compartment

To determine whether exogenous Gal-3 in the plasma may account for the differences observed in binding to E-selectin, the effect of the plasma compartment was examined. C57BL/6 or Gal-3$^{-/-}$ whole blood was collected by cardiac puncture and the platelet-poor plasma from both genotypes was then isolated and delivered back to the cells. The C57BL/6 cells were gently mixed with the Gal-3$^{-/-}$ plasma and vice versa, before immediate flow over E-selectin. Videos of 10s were captured for a total of 6 frames per mouse and 3-4 mice per group; captured leukocytes in each frame were quantified and classified as phase light or dark. Results are expressed as mean±SEM and significance was assessed by two-way ANOVA followed by Bonferroni's multiple comparison post-test.

In the absence of both wild type plasma and wild type leukocytes, there was significantly reduced capture of phase light and phase dark cells to the E-selectin. When compared to the control well containing wild type cells flown with wild type platelet-poor plasma, wild type cells flown with Gal-3$^{-/-}$ platelet-poor plasma exhibited reduced phase light (Figure 3.9A; WT/WT 15.9±2.2 *vs.* WT/KO 4.2±0.5, P<0.001, n=3-4) and phase dark leukocyte capture (Figure 3.9A; WT/WT 9.9±2.7 *vs.* WT/KO1.0±0.3, P<0.001, n=3-4). Similarly, Gal-3$^{-/-}$ cells flown with wild type platelet-poor plasma also exhibited significantly reduced capture of phase dark (Figure 3.9A; WT/WT 9.9±2.7 *vs.* KO/WT 1.3±0.3, P<0.001, n=3-4) and phase light (Figure 3.9A; WT/WT 15.9±2.2 *vs.* KO/WT 9.5±1.6, P<0.01, n=3-4) cells when compared to wild type cells flown with wild type plasma.

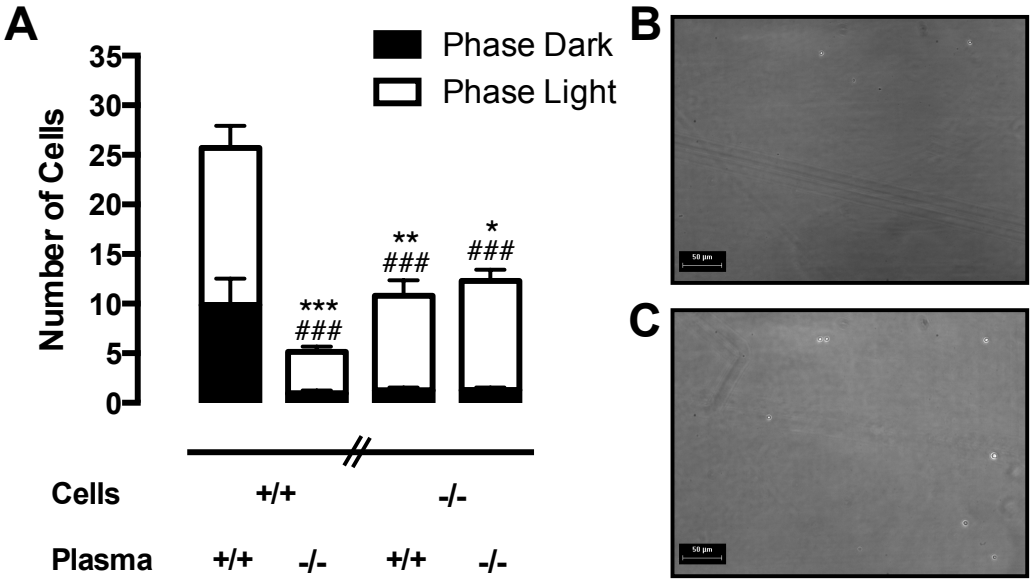

Figure 4.13 Exogenous Gal-3 in the plasma compartment is required for wild type though can not rescue Gal-3$^{-/-}$ leukocyte capture to E-selectin under conditions of flow

Ibidi flow chamber μ-slides were coated with recombinant E-selectin (2μg/ml) and blocked using 0.5% Tween-20. C57BL/6 or Gal-3$^{-/-}$ whole blood was collected by cardiac puncture using heparin (10U/mL) and immediately centrifuged at 200 *g* for 8min to pellet the white and red blood cells. The platelet-rich plasma was collected and centrifuged again at 1000 *g* for 5min; the platelet-poor plasma was then collected and delivered back to the cells. The C57BL/6 cells were gently mixed with the Gal-3$^{-/-}$ plasma and vice versa. The blood was diluted 1:10 in HBSS and flown for 3mins at 1.010mL/min, followed by 1min HBSS. Videos of 10s were captured for a total of 6 frames per mouse and 3-4 mice per group. **A)** Captured leukocytes in each frame were quantified and classified as phase light or dark. Results are expressed as mean±SEM and significance was assessed by two-way ANOVA followed by Bonferroni's multiple comparison post-test between selected groups, denoted by asterisks * P<0.05 and ** P<0.01 and *** P<0.001 when comparing phase light cells to phase light cells in the control WT/WT group and # P<0.05 and ## P<0.01 and ### P<0.001 when comparing phase dark cells to phase dark cells in the control WT/WT group. **B)** Representative images are stills taken from recordings; the top panel shows C57BL/6 cells treated with Gal-3$^{-/-}$ plasma and the lower panel shows Gal-3$^{-/-}$cells treated with C57BL/6 plasma.

4.3 Intravenous administration of rGal-3 to C57BL/6 mice

4.3.1 Analysis by intravital microscopy

Mice were anaesthetized and their jugular vein cannulated before IVM was performed, as detailed in Methods. Briefly, the cremasteric microcirculation in C57BL/6 mice was assessed following intravenous administration of vehicle (saline, 200μL) or recombinant rGal-3 (150ng). Leukocyte flux, rolling velocity, adhesion and emigration was investigated in segments of 100μm in 3-5 vessels per mouse and results are expressed as mean±SEM of 2-3 mice per group. Statistical significance was assessed by two-way ANOVA and Bonferroni's multiple comparison post-test.

Administration of rGal-3 i.v. did not affect leukocyte recruitment over the 60 min time-course. Leukocyte flux remained the same immediately after rGal-3 administration at 15 min (Figure 4.14A; Vehicle 65.0±13.5 *vs.* rGal-3 60.0±17.2, not significant) and also at the 60 min time-point (Figure 4.14A; Vehicle 73.5±4.0 *vs.* rGal-3 39.5±12.2, not significant).

In addition, leukocyte rolling velocities were calculated as percentage of baseline and remained steady over the time-course in both treatment groups, where at 60 min rGal-3 treated animals did not display different rolling velocities when compared to the vehicle-treated group (Figure 4.14B; Vehicle 92.2±41.2 *vs.* rGal-3 126.5±33.4, not significant). Furthermore, Adhesion was unchanged by the addition of rGal-3 i.v., even at the longest 60 min post-administration analysis (Figure 4.14C;

Vehicle 1.0±0.5 *vs.* rGal-3 1.7±0.3, not significant). Finally, administration of rGal-3 i.v. did not increase leukocyte emigration, which remained unchanged from vehicle-treated animals at the 60min time-point (Figure 4.14D; Vehicle 3.3±0.3 *vs.* rGal-3 2.7±0.2, not significant).

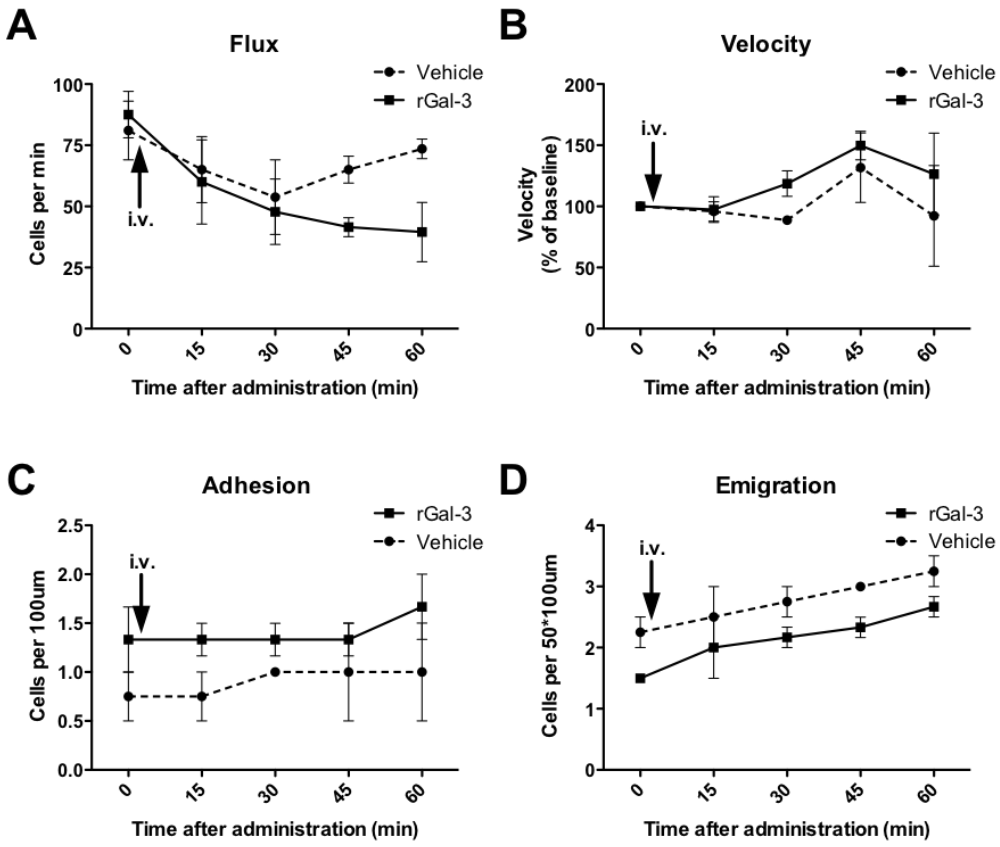

Figure 4.14 Administration of rGal-3 intravenously does not affect leukocyte recruitment in the short-term

Mice were anaesthetized and their jugular vein cannulated before IVM was performed, as detailed in Methods. Briefly, the cremasteric microcirculation in C57BL/6 mice was assessed following intravenous administration of vehicle saline (200μL) or recombinant rGal-3 (150ng in 200μL saline). Leukocyte flux (**A**), rolling velocity (**B**), adhesion (**C**) and emigration (**D**) was investigated in segments of 100μm in 3-5 vessels per mouse and results are expressed as mean±SEM of 2-3 mice per group. Statistical significance was assessed by two-way ANOVA and Bonferroni's multiple comparison post-test.

4.3.2 Analysis of leukocyte adhesion molecule expression by flow cytometry

Wild type C57BL/6 mice were treated intravenously for 4h with vehicle (200μL saline) or rGal-3 (150ng in 200μL saline)$^{-}$ before blood was collected by cardiac puncture using heparin (10U/mL). Murine Fc Receptors were blocked before cell staining with antibodies against PSGL-1, CD11a, CD11b, CD11c, CD44 or CD62L (L-selectin) and analysis by flow cytometry. MFI values were plotted and the data are shown as mean±SEM of 3 mice per group, significance was assessed using an unpaired student's t-test.

When compared to the expression on vehicle-treated counterparts, rGal-3-treated mice displayed unchanged expression of PSGL-1 (Figure 4.15A; Vehicle 11.8±4.4 *vs.* rGal-3 19.6±7.1, not significant), CD11a (Figure 4.15A; Vehicle 100.5±16.2 *vs.* rGal-3 134.0±17.8, not significant), CD11b (Figure 4.15A; Vehicle 0.4±0.08 *vs.* rGal-3 0.8±0.2, not significant), CD11c (Figure 4.15A; Vehicle 1.0±0.6 *vs.* rGal-3 1.1±0.3, not significant), CD44 (Figure 4.15A; Vehicle 33.5±2.8 *vs.* rGal-3 51.0±6.4, not significant) or L-selectin (Figure 4.15A; Vehicle 164.5±33.0 *vs.* rGal-3 177.3±7.1, not significant).

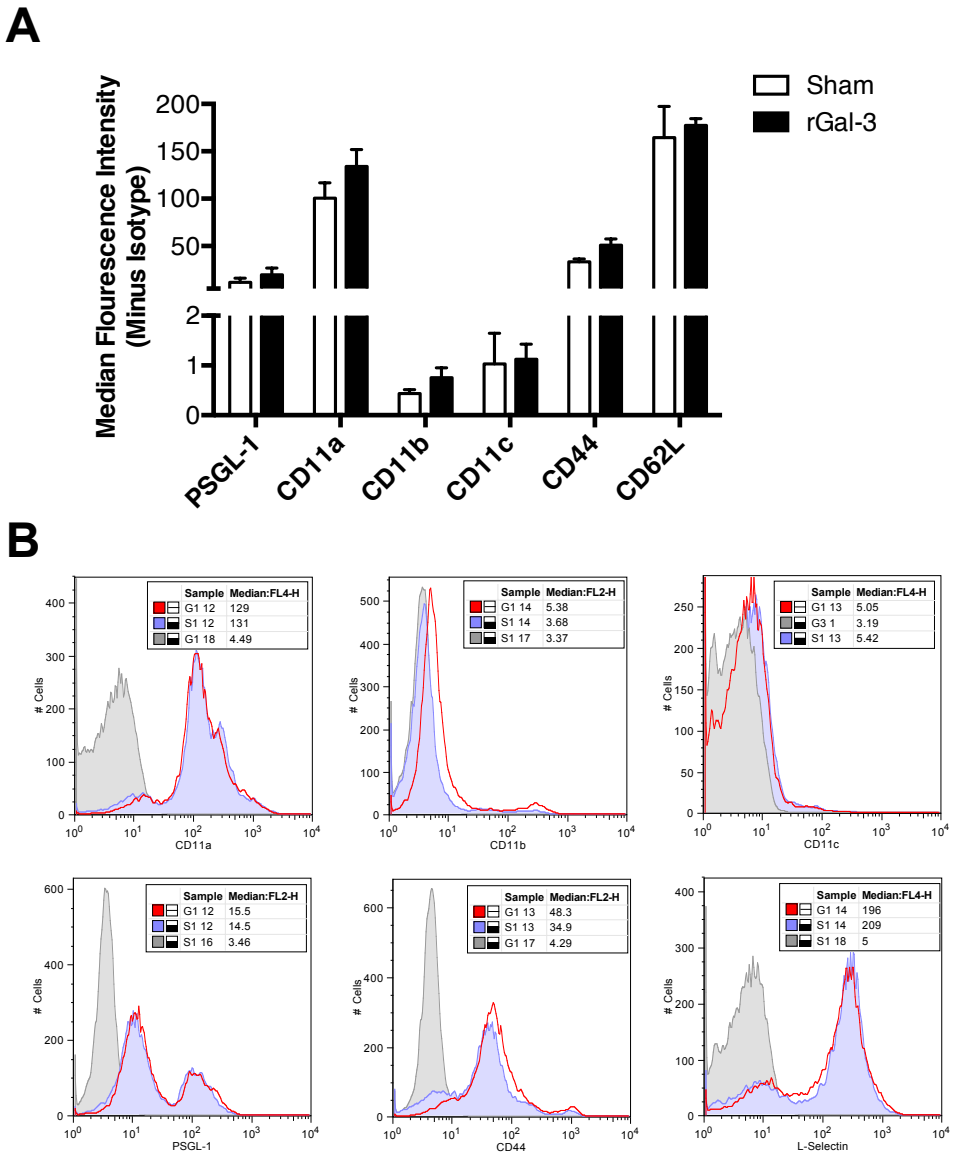

Figure 4.15 Intravenous administration of rGal-3 does not affect leukocyte adhesion molecule expression in the short term

Wild type C57BL/6 mice were treated intravenously for 4h with vehicle (200μL saline) or rGal-3 (150ng in 200μL saline)˙ before whole blood was collected by cardiac puncture using heparin (10U/mL). Murine Fc Receptors were blocked before cell staining with antibodies against PSGL-1, CD11a, CD11b, CD11c, CD44 or CD62L (L-selectin); analysis was carried out with the FACSCalibur Flow cytometer and FlowJo software, as detailed in Methods. **A**) MFI values were plotted and the data are shown as mean±SEM of 3 mice per group, significance was assessed using an unpaired student's t-test. **B**) Representative histogram plots showing leukocytes stained for isotype control (grey) or cell adhesion molecule after treatment with vehicle (blue) or rGal-3 (red line).

4.4 Analysis of cell adhesion molecule expression after treatment with rGal-3

4.4.1 Surface expression of E-selectin and ICAM-1 on MLEC after rGal-3 treatment

Confluent wild type and Gal-3$^{-/-}$ MLEC were treated overnight with vehicle (PBS) or rGal-3 (10 or 100ng/mL). The MLEC were collected and murine Fc receptors were blocked before cell staining for surface ICAM-1 and E-selectin and their isotype controls and analysis by flow cytometry**.** MFI was expressed as mean±SEM of 3 mice sets and statistical significance was assessed using two-way ANOVA followed by Bonferroni's multiple comparison post-test. Similarly to the expression pattern seen after treatment with IL-1β and TNFα, when compared to their wild type counterparts the Gal-3$^{-/-}$ cells displayed reduced E-selectin (Figure 4.16A, upper panel; P=0.0187, n=3) and ICAM-1 (Figure 4.16A, lower panel; P=0.0001, n=3) expression overall. However, in wild type cells rGal-3 treatment itself did not alter expression of E-selectin (Figure 4.16, upper panel; Vehicle 8.7±2.8, 100ng/mL 8.6±0.7, not significant) or ICAM-1 (Figure 4.16, lower panel; Vehicle 623.7±110.0, 100ng/mL 586.0±115.7, not significant). This was also the case in Gal-3$^{-/-}$ cells for both E-selectin (Figure 4.16, upper panel; Vehicle 5.3±0.6, 100ng/mL 6.1±0.9, not significant) and ICAM-1 (Figure 4.16, lower panel; Vehicle 121.6±106.2, 100ng/mL 124.6±109.2, not significant).

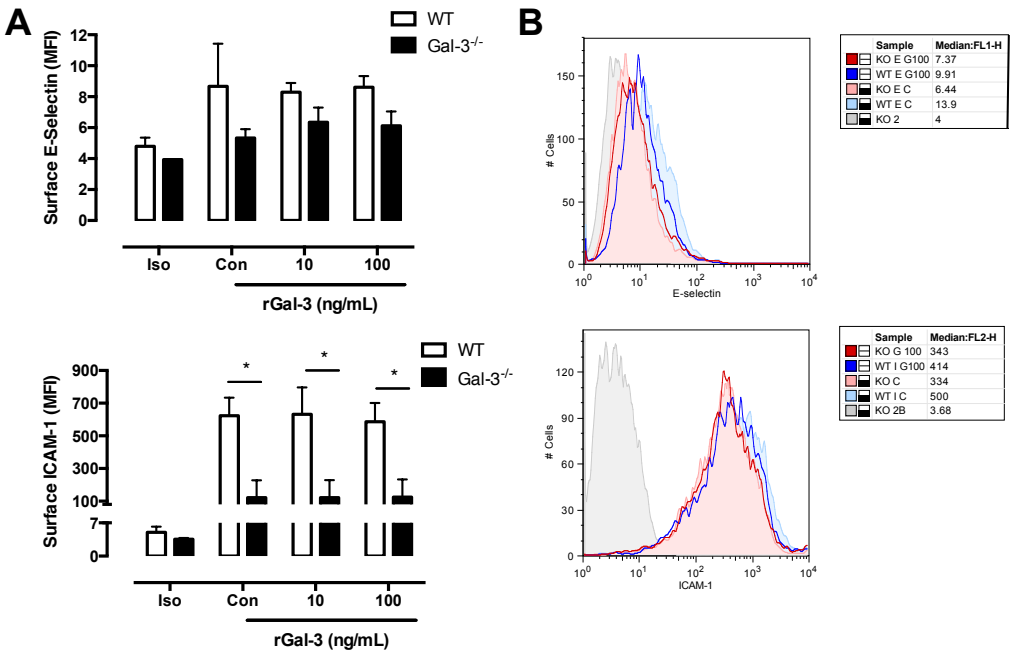

Figure 4.16 Surface expression of E-selectin and ICAM-1 on wild type and Gal-3$^{-/-}$ MLEC after rGal-3 treatment

Confluent wild type and Gal-3$^{-/-}$ MLEC were treated overnight with vehicle (PBS) or rGal-3 (10 or 100ng/mL). The MLEC were collected and murine Fc receptors were blocked before cell staining for surface ICAM-1 and E-selectin and their isotype controls before analysis with the FACSCalibur Flow cytometer and FlowJo software, as detailed in Methods. **A)** MFI was expressed as mean±SEM of 2-3 mice sets for E-selectin (upper panel) and ICAM-1 (lower panel). Statistical significance was assessed using two-way ANOVA followed by Bonferroni's multiple comparison post-test and is denoted by asterisks * P<0.05 and ** P<0.01. **B)** Representative histogram plots showing isotype control (grey tinted), vehicle (PBS) treated wild type cells (filled pale blue), rGal-3 (10ng/mL)-treated wild type cells (blue line), vehicle (PBS) treated Gal-3$^{-/-}$ cells (filled pale red) and rGal-3 (100ng/mL)-treated Gal-3$^{-/-}$ cells (red line) stained for E-selectin (upper panel) and ICAM-1 (lower panel).

4.4.2 Analysis by confocal microscopy of murine cremaster cell adhesion molecule expression after *in vivo* treatment with rGal-3

Cremasters from wild type C57BL/6 mice treated intrascrotally for 4h with PBS, rGal-3, rGal-3 plus lactose or rTNFα were exteriorised and stained as detailed in section 2.6; images are representative of 3 mice per group. Local treatment with TNFα increased expression of ICAM-1 and PECAM-1 in the cremasteric microcirculation (Figure 4.17; 2nd column) when compared to sham-treated vessels. In addition, treatment with rGal-3 also increases PECAM-1 expression above basal levels, though did not affect expression of ICAM-1 (Figure 4.17; 3rd column). Again, local treatment with TNFα increased expression of VCAM-1 and E-selectin in the cremasteric microcirculation compared to sham-treated animals (Figure 4.18; 1st and 2nd columns). Furthermore, these increases in VCAM-1 and E-selectin expression were also seen in rGal-3-treated animals (Figure 4.18; 3rd column). However, local treatment with rGal-3 plus Lactose also increased expression of these two cell adhesion molecules (Figure 4.18; 4th column).

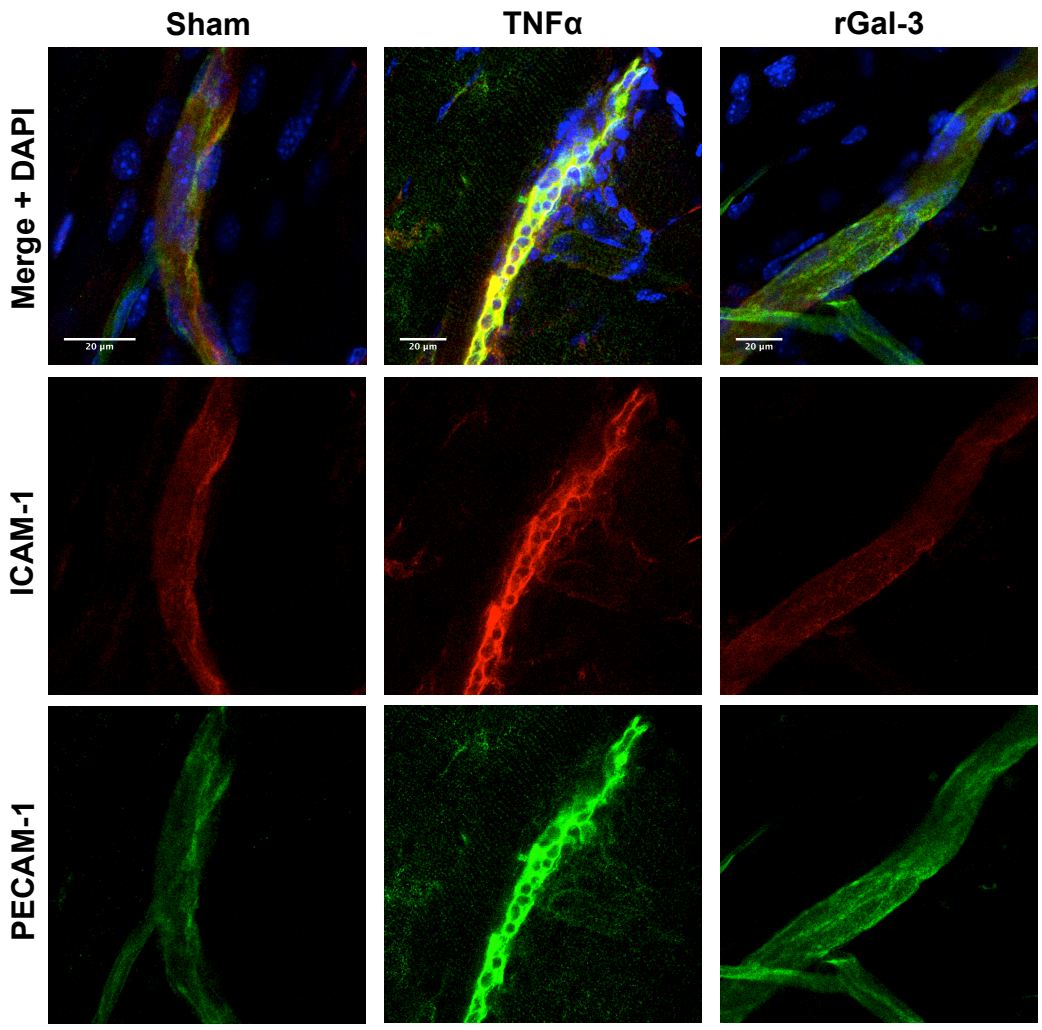

Figure 4.17 Treatment with rGal-3 may increase expression of PECAM-1 in the cremasteric microcirculation

Cremasters from wild type C57BL/6 mice treated intrascrotally for 4h with sham PBS (400µL), rGal-3 (1000ng) or rTNFα (300ng) were exteriorised and fixed flat on wax sheets in 4% PFA before permeabilisation and blocking for 2h at room temperature, as detailed in Methods. Cremasters were stained with antibodies against PECAM-1 (Alexa Fluor® 488 secondary-conjugated) and ICAM-1 (PE-conjugated) and their relevant isotype controls, then washed before mounting in DAPI-containing medium and imaging by confocal microscopy, as detailed in Methods. Merged antibody staining is shown in the top row, ICAM-1 in red in the middle row and PECAM-1 in green in the lower row, with different cremaster treatments in columns, labelled along the top.

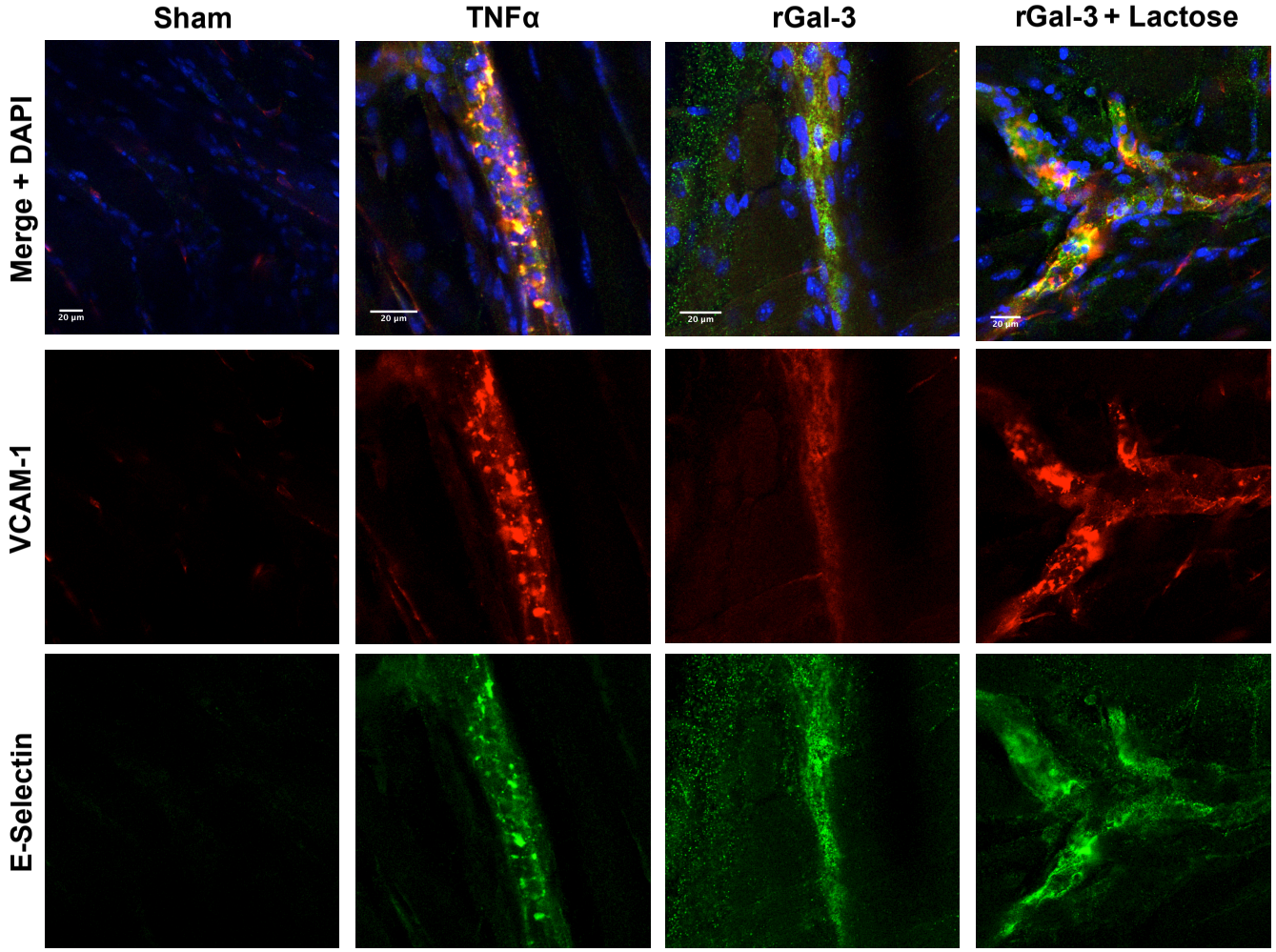

Figure 4.18 rGal-3 treatment may increase expression of E-selectin and VCAM-1 in the cremasteric microcirculation
Cremasters from wild type C57BL/6 mice treated intrascrotally for 4h with sham PBS (400μL), rGal-3 (1000ng) , rGal-3 plus lactose (30mM) or rTNFα (300ng) were exteriorised and fixed flat on wax sheets in 4% PFA before permeabilisation and blocking for 2h at room temperature, as detailed in Methods. Cremasters were stained with antibodies against E-selectin (Alexa Fluor® 488 secondary-conjugated) and VCAM-1 (PE-conjugated) and their relevant isotype controls, then washed before mounting in DAPI-containing medium and imaging by confocal microscopy, as detailed in Methods. Merged antibody staining is shown in the top row, ICAM-1 in red in the middle row and PECAM-1 in green in the lower row, with different cremaster treatments in columns, labelled along the top.

4.5 Discussion

In addition to its intracellular localisation, Gal-3 is secreted and thus found extracellularly, where it exerts its effects predominantly by interacting with glycans on the cell surface and associated with the extracellular matrix. In order to investigate the effects of exogenous Gal-3 intravital microscopy was again used, in this case to examine the leukocyte response to local treatment with the recombinant protein. A time-course was first carried out and it was found that the vessels were highly inflamed after 4h intrascrotal treatment with the lectin, when the leukocyte flux and rolling velocities were significantly reduced and the numbers of adherent and emigrated cells were significantly increased. Once we had established that Gal-3 could elicit an inflammatory response, we were interested to see whether the lectin would act dose-dependently and exhibit cell-type specific responses.

In order to examine the effects of Gal-3 on neutrophils specifically, the recombinant protein was administered i.s. following injection with anti-Ly-6G i.v. and neutrophil recruitment was recorded by intravital microscopy. However, it was first important to establish that the anti-Ly-6G did not affect leukocyte recruitment in this system. The use of anti-Ly-6G antibodies has been shown to impair murine bone marrow neutrophil migration to LTB4 in transwell assays in addition to being routinely used *in vivo* to deplete circulating neutrophils via a complement-dependent mechanism (Abbitt *et al*., 2009). The same study also reported anti-Ly-6G to be lethal when combined with a local i.s. injection of TNFα;

however, these *in vivo* studies use a 5-fold higher dose of anti-Ly-6G given after the local area had been primed for 4h with a higher concentration of TNFα. In addition to this, even the higher dose of anti-Ly-6G did not affect expression of activation markers CD11b and L-selectin or release of ROS from murine neutrophils (Abbitt *et al*., 2009). Furthermore the use of the anti-Ly-6G clone 1A8 rather than clone RB6-8C5, which binds both Ly-6G and Ly-6C, a marker found not only on neutrophils but on dendritic cells, monocytes and lymphocytes increases neutrophil-specificity of the antibody (Daley *et al*., 2008).

Consequently, the use of anti-Ly-6G antibody to label neutrophils was validated in our system. Anti-Ly-6G administration did not alter the number of recruited leukocytes, as levels of flux, velocity, adhesion and emigration were unchanged from vehicle and isotype-treated animals. The isotype control antibody was used to measure the levels of non-specific binding of the Ly-6G antibody and indeed no vascular components were stained by isotype control IgG2a, confirming that the binding seen in anti-Ly-6G-treated animals was specific to this neutrophil antigen. In addition, analysis of whole blood taken after IVM was carried out by flow cytometry confirmed that there was no staining of either the monocytes or lymphocytes, while over 90% of the neutrophils were labelled.

A dose response was then carried out where animals were treated intrascrotally with increasing doses of recombinant Gal-3 in addition to

receiving anti-Ly6G to label the neutrophils. Whilst leukocyte flux was unaffected, there was a dose-dependent increase in the number of adherent or emigrated neutrophils, as well as a reduction in rolling velocity of the neutrophils to a similar extent as the non-labelled leukocytes. This confirms that in this system exogenous Gal-3 can act specifically to increase neutrophil trafficking to the inflamed area *in vivo,* however, approximately half of the recruited cells remained unidentified.

In order to examine the monocyte response to exogenous Gal-3 in isolation, mice containing GFP under their CX_3CR1 promoter were used. The mice were treated with the highest dose of rGal-3 to elicit an inflammatory response, and then monocyte recruitment was examined using IVM. Once more, the mice exhibited increased recruitment of all leukocytes in response to rGal-3. Furthermore, it was apparent that the monocytes exhibited reduced rolling velocities to similar levels as the remaining leukocytes, as well as making up approximately half of the total cells recruited. This was confirmed using confocal microscopy and staining for MRP14 (to label neutrophils), which again showed that rGal-3 elicited increased levels of neutrophil and monocyte recruitment compared to sham-treated animals, as well as almost equal numbers of the two cell types emigrating in to the tissue. These *in vivo* results are in line with papers reporting Gal-3 action as a chemoattractant for neutrophils as well as monocytes and macrophages in static assays (Sano *et al*., 2000).

The recruitment of neutrophils and monocytes in response to local treatment with exogenous Gal-3 was further examined, the cremasters were collected and analysed by real-time PCR to give a snapshot of the cytokines and chemokines present after 4h treatment with the lectin. Expression of IL-1β, TNFα, KC, MCP-1 and IL-6 was significantly increased in response to Gal-3 whereas SDF-1 levels were unchanged. This data suggests that Gal-3 is able to activate cells present in the local area, such as the stromal and endothelial cells to induce release of cytokines and chemokines, which would initiate and potentiate a local inflammatory response, which is consistent with reports in the literature. Since levels of Gal-3 are increased at sites of joint destruction in RA, Filer *et al.* investigated the effect of exogenous Gal-3 treatment of human synovial fibroblasts, which increased their production of IL-6, GM-CSF, TNFα and MMP-3 as well as the neutrophil chemoattractant IL-8 and the monocyte chemoattractants MCP-1, MIP-1α and RANTES. The authors established that autocrine TNFα stimulation was not the cause of this release; in fact ERK MAPK activation occurred within 5 min and JNK, p38 MAPK and Akt phosphorylation was evident at 15 min as well as activation of NFκB (Filer *et al*., 2009). The activation of PI3K by Gal-3 has also been demonstrated in macrophages, which is often associated with chemokine production by stromal cells (MacKinnon *et al*., 2008) as well as E-selectin-dependent neutrophil rolling and trafficking (Puri *et al*., 2005), both cell types that are abundant in the cremaster muscle. To investigate this further, cremasters treated intrascrotally for 4h with rGal-3 were analysed by proteome profile array, which evaluates expression of

many cytokines and chemokines present in the sample. When compared to sham, rGal-3-treated cremaster samples exhibited increased binding of the array, thus many more of these inflammatory mediators were present in higher quantities in these tissues. Among these were TNFα, IFNγ, the neutrophil chemoattractants KC and MIP-2 (CXCL2) and the monocyte chemoattractants MCP-1 and MIP-1α. These arrays provide semi quantitative data, but are useful to show a snapshot of the local tissue microenvironment after treatment with the lectin and support the presence of pro-inflammatory mediators.

Despite treating locally with rGal-3, we wanted to ensure that the lectin was not entering the systemic circulation and acting on neutrophils and monocytes directly. Of note here are previous papers suggesting that Gal-3 may act as a soluble adhesion molecule for neutrophils *in vitro*, where it increased their binding to endothelial monolayers, this effect was dependent on its ability to oligomerise at the cell surface (Kuwabara and Liu, 1996, Sato *et al*., 2002). Furthermore, when the two cell types are incubated together *in vitro,* Gal-3 forms clusters between the endothelial cell surface and adherent neutrophils, these are concentrated at tricellular corners of the endothelium where these cells preferentially transmigrate (Nieminen *et al*., 2007). In addition, Melo *et al.* found that treatment with Gal-3 of sarcoma cells null for endogenous Gal-3 increased migration on laminin suggesting that any defects in the cells could be rescued by a direct effect of the recombinant protein. This was CRD-dependent and associated with SHP-2 tyrosine phosphatase-dependent increased

FAK/paxillin turnover at focal adhesion complexes as well as increased Akt phosphorylation and PI3K-dependence (Melo *et al*., 2011). In order to investigate whether extracellular Gal-3 has a direct effect in *ex vivo* flow chamber assays the quantity of Gal-3 in the plasma was analysed and found to be approximately 10ng/mL. However, treating Gal-$3^{-/-}$ leukocytes with plasma levels of rGal-3 was unable to rescue their phenotype and did not increase their capture to E-selectin under conditions of flow. Secondly, the plasma compartment of wild type mice was compared to that from Gal-$3^{-/-}$ blood. It was found that plasma from wild type mice did not increase capture of Gal-$3^{-/-}$ leukocytes to E-selectin, as well as Gal-$3^{-/-}$ plasma reducing the levels of capture of wild type cells. These results suggest further that, in our systems, the lack of both intracellular and extracellular Gal-3 results in impaired leukocyte function.

The flow chamber is useful to investigate interactions with E-selectin in isolation, however it was also interesting to determine if these results would be confirmed *in vivo*; rGal-3 was administered intravenously during analysis by IVM and the leukocyte recruitment followed over a time-course. It was found that rGal-3 had no effect on leukocyte recruitment to the area over a 60 min period, suggesting that exogenous Gal-3 does not act on leukocytes or vascular endothelial cells directly, at least within 60 min. Furthermore, after rGal-3 treatment *in vivo* in the short term, leukocytes were analysed by flow cytometry, however, their expression of

CAMs such as PSGL-1, L-selectin, CD44 or CD11a, b and c were unchanged in response to this lectin.

Endothelial cell function and particularly the upregulation of CAM expression, is vital to the leukocyte recruitment cascade; consequently, exogenous Gal-3 effects on this cell type were investigated. Isolated MLECs were treated with increasing concentrations of rGal-3 and analysed by flow cytometry; however, they did not alter their expression of ICAM-1 or E-selectin. As this simplified *in vitro* analysis may not support Gal-3 effects and since we know the recombinant protein initiates an inflammatory response *in vivo*, CAM expression in the cremaster after rGal-3 treatment was then investigated by confocal microscopy, using TNFα as a positive control. Using this method to view protein expression, it is possible that rGal-3 treatment results in increased expression of PECAM-1, VCAM-1 and E-selectin. The pan-Galectin inhibitor lactose also resulted in a robust increase in VCAM-1 and E-selectin expression, however, this could be acting via many mechanisms and pathways that do not involve Gal-3 as it would bind all galectins and many unrelated cell surface molecules. These data are interesting and may indicate that exogenous Gal-3 can stimulate endothelial cells directly to upregulate CAM expression or it could be acting on another cell type in vivo and causing that cell to bring about endothelial cell activation. However, the images provide qualitative information only and do not give any idea as to the mechanism of action of the lectin, which in future should be dissected further in the context of most recent literature.

Galectins that bind to cell surface glycoproteins are known to form lattices and transduce signals by crosslinking these glycotopes; due to its chimeric structure, Gal-3 forms large heterogeneous and disorganised lattices. Instances of exogenous Gal-3 forming lattices and interacting with integrins at the cell surface have been investigated in the context of various processes and disease states, resulting in the hypothesis of outside-in signalling pathways by which Gal-3 modulates integrin function. This was studied in cancer cells where the lectin binding to Mgat5-modified glycans and subsequent lattice-formation activated integrins leading to fibronectin remodelling and cell migration. Further investigation found that epidermal growth factor binding triggered Gal-3 lattice and ILK-dependent integrin signalling with subsequent src/pCav1/RhoA/ROCK-dependent production of focal actin structures, fibronectin remodelling and cell migration (Boscher and Nabi, 2013). More recently, Gal-3 was found to form a complex with β1-6 N-glycans on CD147 and β_1-integrin, resulting in their redistribution and clustering on the surface of retinal pigment epithelial cells. The exact functional implications of this association are still unclear, though it contributes to the pathogenesis of proliferative vitreoretinopathy (Priglinger *et al*., 2013). Similar associations have been found with the integrins $\alpha_v\beta_3$, which lead to endothelial cell migration and angiogenesis (Markowska *et al*., 2010, Ochieng *et al*., 1998); $\alpha_5\beta_1$, which affected carcinoma cell motility (Lagana *et al*., 2006); and $\alpha_3\beta_1$, where Gal-3 cross-linking led to lamellipodia development in a model of corneal injury (Saravanan *et al*., 2009b). In addition, Gal-3 binding to VEGF-R2 results in its retention at

the cell membrane and subsequent interaction with $\alpha_v\beta_3$-integrin leads to ILK-dependent increases in endothelial cell migration and proliferation (Markowska *et al*., 2011). There is also an epigenetic link between Gal-3 and members of the integrin family; a functional feedback loop occurs with β-integrins whereby Gal-3 expression in GE11 epithelial cells is increased in cells also expressing β_1-integrins due to demethylation of the Lgals3 promoter. Gal-3 then promotes β_1-integrin-mediated cell adhesion to laminin and fibronectin as well as cell migration (Margadant *et al*., 2012). In future, Gal-3 interactions with remaining members of the integrin family should be studied in the context of neutrophil and monocyte recruitment *in vivo* with the use of blocking antibodies.

Gal-3 effects on monocyte migration have been studied *in vitro*; Polli *et al.* investigated whether exogenous Gal-3 acts as a haptotactic agent – one that is immobilised on extracellular matrix components of endothelial cells, the basement membrane or connective tissue to facilitate cellular migration. This is particularly interesting since Gal-3 interacts with the extracellular matrix and promotes adhesion of neutrophils to laminin and fibronectin (Kuwabara and Liu, 1996). They found that Gal-3 binds to monocyte cell surface glycoproteins in a CRD-dependent manner and that while soluble Gal-3 induced monocyte migration in transwell assays, this was increased when the lectin itself was immobilised or present with laminin or fibronectin but not vitronectin. Furthermore, this was replicated for human macrophages, though only in the presence of laminin, suggesting extracellular matrix components can also control leukocyte

trafficking and that Gal-3 interacts selectively with them in the presence of different cell types. In addition and in concert with findings presented here, the authors found no difference in levels of CD11b, CD11c or L-selectin in monocytes stimulated with exogenous Gal-3 (Danella Polli et al., 2013). Taken together, these studies further suggest that Gal-3 lattice formation has pleiotropic effects on cell migration and specifically on the initiation and continuation of leukocyte adhesion by interacting with carbohydrate counterparts such as those exposed on integrins and the extracellular matrix.

Despite this, it is important to note that though extracellular Gal-3 effects are predominantly mediated by glycan interactions and thus are usually dependent on the CRD of the lectin, there may be CRD-independent and thus protein-protein interaction effects of the molecule at play here. One study describes exogenous Gal-3 effects on the JAK-STAT gene expression pathway in microglial cells where treatment with the lectin increased phosphorylation of JAK2 and STAT 1, 3 and 5, which regulate expression of pro-inflammatory genes; though CRD-independent, this required the presence of the IFNγR1. Furthermore, Gal-3 treatment increased levels of TNFα, IL-6, IL-1β, IP-10, IL-12p40 and IFNγ mRNA, while TGFβ, IL-10 and IL-13 remained the same; this was in addition to increasing expression of ICAM-1, MCP-1 and IL-8 in microglia (Jeon *et al*., 2010). Though this study was carried out to investigate traumatic brain injury, it is interesting that in other inflammatory models Gal-3 can affect expression of chemokines and cell adhesion molecules

independent of its CRD and highlights that N-terminus-dependent mechanisms of Gal-3 action may operate. In future, in vivo effects of rGal-3 should be dissected with respect to CRD or N-terminus dependency, using lactose or fragments of the Gal-3 N-terminus.

Chapter 5: Concluding remarks and future directions

This study has used *in vivo* imaging to explore the hypothesis that Gal-3 acts as a positive regulator of leukocyte recruitment to the inflamed microcirculation and unveils novel biology for exogenous and endogenous Gal-3 in controlling vascular inflammation. The results obtained throughout this PhD studentship are summarised in **Error! Reference source not found.**.

The data presented in Chapter 3 show that endogenous Gal-3 is required for slow rolling of leukocytes in response to local treatment with IL-1β and TNFα as well as for the emigration of leukocytes in response to IL-1β. These stimulus-specific effects can be attributed to further inherent changes in the cells such as their gene expression profile and glycosylation pattern. This is demonstrated by reduced levels of HPA and PNA lectin binding and CD11b expression basally on neutrophils, which when stimulated with TNFα also express reduced PSGL-1 and CD11b. Finally, Gal-3$^{-/-}$ endothelial cells express reduced ICAM-1 basally and after TNFα or IL-1β treatment, in addition to expressing reduced E-selectin after IL-1β treatment only.

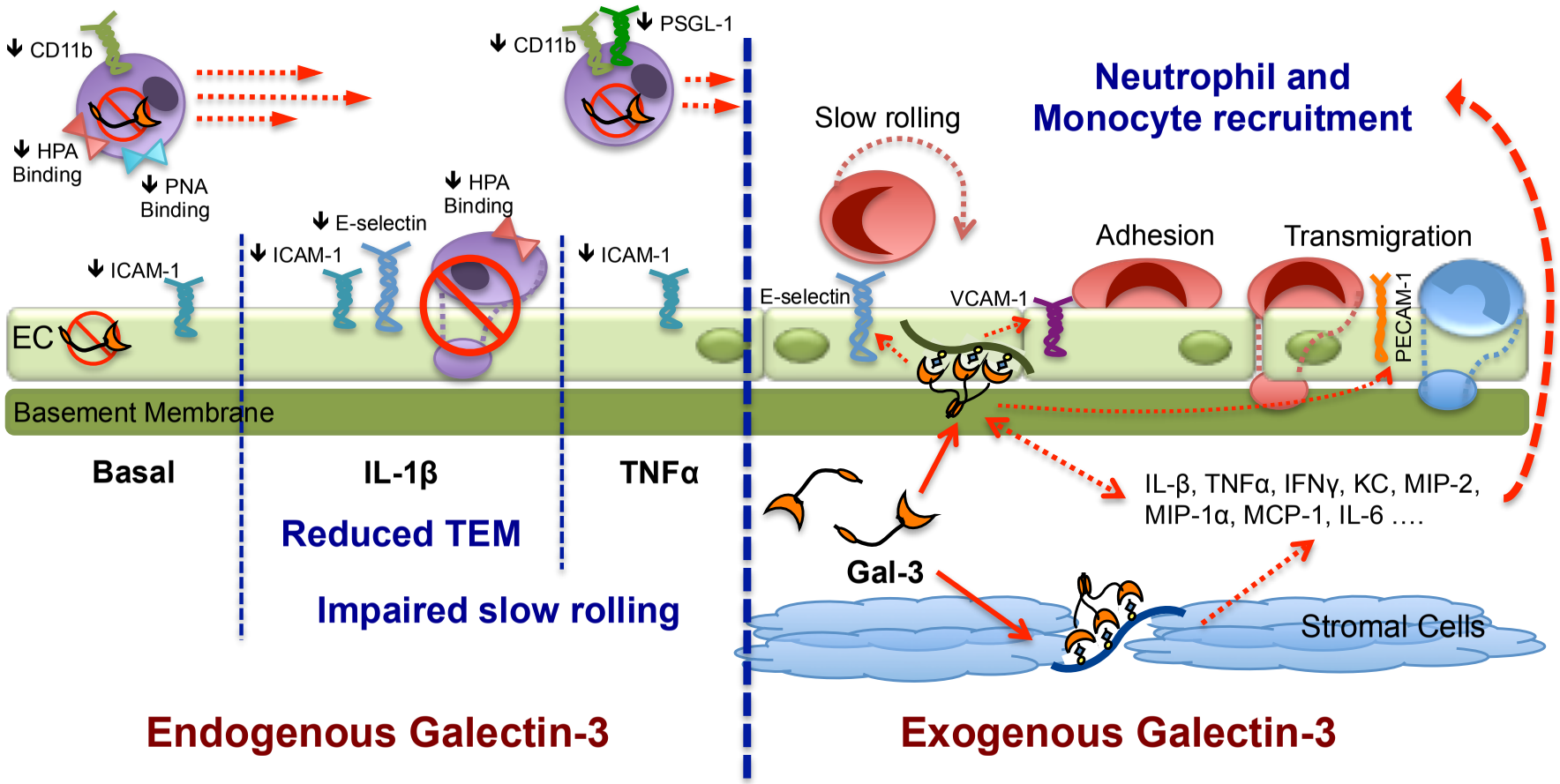

Figure 5.1 Exogenous and endogenous Gal-3 are positive regulators of leukocyte recruitment to the inflamed microcirculation

These findings have raised many points of interest that could be addressed and though some may be broader in scope than others, they include:

1. Assessing the glycosylation profile of Gal-3$^{-/-}$ endothelial cells; it has long been established that endothelial cells upregulate cell adhesion molecules to facilitate leukocyte recruitment, but it is important that these molecules also present the correct glycosylation profile to the leukocyte. For example, differential glycan expression is associated with inflammatory diseases that have a vascular component, such as psoriasis, myocarditis, ulcerative colitis and vasculitis; furthermore, the glycosylation profile has been postulated to act as a zip code, targeting cells to different organs and sites of inflammation (Renkonen *et al*., 2002). Studies investigating primary human monocyte adhesion found that TNFα stimulation of HUVEC increases N-glycan expression at cell junctions, possibly by affecting gene expression of the enzymes required for their production (Chacko *et al*., 2011). Further highlighting the importance of appropriate N-glycosylation are studies that found that ICAM-1 protein folding, trafficking and binding to CD11b are affected otherwise (Jimenez *et al*., 2005, Diamond *et al*., 1991).
2. To characterise further endogenous Gal-3 roles on emigration in response to IL-1β; for example with the use of more powerful IVM technology to assess leukocyte crawling and the proportion of para- versus transcellular emigration in Gal-3$^{-/-}$ animals. In

addition to using longer fixed-time models of leukocyte recruitment such as recruitment to the murine air pouch.

3. Characterise further the Gal-3$^{-/-}$ response to additional inflammatory stimuli, with the use of tri-colour IVM using antibodies to identify leukocyte subsets affected.
4. Quantify expression of molecules involved in emigration, particularly PECAM-1, ICAM-2, JAM-A and integrin-α_6 in Gal-3$^{-/-}$ mice after treatment *in vivo*.
5. The use of blocking antibodies against E-selectin, ICAM-1, CD11b and integrin family members in vivo and in vitro to assess which molecules are involved in Gal-3-dependent slow rolling and emigration.
6. Whether signalling pathways and cellular activation are compromised in Gal-3$^{-/-}$ cells after treatment with classical stimuli, particularly the MAPK system after binding to E-selectin.

Concurrently, the data presented in Chapter 4 indicate that exogenous Gal-3 elicits an inflammatory response alone and induced both neutrophil and monocyte recruitment to the area. After 4 h treatment with the lectin the cremaster contained increased mRNA for IL-1β, TNFα, KC, MCP-1 and IL-6; increased protein expression of these mediators with the exception of IL-1β, was confirmed by proteome profile array alongside IFNγ, MIP-2 and MIP-1α. The recombinant lectin does not act directly on the leukocytes, which was confirmed using various techniques including intravenous administration of the lectin during intravital microscopy.

Finally, endothelial cells treated *in vitro* with Gal-3 did not increase ICAM-1 or E-selectin expression however, treatment *in vivo* followed by confocal analysis showed possible increases in PECAM-1, VCAM-1 and E-selectin expression.

In the context of work presented here, exogenous Gal-3 may have multiple effects on the local tissue microenvironment – firstly, to stimulate the production of classical neutrophil and monocyte chemoattractants by stromal cells and secondly, it may interact with glycoproteins to provide a 'pro-recruitment' status at the endothelial cell surface. Furthermore by acting as a haptotactic agent, the lectin may use selective interactions with the extracellular matrix to modulate trafficking of leukocyte subsets differentially. Addressing the following aims would elucidate the mechanism of exogenous Gal-3 action further:

1. To identify which cells are secreting the chemokine and cytokine panel observed in response to Gal-3 treatment; for example by analysing supernatants of fibroblast and endothelial cells cultured with the lectin.
2. To then examine which signalling pathways Gal-3 acts on; by using inhibitors of kinases known to be associated with various Gal-3 functions: PI3K, MAPK systems such as ERK1/2, JNK and p38 MAPK, and Akt.
3. To establish the localisation of Gal-3 itself after in vivo treatment; for example imaging by confocal microscopy to confirm which cells

Gal-3 acts on, whether it forms clusters at the cell surface and if it is interacting with integrins or members of the extracellular matrix.

4. To use Gal-3 CRD inhibitors such as lactose or the N-terminus fragment of the lectin to determine which portion of the molecule elicits an inflammatory response *in vivo*.

Finally, to highlight the clinical relevance of this study, Gal-3 is a multi-faceted carbohydrate binding protein that exhibits modulatory properties on many aspects of the immune response to disease; it has been implicated in RA, atherosclerosis, *S. pneumoniae* infection, metastatic cancers, stroke and bacterial sepsis. Recently, a genome wide association study was carried out on circulating Gal-3 and two loci were found; the gene itself Lgals3 was found, indeed this is the only study so far to do so. The second is the ABO gene locus though the study concludes that it is still unknown how the ABO gene variants may affect circulating Gal-3 levels (de Boer *et al*., 2012). However, the ABO gene variant is associated with many inflammatory markers, haematological parameters, cancers and cardiovascular diseases, which are all pathophysiologies that Gal-3 itself has roles in. In future, elucidating the cellular mechanisms behind Gal-3 action might provide therapeutic benefit to many patients suffering from these inflammatory disorders.

BIBLIOGRAPHY

ABBITT, K. B., COTTER, M. J., RIDGER, V. C., CROSSMAN, D. C., HELLEWELL, P. G. & NORMAN, K. E. 2009. Antibody ligation of murine Ly-6G induces neutropenia, blood flow cessation, and death via complement-dependent and independent mechanisms. *J Leukoc Biol,* 85**,** 55-63.

ACOSTA-RODRÍGUEZ, E. V., MONTES, C. L., MOTRÁN, C. C., ZUNIGA, E. I., LIU, F. T., RABINOVICH, G. A. & GRUPPI, A. 2004. Galectin-3 mediates IL-4-induced survival and differentiation of B cells: functional cross-talk and implications during Trypanosoma cruzi infection. *J Immunol,* 172**,** 493-502.

ALMKVIST, J., FÄLDT, J., DAHLGREN, C., LEFFLER, H. & KARLSSON, A. 2001. Lipopolysaccharide-induced gelatinase granule mobilization primes neutrophils for activation by galectin-3 and formylmethionyl-Leu-Phe. *Infect Immun,* 69**,** 832-7.

ALVES, C. M., SILVA, D. A., AZZOLINI, A. E., MARZOCCHI-MACHADO, C. M., LUCISANO-VALIM, Y. M., ROQUE-BARREIRA, M. C. & MINEO, J. R. 2013. Galectin-3 is essential for reactive oxygen species production by peritoneal neutrophils from mice infected with a virulent strain of Toxoplasma gondii. *Parasitology,* 140**,** 210-9.

ARGÜESO, P. & PANJWANI, N. 2011. Focus on molecules: galectin-3. *Exp Eye Res,* 92**,** 2-3.

BAHAIE, N. S., KANG, B. N., FRENZEL, E. M., HOSSEINKHANI, M. R., GE, X. N., GREENBERG, Y., HA, S. G., DEMETRIOU, M., RAO, S. P. & SRIRAMARAO, P. 2011. N-Glycans differentially regulate eosinophil and neutrophil recruitment during allergic airway inflammation. *J Biol Chem,* 286**,** 38231-41.

BARBONI, E. A., BAWUMIA, S. & HUGHES, R. C. 1999. Kinetic measurements of binding of galectin 3 to a laminin substratum. *Glycoconj J,* 16**,** 365-73.

BERNARDES, E. S., SILVA, N. M., RUAS, L. P., MINEO, J. R., LOYOLA, A. M., HSU, D. K., LIU, F. T., CHAMMAS, R. & ROQUE-BARREIRA, M. C. 2006. Toxoplasma gondii infection reveals a novel regulatory role for galectin-3 in the interface of innate and adaptive immunity. *Am J Pathol,* 168**,** 1910-20.

BEVILACQUA, M. P., STENGELIN, S., GIMBRONE, M. A. & SEED, B. 1989. Endothelial leukocyte adhesion molecule 1: an inducible receptor for neutrophils related to complement regulatory proteins and lectins. *Science,* 243**,** 1160-5.

BHAUMIK, P., ST-PIERRE, G., MILOT, V., ST-PIERRE, C. & SATO, S. 2013. Galectin-3 facilitates neutrophil recruitment as an innate immune response to a parasitic protozoa cutaneous infection. *J Immunol,* 190**,** 630-40.

BLOCK, H., LEY, K. & ZARBOCK, A. 2012. Severe impairment of leukocyte recruitment in ppGalNAcT-1-deficient mice. *J Immunol,* 188**,** 5674-81.

BOSCHER, C. & NABI, I. R. 2013. Galectin-3- and phospho-caveolin-1-dependent outside-in integrin signaling mediates the EGF motogenic response in mammary cancer cells. *Mol Biol Cell,* 24**,** 2134-45.

BRADFIELD, P. F., SCHEIERMANN, C., NOURSHARGH, S., ODY, C., LUSCINSKAS, F. W., RAINGER, G. E., NASH, G. B., MILJKOVIC-LICINA, M., AURRAND-LIONS, M. & IMHOF, B. A. 2007. JAM-C regulates unidirectional monocyte transendothelial migration in inflammation. *Blood,* 110**,** 2545-55.

BRUEHL, R. E., MOORE, K. L., LORANT, D. E., BORREGAARD, N., ZIMMERMAN, G. A., MCEVER, R. P. & BAINTON, D. F. 1997. Leukocyte activation induces surface redistribution of P-selectin glycoprotein ligand-1. *J Leukoc Biol,* 61**,** 489-99.

BURNS, A. R., BOWDEN, R. A., MACDONELL, S. D., WALKER, D. C., ODEBUNMI, T. O., DONNACHIE, E. M., SIMON, S. I., ENTMAN, M. L. & SMITH, C. W. 2000. Analysis of tight junctions during neutrophil transendothelial migration. *J Cell Sci,* 113 (Pt 1)**,** 45-57.

CABEROY, N. B., ALVARADO, G., BIGCAS, J. L. & LI, W. 2012. Galectin-3 is a new MerTK-specific eat-me signal. *J Cell Physiol,* 227**,** 401-7.

CARMAN, C. V. & SPRINGER, T. A. 2004. A transmigratory cup in leukocyte diapedesis both through individual vascular endothelial cells and between them. *J Cell Biol,* 167**,** 377-88.

CERLIANI, J. P., STOWELL, S. R., MASCANFRONI, I. D., ARTHUR, C. M., CUMMINGS, R. D. & RABINOVICH, G. A. 2011. Expanding the universe of cytokines and pattern recognition receptors: galectins and glycans in innate immunity. *J Clin Immunol,* 31**,** 10-21.

CFG. 2013. *Galectin 3 null mouse phenotype* [Online]. Available: http://www.functionalglycomics.org/glycomics/search/jsp/result.jsp?query=galectin 3&cat=coreg.

CHACKO, B. K., SCOTT, D. W., CHANDLER, R. T. & PATEL, R. P. 2011. Endothelial surface N-glycans mediate monocyte adhesion and are targets for anti-inflammatory effects of peroxisome proliferator-activated receptor gamma ligands. *J Biol Chem,* 286**,** 38738-47.

CHAVAKIS, T., KEIPER, T., MATZ-WESTPHAL, R., HERSEMEYER, K., SACHS, U. J., NAWROTH, P. P., PREISSNER, K. T. & SANTOSO, S. 2004. The junctional adhesion molecule-C promotes neutrophil transendothelial migration in vitro and in vivo. *J Biol Chem,* 279**,** 55602-8.

CHEN, H. Y., LIU, F. T. & YANG, R. Y. 2005. Roles of galectin-3 in immune responses. *Arch Immunol Ther Exp (Warsz),* 53**,** 497-504.

CHEN, H. Y., SHARMA, B. B., YU, L., ZUBERI, R., WENG, I. C., KAWAKAMI, Y., KAWAKAMI, T., HSU, D. K. & LIU, F. T. 2006. Role of galectin-3 in mast cell functions: galectin-3-deficient mast cells exhibit impaired mediator release and defective JNK expression. *J Immunol,* 177**,** 4991-7.

COLNOT, C., RIPOCHE, M. A., MILON, G., MONTAGUTELLI, X., CROCKER, P. R. & POIRIER, F. 1998. Maintenance of

granulocyte numbers during acute peritonitis is defective in galectin-3-null mutant mice. *Immunology,* 94**,** 290-6.

COOPER, D., IQBAL, A. J., GITTENS, B. R., CERVONE, C. & PERRETTI, M. 2012. The effect of galectins on leukocyte trafficking in inflammation: sweet or sour? *Ann N Y Acad Sci,* 1253**,** 181-92.

CRAIG, S. S., KRISHNASWAMY, P., IRANI, A. M., KEPLEY, C. L., LIU, F. T. & SCHWARTZ, L. B. 1995. Immunoelectron microscopic localization of galectin-3, an IgE binding protein, in human mast cells and basophils. *Anat Rec,* 242**,** 211-9.

DALEY, J. M., THOMAY, A. A., CONNOLLY, M. D., REICHNER, J. S. & ALBINA, J. E. 2008. Use of Ly6G-specific monoclonal antibody to deplete neutrophils in mice.

DANELLA POLLI, C., ALVES TOLEDO, K., FRANCO, L. H., SAMMARTINO MARIANO, V., DE OLIVEIRA, L. L., SOARES BERNARDES, E., ROQUE-BARREIRA, M. C. & PEREIRA-DA-SILVA, G. 2013. Monocyte Migration Driven by Galectin-3 Occurs through Distinct Mechanisms Involving Selective Interactions with the Extracellular Matrix. *ISRN Inflamm,* 2013**,** 259256.

DANGERFIELD, J. P., WANG, S. & NOURSHARGH, S. 2005. Blockade of alpha6 integrin inhibits IL-1beta- but not TNF-alpha-induced neutrophil transmigration in vivo. *J Leukoc Biol,* 77**,** 159-65.

DE BOER, R. A., VERWEIJ, N., VAN VELDHUISEN, D. J., WESTRA, H. J., BAKKER, S. J. L., GANSEVOORT, R. T., MULLER KOBOLD, A. C., VAN GILST, W. H., FRANKE, L., LEACH, I. M. & VAN DER HARST, P. 2012. A Genome-Wide Association Study of Circulating Galectin-3. *PLoS One,* 7.

DE BOER, R. A., YU, L. & VAN VELDHUISEN, D. J. 2010. Galectin-3 in cardiac remodeling and heart failure. *Curr Heart Fail Rep,* 7**,** 1-8.

DEMETRIOU, M., GRANOVSKY, M., QUAGGIN, S. & DENNIS, J. W. 2001. Negative regulation of T-cell activation and autoimmunity by Mgat5 N-glycosylation. *Nature,* 409**,** 733-9.

DHIRAPONG, A., LLEO, A., LEUNG, P., GERSHWIN, M. E. & LIU, F. T. 2009. The immunological potential of galectin-1 and -3. *Autoimmun Rev,* 8**,** 360-3.

DI LELLA, S., SUNDBLAD, V., CERLIANI, J. P., GUARDIA, C. M., ESTRIN, D. A., VASTA, G. R. & RABINOVICH, G. A. 2011. When galectins recognize glycans: from biochemistry to physiology and back again. *Biochemistry,* 50**,** 7842-57.

DIAMOND, M. S., STAUNTON, D. E., MARLIN, S. D. & SPRINGER, T. A. 1991. Binding of the integrin Mac-1 (CD11b/CD18) to the third immunoglobulin-like domain of ICAM-1 (CD54) and its regulation by glycosylation. *Cell,* 65**,** 961-71.

DINARELLO, C. A. 2000. Proinflammatory Cytokines. *CHEST Journal,* 118**,** 503-508.

DINARELLO, C. A. 2011. A clinical perspective of IL-1β as the gatekeeper of inflammation. *Eur J Immunol,* 41**,** 1203-17.

DUNNE, J. L., COLLINS, R. G., BEAUDET, A. L., BALLANTYNE, C. M. & LEY, K. 2003. Mac-1, but not LFA-1, uses intercellular adhesion molecule-1 to mediate slow leukocyte rolling in TNF-alpha-induced inflammation. *J Immunol,* 171**,** 6105-11.

FARNWORTH, S. L., HENDERSON, N. C., MACKINNON, A. C., ATKINSON, K. M., WILKINSON, T., DHALIWAL, K., HAYASHI, K., SIMPSON, A. J., ROSSI, A. G., HASLETT, C. & SETHI, T. 2008. Galectin-3 reduces the severity of pneumococcal pneumonia by augmenting neutrophil function. *Am J Pathol,* 172**,** 395-405.

FEDUSKA, J. M., GARCIA, P. L., BRENNAN, S. B., BU, S., COUNCIL, L. N. & YOON, K. J. 2013. N-glycosylation of ICAM-2 is required for ICAM-2-mediated complete suppression of metastatic potential of SK-N-AS neuroblastoma cells. *BMC Cancer,* 13**,** 261.

FENG, D., NAGY, J. A., PYNE, K., DVORAK, H. F. & DVORAK, A. M. 1998. Neutrophils emigrate from venules by a transendothelial cell pathway in response to FMLP. *J Exp Med,* 187**,** 903-15.

FERNÁNDEZ, G. C., ILARREGUI, J. M., RUBEL, C. J., TOSCANO, M. A., GÓMEZ, S. A., BEIGIER BOMPADRE, M., ISTURIZ, M. A., RABINOVICH, G. A. & PALERMO, M. S. 2005. Galectin-3 and

soluble fibrinogen act in concert to modulate neutrophil activation and survival: involvement of alternative MAPK pathways. *Glycobiology,* 15**,** 519-27.

FEUK-LAGERSTEDT, E., JORDAN, E. T., LEFFLER, H., DAHLGREN, C. & KARLSSON, A. 1999. Identification of CD66a and CD66b as the major galectin-3 receptor candidates in human neutrophils. *J Immunol,* 163**,** 5592-8.

FILER, A., BIK, M., PARSONAGE, G. N., FITTON, J., TREBILCOCK, E., HOWLETT, K., COOK, M., RAZA, K., SIMMONS, D. L., THOMAS, A. M., SALMON, M., SCHEEL-TOELLNER, D., LORD, J. M., RABINOVICH, G. A. & BUCKLEY, C. D. 2009. Galectin 3 induces a distinctive pattern of cytokine and chemokine production in rheumatoid synovial fibroblasts via selective signaling pathways. *Arthritis Rheum,* 60**,** 1604-14.

FORSMAN, H., ISLANDER, U., ANDRÉASSON, E., ANDERSSON, A., ONNHEIM, K., KARLSTRÖM, A., SÄVMAN, K., MAGNUSSON, M., BROWN, K. L. & KARLSSON, A. 2011. Galectin 3 aggravates joint inflammation and destruction in antigen-induced arthritis. *Arthritis Rheum,* 63**,** 445-54.

FORSMAN, H., SALOMONSSON, E., ONNHEIM, K., KARLSSON, J., BJÖRSTAD, A., LEFFLER, H., BYLUND, J., KARLSSON, A. & DAHLGREN, C. 2008. The beta-galactoside binding immunomodulatory lectin galectin-3 reverses the desensitized state induced in neutrophils by the chemotactic peptide f-Met-Leu-Phe: role of reactive oxygen species generated by the NADPH-oxidase and inactivation of the agonist. *Glycobiology,* 18**,** 905-12.

FRIGERI, L. G. & LIU, F. T. 1992. Surface expression of functional IgE binding protein, an endogenous lectin, on mast cells and macrophages. *J Immunol,* 148**,** 861-7.

FRIGERI, L. G., ZUBERI, R. I. & LIU, F. T. 1993. Epsilon BP, a beta-galactoside-binding animal lectin, recognizes IgE receptor (Fc epsilon RI) and activates mast cells. *Biochemistry,* 32**,** 7644-9.

FUKUMORI, T., TAKENAKA, Y., YOSHII, T., KIM, H. R., HOGAN, V., INOHARA, H., KAGAWA, S. & RAZ, A. 2003. CD29 and CD7

mediate galectin-3-induced type II T-cell apoptosis. *Cancer Res,* 63**,** 8302-11.

FUKUSHI, J., MAKAGIANSAR, I. T. & STALLCUP, W. B. 2004. NG2 proteoglycan promotes endothelial cell motility and angiogenesis via engagement of galectin-3 and alpha3beta1 integrin. *Mol Biol Cell,* 15**,** 3580-90.

GAO, X., LIU, D., FAN, Y., LI, X., XUE, H., MA, Y., ZHOU, Y. & TAI, G. 2012. The two endocytic pathways mediated by the carbohydrate recognition domain and regulated by the collagen-like domain of galectin-3 in vascular endothelial cells. *PLoS One,* 7**,** e52430.

GE, X. N., BAHAIE, N. S., KANG, B. N., HOSSEINKHANI, M. R., HA, S. G., FRENZEL, E. M., LIU, F. T., RAO, S. P. & SRIRAMARAO, P. 2010. Allergen-induced airway remodeling is impaired in galectin-3-deficient mice. *J Immunol,* 185**,** 1205-14.

GE, X. N., HA, S. G., LIU, F. T., RAO, S. P. & SRIRAMARAO, P. 2013. Eosinophil-expressed galectin-3 regulates cell trafficking and migration. *Front Pharmacol,* 4**,** 37.

GIL, C. D., COOPER, D., ROSIGNOLI, G., PERRETTI, M. & OLIANI, S. M. 2006. Inflammation-induced modulation of cellular galectin-1 and -3 expression in a model of rat peritonitis. *Inflamm Res,* 55**,** 99-107.

GREEN, C. E., PEARSON, D. N., CAMPHAUSEN, R. T., STAUNTON, D. E. & SIMON, S. I. 2004. Shear-dependent capping of L-selectin and P-selectin glycoprotein ligand 1 by E-selectin signals activation of high-avidity beta2-integrin on neutrophils. *J Immunol,* 172**,** 7780-90.

HAUDEK, K. C., SPRONK, K. J., VOSS, P. G., PATTERSON, R. J., WANG, J. L. & ARNOYS, E. J. 2010. Dynamics of galectin-3 in the nucleus and cytoplasm. *Biochim Biophys Acta,* 1800**,** 181-9.

HENDERSON, N. C. & SETHI, T. 2009. The regulation of inflammation by galectin-3. *Immunol Rev,* 230**,** 160-71.

HOGG, J. C. & DOERSCHUK, C. M. 1995. Leukocyte traffic in the lung. *Annu Rev Physiol,* 57**,** 97-114.

HOGG, N., PATZAK, I. & WILLENBROCK, F. 2011. The insider's guide to leukocyte integrin signalling and function. *Nat Rev Immunol,* 11**,** 416-26.

HOYER, K. K., PANG, M., GUI, D., SHINTAKU, I. P., KUWABARA, I., LIU, F. T., SAID, J. W., BAUM, L. G. & TEITELL, M. A. 2004. An anti-apoptotic role for galectin-3 in diffuse large B-cell lymphomas. *Am J Pathol,* 164**,** 893-902.

HSU, D. K., CHEN, H. Y. & LIU, F. T. 2009a. Galectin-3 regulates T-cell functions. *Immunol Rev,* 230**,** 114-27.

HSU, D. K., CHERNYAVSKY, A. I., CHEN, H. Y., YU, L., GRANDO, S. A. & LIU, F. T. 2009b. Endogenous galectin-3 is localized in membrane lipid rafts and regulates migration of dendritic cells. *J Invest Dermatol,* 129**,** 573-83.

HSU, D. K., YANG, R. Y., PAN, Z., YU, L., SALOMON, D. R., FUNG-LEUNG, W. P. & LIU, F. T. 2000. Targeted disruption of the galectin-3 gene results in attenuated peritoneal inflammatory responses. *Am J Pathol,* 156**,** 1073-83.

HU, Y., KIELY, J. M., SZENTE, B. E., ROSENZWEIG, A. & GIMBRONE, M. A. 2000. E-selectin-dependent signaling via the mitogen-activated protein kinase pathway in vascular endothelial cells. *J Immunol,* 165**,** 2142-8.

HUDSON, D. L., SLEEMAN, J. & WATT, F. M. 1995. CD44 is the major peanut lectin-binding glycoprotein of human epidermal keratinocytes and plays a role in intercellular adhesion. *J Cell Sci,* 108 (Pt 5)**,** 1959-70.

IURISCI, I., TINARI, N., NATOLI, C., ANGELUCCI, D., CIANCHETTI, E. & IACOBELLI, S. 2000. Concentrations of galectin-3 in the sera of normal controls and cancer patients. *Clin Cancer Res,* 6**,** 1389-93.

JANTSCHEFF, P., NAGEL, G., THOMPSON, J., KLEIST, S. V., EMBLETON, M. J., PRICE, M. R. & GRUNERT, F. 1996. A CD66a-specific, activation-dependent epitope detected by recombinant human single chain fragments (scFvs) on CHO transfectants and activated granulocytes. *J Leukoc Biol,* 59**,** 891-901.

JEON, S. B., YOON, H. J., CHANG, C. Y., KOH, H. S., JEON, S. H. & PARK, E. J. 2010. Galectin-3 exerts cytokine-like regulatory actions through the JAK-STAT pathway. *J Immunol,* 185**,** 7037-46.

JIANG, H. R., AL RASEBI, Z., MENSAH-BROWN, E., SHAHIN, A., XU, D., GOODYEAR, C. S., FUKADA, S. Y., LIU, F. T., LIEW, F. Y. & LUKIC, M. L. 2009. Galectin-3 deficiency reduces the severity of experimental autoimmune encephalomyelitis. *J Immunol,* 182**,** 1167-73.

JIMENEZ, D., RODA-NAVARRO, P., SPRINGER, T. A. & CASASNOVAS, J. M. 2005. Contribution of N-linked glycans to the conformation and function of intercellular adhesion molecules (ICAMs). *J Biol Chem,* 280**,** 5854-61.

JUNG, U. & LEY, K. 1997. Regulation of E-selectin, P-selectin, and intercellular adhesion molecule 1 expression in mouse cremaster muscle vasculature. *Microcirculation,* 4**,** 311-9.

JUNG, U., NORMAN, K. E., SCHARFFETTER-KOCHANEK, K., BEAUDET, A. L. & LEY, K. 1998. Transit time of leukocytes rolling through venules controls cytokine-induced inflammatory cell recruitment in vivo. *J Clin Invest,* 102**,** 1526-33.

KARLSSON, A., CHRISTENSON, K., MATLAK, M., BJÖRSTAD, A., BROWN, K. L., TELEMO, E., SALOMONSSON, E., LEFFLER, H. & BYLUND, J. 2009. Galectin-3 functions as an opsonin and enhances the macrophage clearance of apoptotic neutrophils. *Glycobiology,* 19**,** 16-20.

KARLSSON, A., FOLLIN, P., LEFFLER, H. & DAHLGREN, C. 1998. Galectin-3 activates the NADPH-oxidase in exudated but not peripheral blood neutrophils. *Blood,* 91**,** 3430-8.

KOENEN, R. R., PRUESSMEYER, J., SOEHNLEIN, O., FRAEMOHS, L., ZERNECKE, A., SCHWARZ, N., REISS, K., SARABI, A., LINDBOM, L., HACKENG, T. M., WEBER, C. & LUDWIG, A. 2009. Regulated release and functional modulation of junctional adhesion molecule A by disintegrin metalloproteinases. *Blood,* 113**,** 4799-809.

KOHLER, S., ULLRICH, S., RICHTER, U. & SCHUMACHER, U. 2010. E-/P-selectins and colon carcinoma metastasis: first in vivo evidence for their crucial role in a clinically relevant model of spontaneous metastasis formation in the lung. *Br J Cancer,* 102**,** 602-9.

KOLLIAS, G., DOUNI, E., KASSIOTIS, G. & KONTOYIANNIS, D. 1999. The function of tumour necrosis factor and receptors in models of multi-organ inflammation, rheumatoid arthritis, multiple sclerosis and inflammatory bowel disease. *Ann Rheum Dis,* 58 Suppl 1**,** I32-9.

KUBES, P., JUTILA, M. & PAYNE, D. 1995. Therapeutic potential of inhibiting leukocyte rolling in ischemia/reperfusion.

KUBES, P. & KERFOOT, S. M. 2001. Leukocyte recruitment in the microcirculation: the rolling paradigm revisited. *News Physiol Sci,* 16**,** 76-80.

KUNKEL, E. J., DUNNE, J. L. & LEY, K. 2000. Leukocyte arrest during cytokine-dependent inflammation in vivo. *J Immunol,* 164**,** 3301-8.

KUNKEL, E. J. & LEY, K. 1996. Distinct phenotype of E-selectin-deficient mice. E-selectin is required for slow leukocyte rolling in vivo. *Circ Res,* 79**,** 1196-204.

KUWABARA, I. & LIU, F. T. 1996. Galectin-3 promotes adhesion of human neutrophils to laminin. *J Immunol,* 156**,** 3939-44.

KUWANO, Y., SPELTEN, O., ZHANG, H., LEY, K. & ZARBOCK, A. 2010. Rolling on E- or P-selectin induces the extended but not high-affinity conformation of LFA-1 in neutrophils. *Blood,* 116**,** 617-24.

LAGANA, A., GOETZ, J. G., CHEUNG, P., RAZ, A., DENNIS, J. W. & NABI, I. R. 2006. Galectin binding to Mgat5-modified N-glycans regulates fibronectin matrix remodeling in tumor cells. *Mol Cell Biol,* 26**,** 3181-93.

LEY, K., BULLARD, D. C., ARBONÉS, M. L., BOSSE, R., VESTWEBER, D., TEDDER, T. F. & BEAUDET, A. L. 1995. Sequential contribution of L- and P-selectin to leukocyte rolling in vivo. *J Exp Med,* 181**,** 669-75.

LEY, K., LAUDANNA, C., CYBULSKY, M. I. & NOURSHARGH, S. 2007. Getting to the site of inflammation: the leukocyte adhesion cascade updated. *Nat Rev Immunol,* 7**,** 678-89.

LI, Z., BURNS, A. R. & SMITH, C. W. 2006. Two waves of neutrophil emigration in response to corneal epithelial abrasion: distinct adhesion molecule requirements. *Invest Ophthalmol Vis Sci,* 47**,** 1947-55.

LIU, F. T., HSU, D. K., ZUBERI, R. I., KUWABARA, I., CHI, E. Y. & HENDERSON, W. R. 1995. Expression and function of galectin-3, a beta-galactoside-binding lectin, in human monocytes and macrophages. *Am J Pathol,* 147**,** 1016-28.

LIU, F. T., PATTERSON, R. J. & WANG, J. L. 2002. Intracellular functions of galectins. *Biochim Biophys Acta,* 1572**,** 263-73.

LIU, W., HSU, D. K., CHEN, H. Y., YANG, R. Y., CARRAWAY, K. L., ISSEROFF, R. R. & LIU, F. T. 2012. Galectin-3 regulates intracellular trafficking of EGFR through Alix and promotes keratinocyte migration. *J Invest Dermatol,* 132**,** 2828-37.

LUND-JOHANSEN, F., OLWEUS, J., SYMINGTON, F. W., ARLI, A., THOMPSON, J. S., VILELLA, R., SKUBITZ, K. & HOREJSI, V. 1993. Activation of human monocytes and granulocytes by monoclonal antibodies to glycosylphosphatidylinositol-anchored antigens. *Eur J Immunol,* 23**,** 2782-91.

MACKINNON, A. C., FARNWORTH, S. L., HODKINSON, P. S., HENDERSON, N. C., ATKINSON, K. M., LEFFLER, H., NILSSON, U. J., HASLETT, C., FORBES, S. J. & SETHI, T. 2008. Regulation of alternative macrophage activation by galectin-3. *J Immunol,* 180**,** 2650-8.

MACKINNON, A. C., LIU, X., HADOKE, P. W., MILLER, M. R., NEWBY, D. E. & SETHI, T. 2013. Inhibition of galectin-3 reduces atherosclerosis in apolipoprotein E-deficient mice. *Glycobiology,* 23**,** 654-63.

MAMDOUH, Z., CHEN, X., PIERINI, L. M., MAXFIELD, F. R. & MULLER, W. A. 2003. Targeted recycling of PECAM from endothelial

surface-connected compartments during diapedesis. *Nature,* 421**,** 748-53.

MAMDOUH, Z., KREITZER, G. E. & MULLER, W. A. 2008. Leukocyte transmigration requires kinesin-mediated microtubule-dependent membrane trafficking from the lateral border recycling compartment. *J Exp Med,* 205**,** 951-66.

MAMDOUH, Z., MIKHAILOV, A. & MULLER, W. A. 2009. Transcellular migration of leukocytes is mediated by the endothelial lateral border recycling compartment. *J Exp Med,* 206**,** 2795-808.

MARGADANT, C., VAN DEN BOUT, I., VAN BOXTEL, A. L., THIJSSEN, V. L. & SONNENBERG, A. 2012. Epigenetic regulation of galectin-3 expression by beta1 integrins promotes cell adhesion and migration. *J Biol Chem,* 287**,** 44684-93.

MARKOWSKA, A. I., JEFFERIES, K. C. & PANJWANI, N. 2011. Galectin-3 protein modulates cell surface expression and activation of vascular endothelial growth factor receptor 2 in human endothelial cells. *J Biol Chem,* 286**,** 29913-21.

MARKOWSKA, A. I., LIU, F. T. & PANJWANI, N. 2010. Galectin-3 is an important mediator of VEGF- and bFGF-mediated angiogenic response. *J Exp Med,* 207**,** 1981-93.

MATARRESE, P., TINARI, N., SEMERARO, M. L., NATOLI, C., IACOBELLI, S. & MALORNI, W. 2000. Galectin-3 overexpression protects from cell damage and death by influencing mitochondrial homeostasis. *FEBS Lett,* 473**,** 311-5.

MAZUREK, N., CONKLIN, J., BYRD, J. C., RAZ, A. & BRESALIER, R. S. 2000. Phosphorylation of the beta-galactoside-binding protein galectin-3 modulates binding to its ligands. *J Biol Chem,* 275**,** 36311-5.

MELO, F. H., BUTERA, D., JUNQUEIRA MDE, S., HSU, D. K., DA SILVA, A. M., LIU, F. T., SANTOS, M. F. & CHAMMAS, R. 2011. The promigratory activity of the matricellular protein galectin-3 depends on the activation of PI-3 kinase. *PLoS One,* 6**,** e29313.

MIZGERD, J. P., HORWITZ, B. H., QUILLEN, H. C., SCOTT, M. L. & DOERSCHUK, C. M. 1999. Effects of CD18 Deficiency on the Emigration of Murine Neutrophils During Pneumonia.

MIZGERD, J. P., KUBO, H., KUTKOSKI, G. J., BHAGWAN, S. D., SCHARFFETTER-KOCHANEK, K., BEAUDET, A. L. & DOERSCHUK, C. M. 1997. Neutrophil emigration in the skin, lungs, and peritoneum: different requirements for CD11/CD18 revealed by CD18-deficient mice. *J Exp Med,* 186**,** 1357-64.

MULLER, W. A. 2011. Mechanisms of leukocyte transendothelial migration. *Annu Rev Pathol,* 6**,** 323-44.

NACHTIGAL, M., AL-ASSAAD, Z., MAYER, E. P., KIM, K. & MONSIGNY, M. 1998. Galectin-3 expression in human atherosclerotic lesions. *Am J Pathol,* 152**,** 1199-208.

NAKAHARA, S., OKA, N. & RAZ, A. 2005. On the role of galectin-3 in cancer apoptosis. *Apoptosis,* 10**,** 267-75.

NANGIA-MAKKER, P., HONJO, Y., SARVIS, R., AKAHANI, S., HOGAN, V., PIENTA, K. J. & RAZ, A. 2000. Galectin-3 induces endothelial cell morphogenesis and angiogenesis. *Am J Pathol,* 156**,** 899-909.

NEWTON, J. P., HUNTER, A. P., SIMMONS, D. L., BUCKLEY, C. D. & HARVEY, D. J. 1999. CD31 (PECAM-1) exists as a dimer and is heavily N-glycosylated. *Biochem Biophys Res Commun,* 261**,** 283-91.

NIEMINEN, J., KUNO, A., HIRABAYASHI, J. & SATO, S. 2007. Visualization of galectin-3 oligomerization on the surface of neutrophils and endothelial cells using fluorescence resonance energy transfer. *J Biol Chem,* 282**,** 1374-83.

NIEMINEN, J., ST-PIERRE, C., BHAUMIK, P., POIRIER, F. & SATO, S. 2008. Role of galectin-3 in leukocyte recruitment in a murine model of lung infection by Streptococcus pneumoniae. *J Immunol,* 180**,** 2466-73.

NIEMINEN, J., ST-PIERRE, C. & SATO, S. 2005. Galectin-3 interacts with naive and primed neutrophils, inducing innate immune responses. *J Leukoc Biol,* 78**,** 1127-35.

OCHIENG, J., LEITE-BROWNING, M. L. & WARFIELD, P. 1998. Regulation of cellular adhesion to extracellular matrix proteins by galectin-3. *Biochem Biophys Res Commun,* 246**,** 788-91.

OHSHIMA, S., KUCHEN, S., SEEMAYER, C. A., KYBURZ, D., HIRT, A., KLINZING, S., MICHEL, B. A., GAY, R. E., LIU, F. T., GAY, S. & NEIDHART, M. 2003. Galectin 3 and its binding protein in rheumatoid arthritis. *Arthritis Rheum,* 48**,** 2788-95.

OSBORN, L., HESSION, C., TIZARD, R., VASSALLO, C., LUHOWSKYJ, S., CHI-ROSSO, G. & LOBB, R. 1989. Direct expression cloning of vascular cell adhesion molecule 1, a cytokine-induced endothelial protein that binds to lymphocytes. *Cell,* 59**,** 1203-11.

PAN, J., XIA, L. & MCEVER, R. P. 1998. Comparison of promoters for the murine and human P-selectin genes suggests species-specific and conserved mechanisms for transcriptional regulation in endothelial cells. *J Biol Chem,* 273**,** 10058-67.

PARTRIDGE, E. A., LE ROY, C., DI GUGLIELMO, G. M., PAWLING, J., CHEUNG, P., GRANOVSKY, M., NABI, I. R., WRANA, J. L. & DENNIS, J. W. 2004. Regulation of cytokine receptors by Golgi N-glycan processing and endocytosis. *Science,* 306**,** 120-4.

PETRI, B., PHILLIPSON, M. & KUBES, P. 2008. The physiology of leukocyte recruitment: an in vivo perspective. *J Immunol,* 180**,** 6439-46.

PFAFFL, M. W. 2001. A new mathematical model for relative quantification in real-time RT-PCR. *Nucleic Acids Res,* 29**,** e45.

PHILLIPSON, M., HEIT, B., COLARUSSO, P., LIU, L., BALLANTYNE, C. M. & KUBES, P. 2006. Intraluminal crawling of neutrophils to emigration sites: a molecularly distinct process from adhesion in the recruitment cascade. *J Exp Med,* 203**,** 2569-75.

POBER, J. S., GIMBRONE, M. A., LAPIERRE, L. A., MENDRICK, D. L., FIERS, W., ROTHLEIN, R. & SPRINGER, T. A. 1986. Overlapping patterns of activation of human endothelial cells by interleukin 1, tumor necrosis factor, and immune interferon. *J Immunol,* 137**,** 1893-6.

PRIGLINGER, C. S., SZOBER, C. M., PRIGLINGER, S. G., MERL, J., EULER, K. N., KERNT, M., GONDI, G., BEHLER, J., GEERLOF, A., KAMPIK, A., UEFFING, M. & HAUCK, S. M. 2013. Galectin-3 induces clustering of CD147 and integrin-beta1 transmembrane glycoprotein receptors on the RPE cell surface. *PLoS One,* 8**,** e70011.

PURI, K. D., DOGGETT, T. A., HUANG, C. Y., DOUANGPANYA, J., HAYFLICK, J. S., TURNER, M., PENNINGER, J. & DIACOVO, T. G. 2005. The role of endothelial PI3Kgamma activity in neutrophil trafficking. *Blood,* 106**,** 150-7.

RAMBARUTH, N. D., GREENWELL, P. & DWEK, M. V. 2012. The lectin Helix pomatia agglutinin recognizes O-GlcNAc containing glycoproteins in human breast cancer. *Glycobiology,* 22**,** 839-48.

RAMPART, M., (UIA), U. O. A., FIERS, W., (RUG), S. U. O. G., SMET, W. D., INNOGENETICS, HERMAN, A. G. & (UIA), U. O. A. 1989. Different pro-inflammatory profiles of interleukin 1 (IL 1) and tumor necrosis factor (TNF) in anin vivo model of inflammation. *Agents and Actions,* 26**,** 186-188.

RAO, R. M., YANG, L., GARCIA-CARDENA, G. & LUSCINSKAS, F. W. 2007a. Endothelial-Dependent Mechanisms of Leukocyte Recruitment to the Vascular Wall.

RAO, S. P., WANG, Z., ZUBERI, R. I., SIKORA, L., BAHAIE, N. S., ZURAW, B. L., LIU, F. T. & SRIRAMARAO, P. 2007b. Galectin-3 functions as an adhesion molecule to support eosinophil rolling and adhesion under conditions of flow. *J Immunol,* 179**,** 7800-7.

REINHARDT, P. H. & KUBES, P. 1998. Differential leukocyte recruitment from whole blood via endothelial adhesion molecules under shear conditions. *Blood,* 92**,** 4691-9.

RENKONEN, J., TYNNINEN, O., HAYRY, P., PAAVONEN, T. & RENKONEN, R. 2002. Glycosylation Might Provide Endothelial Zip Codes for Organ-Specific Leukocyte Traffic into Inflammatory Sites. *Am J Pathol,* 161**,** 543-50.

REYNOLDS, A. R., REYNOLDS, L. E., NAGEL, T. E., LIVELY, J. C., ROBINSON, S. D., HICKLIN, D. J., BODARY, S. C. & HODIVALA-

DILKE, K. M. 2004. Elevated Flk1 (vascular endothelial growth factor receptor 2) signaling mediates enhanced angiogenesis in beta3-integrin-deficient mice. *Cancer Res,* 64**,** 8643-50.

SANO, H., HSU, D. K., YU, L., APGAR, J. R., KUWABARA, I., YAMANAKA, T., HIRASHIMA, M. & LIU, F. T. 2000. Human galectin-3 is a novel chemoattractant for monocytes and macrophages. *J Immunol,* 165**,** 2156-64.

SARAVANAN, C., CAO, Z., HEAD, S. R. & PANJWANI, N. 2009a. Detection of differentially expressed wound-healing-related glycogenes in galectin-3-deficient mice. *Invest Ophthalmol Vis Sci,* 50**,** 5690-6.

SARAVANAN, C., LIU, F. T., GIPSON, I. K. & PANJWANI, N. 2009b. Galectin-3 promotes lamellipodia formation in epithelial cells by interacting with complex N-glycans on alpha3beta1 integrin. *J Cell Sci,* 122**,** 3684-93.

SATO, S., OUELLET, N., PELLETIER, I., SIMARD, M., RANCOURT, A. & BERGERON, M. G. 2002. Role of galectin-3 as an adhesion molecule for neutrophil extravasation during streptococcal pneumonia. *J Immunol,* 168**,** 1813-22.

SCHENKEL, A. R., MAMDOUH, Z. & MULLER, W. A. 2004. Locomotion of monocytes on endothelium is a critical step during extravasation. *Nat Immunol,* 5**,** 393-400.

SCHIFF, M. 2000. Role of interleukin 1 and interleukin 1 receptor antagonist in the mediation of rheumatoid arthritis. *Ann Rheum Dis,* 59**,** i103-8.

SCHRÖDER, A. K., UCIECHOWSKI, P., FLEISCHER, D. & RINK, L. 2006. Crosslinking of CD66B on peripheral blood neutrophils mediates the release of interleukin-8 from intracellular storage. *Hum Immunol,* 67**,** 676-82.

SETIADI, H. & MCEVER, R. P. 2003. Signal-dependent distribution of cell surface P-selectin in clathrin-coated pits affects leukocyte rolling under flow. *J Cell Biol,* 163**,** 1385-95.

SHEKHAR, M. P., NANGIA-MAKKER, P., TAIT, L., MILLER, F. & RAZ, A. 2004. Alterations in galectin-3 expression and distribution correlate

with breast cancer progression: functional analysis of galectin-3 in breast epithelial-endothelial interactions. *Am J Pathol,* 165**,** 1931-41.

SIMON, S. I., HU, Y., VESTWEBER, D. & SMITH, C. W. 2000. Neutrophil tethering on E-selectin activates beta 2 integrin binding to ICAM-1 through a mitogen-activated protein kinase signal transduction pathway. *J Immunol,* 164**,** 4348-58.

SKUBITZ, K. M., CAMPBELL, K. D. & SKUBITZ, A. P. 1996. CD66a, CD66b, CD66c, and CD66d each independently stimulate neutrophils. *J Leukoc Biol,* 60**,** 106-17.

SONG, S., JI, B., RAMACHANDRAN, V., WANG, H., HAFLEY, M., LOGSDON, C. & BRESALIER, R. S. 2012. Overexpressed galectin-3 in pancreatic cancer induces cell proliferation and invasion by binding Ras and activating Ras signaling. *PLoS One,* 7**,** e42699.

SPERANDIO, M., GLEISSNER, C. A. & LEY, K. 2009. Glycosylation in immune cell trafficking. *Immunol Rev,* 230**,** 97-113.

STEIN, J. V., CHENG, G., STOCKTON, B. M., FORS, B. P., BUTCHER, E. C. & VON ANDRIAN, U. H. 1999. L-selectin-mediated leukocyte adhesion in vivo: microvillous distribution determines tethering efficiency, but not rolling velocity. *J Exp Med,* 189**,** 37-50.

STOWELL, S. R., QIAN, Y., KARMAKAR, S., KOYAMA, N. S., DIAS-BARUFFI, M., LEFFLER, H., MCEVER, R. P. & CUMMINGS, R. D. 2008. Differential roles of galectin-1 and galectin-3 in regulating leukocyte viability and cytokine secretion. *J Immunol,* 180**,** 3091-102.

SUNDD, P., POSPIESZALSKA, M. K., CHEUNG, L. S., KONSTANTOPOULOS, K. & LEY, K. 2011. Biomechanics of leukocyte rolling. *Biorheology,* 48**,** 1-35.

TEN OEVER, J., GIAMARELLOS-BOURBOULIS, E. J., VAN DE VEERDONK, F. L., STELMA, F. F., SIMON, A., JANSSEN, M., JOHNSON, M., PACHOT, A., KULLBERG, B. J., JOOSTEN, L. A. & NETEA, M. G. 2013. Circulating galectin-3 in infections and non-infectious inflammatory diseases. *Eur J Clin Microbiol Infect Dis*.

THIJSSEN, V. L., HULSMANS, S. & GRIFFIOEN, A. W. 2008. The galectin profile of the endothelium: altered expression and localization in activated and tumor endothelial cells. *Am J Pathol,* 172**,** 545-53.

THOMPSON, R. D., NOBLE, K. E., LARBI, K. Y., DEWAR, A., DUNCAN, G. S., MAK, T. W. & NOURSHARGH, S. 2001. Platelet-endothelial cell adhesion molecule-1 (PECAM-1)-deficient mice demonstrate a transient and cytokine-specific role for PECAM-1 in leukocyte migration through the perivascular basement membrane. *Blood,* 97**,** 1854-60.

TRUONG, M. J., GRUART, V., LIU, F. T., PRIN, L., CAPRON, A. & CAPRON, M. 1993. IgE-binding molecules (Mac-2/epsilon BP) expressed by human eosinophils. Implication in IgE-dependent eosinophil cytotoxicity. *Eur J Immunol,* 23**,** 3230-5.

VAN STIJN, C. M., VAN DEN BROEK, M., VAN DE WEERD, R., VISSER, M., TAŞDELEN, I., TEFSEN, B. & VAN DIE, I. 2009. Regulation of expression and secretion of galectin-3 in human monocyte-derived dendritic cells. *Mol Immunol,* 46**,** 3292-9.

VLASSARA, H., LI, Y. M., IMANI, F., WOJCIECHOWICZ, D., YANG, Z., LIU, F. T. & CERAMI, A. 1995. Identification of galectin-3 as a high-affinity binding protein for advanced glycation end products (AGE): a new member of the AGE-receptor complex. *Mol Med,* 1**,** 634-46.

VRAY, B., CAMBY, I., VERCRUYSSE, V., MIJATOVIC, T., BOVIN, N. V., RICCIARDI-CASTAGNOLI, P., KALTNER, H., SALMON, I., GABIUS, H. J. & KISS, R. 2004. Up-regulation of galectin-3 and its ligands by Trypanosoma cruzi infection with modulation of adhesion and migration of murine dendritic cells. *Glycobiology,* 14**,** 647-57.

WALDO, S. W., LI, Y., BUONO, C., ZHAO, B., BILLINGS, E. M., CHANG, J. & KRUTH, H. S. 2008. Heterogeneity of human macrophages in culture and in atherosclerotic plaques. *Am J Pathol,* 172**,** 1112-26.

WESLEY, U. V., VEMUGANTI, R., AYVACI, E. R. & DEMPSEY, R. J. 2013. Galectin-3 enhances angiogenic and migratory potential of

microglial cells via modulation of integrin linked kinase signaling. *Brain Res,* 1496**,** 1-9.

WOJCIECHOWSKI, J. C. & SARELIUS, I. H. 2005. Preferential binding of leukocytes to the endothelial junction region in venules in situ. *Microcirculation,* 12**,** 349-59.

WOODFIN, A., VOISIN, M. B., IMHOF, B. A., DEJANA, E., ENGELHARDT, B. & NOURSHARGH, S. 2009. Endothelial cell activation leads to neutrophil transmigration as supported by the sequential roles of ICAM-2, JAM-A, and PECAM-1. *Blood,* 113**,** 6246-57.

YAMAOKA, A., KUWABARA, I., FRIGERI, L. G. & LIU, F. T. 1995. A human lectin, galectin-3 (epsilon bp/Mac-2), stimulates superoxide production by neutrophils. *J Immunol,* 154**,** 3479-87.

YAN, Y. P., LANG, B. T., VEMUGANTI, R. & DEMPSEY, R. J. 2009. Galectin-3 mediates post-ischemic tissue remodeling. *Brain Res,* 1288**,** 116-24.

YANG, E., SHIM, J. S., WOO, H. J., KIM, K. W. & KWON, H. J. 2007. Aminopeptidase N/CD13 induces angiogenesis through interaction with a pro-angiogenic protein, galectin-3. *Biochem Biophys Res Commun,* 363**,** 336-41.

YANG, J., HIRATA, T., CROCE, K., MERRILL-SKOLOFF, G., TCHERNYCHEV, B., WILLIAMS, E., FLAUMENHAFT, R., FURIE, B. C. & FURIE, B. 1999. Targeted gene disruption demonstrates that P-selectin glycoprotein ligand 1 (PSGL-1) is required for P-selectin-mediated but not E-selectin-mediated neutrophil rolling and migration. *J Exp Med,* 190**,** 1769-82.

YANG, L., FROIO, R. M., SCIUTO, T. E., DVORAK, A. M., ALON, R. & LUSCINSKAS, F. W. 2005. ICAM-1 regulates neutrophil adhesion and transcellular migration of TNF-alpha-activated vascular endothelium under flow. *Blood,* 106**,** 584-92.

YANG, L., KOWALSKI, J. R., ZHAN, X., THOMAS, S. M. & LUSCINSKAS, F. W. 2006. Endothelial cell cortactin phosphorylation by Src contributes to polymorphonuclear leukocyte transmigration in vitro. *Circ Res,* 98**,** 394-402.

YANG, R. Y., HSU, D. K. & LIU, F. T. 1996. Expression of galectin-3 modulates T-cell growth and apoptosis. *Proc Natl Acad Sci U S A,* 93**,** 6737-42.

YOON, J., TERADA, A. & KITA, H. 2007. CD66b regulates adhesion and activation of human eosinophils. *J Immunol,* 179**,** 8454-62.

YOSHIDA, M., SZENTE, B. E., KIELY, J. M., ROSENZWEIG, A. & GIMBRONE, M. A., JR. 1998. Phosphorylation of the cytoplasmic domain of E-selectin is regulated during leukocyte-endothelial adhesion. *J Immunol,* 161**,** 933-41.

YOSHIDA, M., WESTLIN, W. F., WANG, N., INGBER, D. E., ROSENZWEIG, A., RESNICK, N. & GIMBRONE, M. A., JR. 1996. Leukocyte adhesion to vascular endothelium induces E-selectin linkage to the actin cytoskeleton. *J Cell Biol,* 133**,** 445-55.

YOUNG, R. E., THOMPSON, R. D. & NOURSHARGH, S. 2002. Divergent mechanisms of action of the inflammatory cytokines interleukin 1-beta and tumour necrosis factor-alpha in mouse cremasteric venules. *Br J Pharmacol,* 137**,** 1237-46.

ZANARDO, R. C., BONDER, C. S., HWANG, J. M., ANDONEGUI, G., LIU, L., VESTWEBER, D., ZBYTNUIK, L. & KUBES, P. 2004. A down-regulatable E-selectin ligand is functionally important for PSGL-1-independent leukocyte-endothelial cell interactions. *Blood,* 104**,** 3766-73.

ZARBOCK, A., LOWELL, C. A. & LEY, K. 2007. Spleen tyrosine kinase Syk is necessary for E-selectin-induced alpha(L)beta(2) integrin-mediated rolling on intercellular adhesion molecule-1. *Immunity,* 26**,** 773-83.